An Electrochemical Treatment for Improving the Activity of Nickel and Other Metals for the
Hydrogen Evolution and Other Reactions

Andrew R.T. Morrison

A Thesis

In the Department

of

Mechanical and Industrial Engineering

Presented in Partial Fulfillment of the Requirements

For the Degree of

Doctor of Philosophy (Mechanical Engineering) at

Concordia University

Montreal, Quebec, Canada

April 2016

Abstract

An Electrochemical Treatment for Improving the Activity of Nickel and Other Metals for the Hydrogen Evolution and Other Reactions

Andrew R.T. Morrison, Ph.D.

Concordia University, 2015

The electrolysis of water to produce hydrogen gas may form an important part of the world's future economy as a way to store the energy for sustainable sources for later use. Part of what will determine if this use is practical is the efficiency of the catalysts used for the two half reactions that make up the electrolysis reaction. Presently in industry the cathodic reaction, the hydrogen evolution reaction (HER), is catalysed by nickel most commonly. Thus, there is a motivation to increase the activity of nickel toward the HER. Traditionally this was done by creating a high specific surface area or by increasing the intrinsic activity of nickel through alloying with other metals. Recently the importance using bifunctional catalysts for the HER was seen, this opened up a new line of investigation for methods to increase the activity of nickel HER catalysts. In this work a novel procedure to modify a nickel surface into highly active bifunctional catalyst is presented. The method is an electrochemical treatment that works by applying an alternating voltage to the nickel surface in a mildly acidic environment that causes it to oxidize in a manner similar to platinum. The platinum-like oxidation of the surface yields the $Ni(OH)_x$ structure (with x=0-2 across the surface), and allows a way to side step the problem of clumping of phases which is seen in bifunctional catalysts. The surface created by the treatment not only catalyses the HER, but also the urea electrooxidation, among other reactions. In this thesis the treated nickel surface is characterized and shown to be a highly active stable bifunctional catalyst, when the optimal parameters for the treatment are used. The characterization also shows that treated surfaces conform to the expectations of the novel $Ni(OH)_x$ structure. The treated surface is also seen to be active toward urea electrooxidation, but for slightly different parameters than the optimal parameters for a HER catalyst. Several practical elements of implementing the treatment in an industrial setting are dealt with. Finally, after concluding remarks, several new lines of enquiry that have been opened by this novel technique are briefly discussed.

Dedication and Acknowledgements

This work is dedicated to all of my family, friends, and colleagues who helped me during this work. I don't know if you know who you are. If you don't, I'm not going to clarify here.

Contributions of Authors

There are three papers included in this thesis which have multiple authors. The contributions of all authors are disclosed here.

In the paper of chapter 5 Andrew Morrison planned and ran experiments, analysed all the data, and wrote the paper. Schwan Hosseiny provided the raw data for the XPS analysis, and provided comments to the writing prior to the final draft. Rolf Wuthrich supervised the work, and edited the paper.

In the paper of chapter 6 Andrew Morrison planned and ran experiments, analysed all the data, and wrote the paper. Louis Juillac and Sébastien Guyomart ran experiments under Andrew's direction. Rolf Wuthrich supervised the work, and edited the paper.

In the paper of chapter 7 Andrew Morrison planned and ran experiments, analysed all the data, and wrote the paper. Rolf Wuthrich supervised the work, and edited the paper.

Table of Contents

List of Figures

List of Tables

List of Symbols and Abbreviations

(Units unless otherwise stated)

AFM	Atomic force microscopy
b	Tafel Slope (mV/dec)
C	Capacitance (F)
C_{AA}	Concentration of ascorbic acid (mM)
C_{SS}	Concentration of sodium sulphate (mM)
CV	Cyclic voltammogram
D	Duty cycle for square wave (percent of full cycle)
E	Energy (J)
E^0	Standard Electrode Potential (V vs NHE)
EDX	Energy dispersive x-ray (spectroscopy)
EIS	Electrochemical impedance spectroscopy
EQCM	Electrochemical quartz Crystal microbalance
FTIR	Fourier transform infrared (spectroscopy)
η	Overvoltage of an electrochemical reaction (mV)
HER	Hydrogen evolution reaction
j	Current density (mA/cm^2)
j_0	Exchange current density (mA/cm^2)
L	Treatment length (number of cycles)
MSE	Mercury sulphate electrode
NP	Nanoparticle
OER	Oxygen evolution reaction
Q	Charge (C)
R	Electrical resistance (Ω)

SEM	Scanning electron microscopy
SPM	Scanning probe microscopy
T	Period for square wave (ms)
t_h	High time for square wave (ms)
t_l	Low time for square wave (ms)
TPB	Triple phase boundary
UOR	Urea oxidation reaction
V	Voltage (mV)
V_{eq}	Equilibrium Voltage (mV)
V_h	High voltage for square wave (mV)
V_l	Low voltage for square wave (mV)
XPS	X-ray photoelectron spectroscopy

Subscripts in Chemical Formula

ads	Adsorbed
aq	Aqueous
s	Solid

List of Equations and Chemical Reactions

xviii

1 Introduction

Electrocatalysts are important in several areas of research and industry. Electrochemical reactions are comprised of two half reactions, each reaction occurs on one of the two electrodes. The surface of these electrodes is actually the electrocatalyst for the respective half-reaction that occurs on it. Having an active electrocatalyst (electrode) for a half-reaction can be important for maximising a signal from an electrochemical sensor [1]. More obviously, active catalysts are important for saving energy. Energy savings by active catalysts are important in fuel cells [2], batteries [3], waste water treatment [4], and the device that will be discussed here, water electrolysers [5].

Water electrolysers are electrochemical devices that use electricity to generate hydrogen gas on the cathode, and some other product on the anode (oxygen, chlorine, etc.). Water electrolysis can be thought of as a way to store energy. Electricity can be converted to hydrogen gas and then back to electricity again through a fuel cell. The ability to store energy efficiently is actually of an important concern to the world. This is because of the need to transition the energy economy away from fossil fuels to a renewables based economy [6, 7]. The generation of energy from renewables is often more periodic (e.g. solar cells, wind turbines, tidal farms) than traditional power sources, so there is a need to make hay while the sun shines, and store energy for when it is required. Water electrolysers may play a large role in the future green energy economy in this capacity [8]. However, challenges must be overcome to make them more efficient at cost effective prices first [6].

A major challenge facing electrolysers is developing better noble metal free catalysts for both the anodic reaction and the cathodic reaction [6]. The performance of a water electrolyser catalyst depends on the type of water electrolyser, but the most common water electrolyser is the alkaline water electrolyser [9]. For this type of electrolyser the most often used material for both electrodes is nickel [5, 10]. Generally speaking the oxygen evolution is harder to catalyse than the hydrogen evolution reaction (HER) [5]. However, some non-traditional anode reactions are possible in the context of alkaline water electrolysers. For example, using the urea oxidization instead can both increase the efficiency of alkaline water electrolysers and give a use for the common pollutant urea, and nickel is again an active catalyst for this reaction.

1

All of this motivates research into Ni as a catalyst for these reactions. In addition to this, alkaline water electrolysers are already being used on an industrial scale [9, 11, 12]. This makes the appeal of finding better Ni electrolysis catalysts not only a matter of some-day, but also of today, because there are real applications that motivate their study.

In this thesis, following some background information, a literature review of nickel hydrogen evolution catalysts is presented. For the main work, an electrochemical treatment that increases the activity of catalysts through a unique process is described and investigated. The use of the treatment is seen to be more widely applicable than only for HER, and indeed other reactions, such as the urea oxidation, are also catalysed.

2 Background

2.1 Tafel Equation

If one had to pick an aspect of electrochemical reactions that makes them particularly interesting compared to other reactions, the obvious answer is that they have an extra control parameter: the electrode potential, which allows the manipulation of the reaction rate. The Tafel equation is a way to describe the relationship between the potential and the rate of an electrochemical (electrical current) reaction. The Tafel equation is written [13, 14]:

$$\eta = b \log \frac{j}{j_0},$$ (2.1)

with η being the overpotential, which is the difference between the potential of the electrode (V) and the equilibrium potential V_{eq} of the electrode. V_{eq} of a reaction is the potential at which the electrochemical reaction does not proceed in either the forward or reverse direction in net. This is a dynamic equilibrium and both directions of an electrochemical reaction are always occurring. More precisely, the equilibrium potential is the potential at which the reaction rates in both directions cancel out.

The variables b and j_0 are called the Tafel parameters. b is the Tafel slope, it is a measure of how much a change in the voltage will change the current. j_0 is the exchange current density. It is the amount of current that would flow at V_{eq} in the hypothetical of eliminating the reverse reaction. Taken together, these parameters are often used as a short hand for the activity an electrocatalyst has for a given reaction. If one desires the reaction to go faster, a higher j_0, and a lower b are desired.

The Tafel equation is only true for high current densities or high overpotentials (because the Tafel equation is a simplification of the Butler-Volmer equation that eliminates negligible terms [13, 14]). This is not the only limitation of the Tafel equation. At high currents the solution resistance and mass transport limitation become significant, both of which are not modeled in the Tafel equation. This leaves a region between high and low overpotentials where the Tafel equation is accurate (sometimes called the Tafel region).

In the literature the Tafel Equation is also widely used in situations where competing or coupled reactions (electrochemical or not) take place. Strictly speaking, the Tafel equation would not be valid in such cases. However, its use is standard, as it allows a first overview of the activity of a given electrode, thorough the two simple parameters j_0 and b.

2.2 Electrochemically Active Surface Area

In the fundamentals laws of electrochemistry the relevant quantity is current density (current normalized by surface area). However, the quantity accessible to measurement is the current. It immediately raises the question of how to measure the surface area. How surface area is measured is often dependant on the context. The context in this case is electrochemistry. Electrochemically active surface area is the surface area available for electrochemical reactions. The concept is fuzzy to a certain extent because it does depend on the reaction under study. It is probably best to think of this value as a measure of the number of active sites a surface contains (although expressed as an area). This value is usually determined through electrochemical means, by the deposition and removal of a mono-layer of some substance (e.g $Ni(OH)_2$ [15] or H_{ads} [16]) or by trying to measure of the double-layer capacitance that exists between the electrode and the bulk electrolyte [17].

2.3 Hydrogen Evolution

The hydrogen evolution reaction is the cathodic half reaction of water electrolysis.

$$2H_2O + 2e- \rightarrow H_2 + 2OH^-_{(aq)}. \qquad\qquad E^0 = 0 \text{ V}[18] \qquad (2.2)$$

The standard presentation of the HER has it happen in two steps. In the first step, hydrogen is adsorbed onto the surface of the electrode. The second is the desorption step, where the adsorbed hydrogen is released from the surface in the form of molecular hydrogen (H_2). The adsorption proceeds through what is known as the Volmer reaction, which in alkaline solution is

$$H_2O + e- \rightarrow H_{ads} + OH^-_{(aq)}. \qquad\qquad\qquad (2.3)$$

It is the water splitting step, splitting a molecule of water into an adsorbed hydrogen and a hydroxide ion. The next step proceeds via either the Heyrovsky reaction (also called electrochemical desorption) in alkaline solution:

$$H_{ads} + H_2O_{(aq)} + e^- \rightarrow H_{2,ads} + OH^-_{(aq)} , \qquad (2.4)$$

or the Tafel reaction:

$$2H_{ads} \rightarrow H_{2,ads}. \qquad (2.5)$$

Whether or not the desorption process is dominated by (2.4) or (2.5) depends on the surface concentration of adsorbed hydrogen, with high concentrations being dominated by the Tafel reaction, though any of the three steps could be rate limiting.

2.4 Nickel Electrochemistry

For discussing the electrochemistry of nickel two cases are distinguished here: the cases of alkaline and weakly acidic solutions. This is followed by comments on the initial surface structures of $Ni(OH)_2$. Finally some general information about working with nickel is given.

2.4.1   Alkaline Solutions
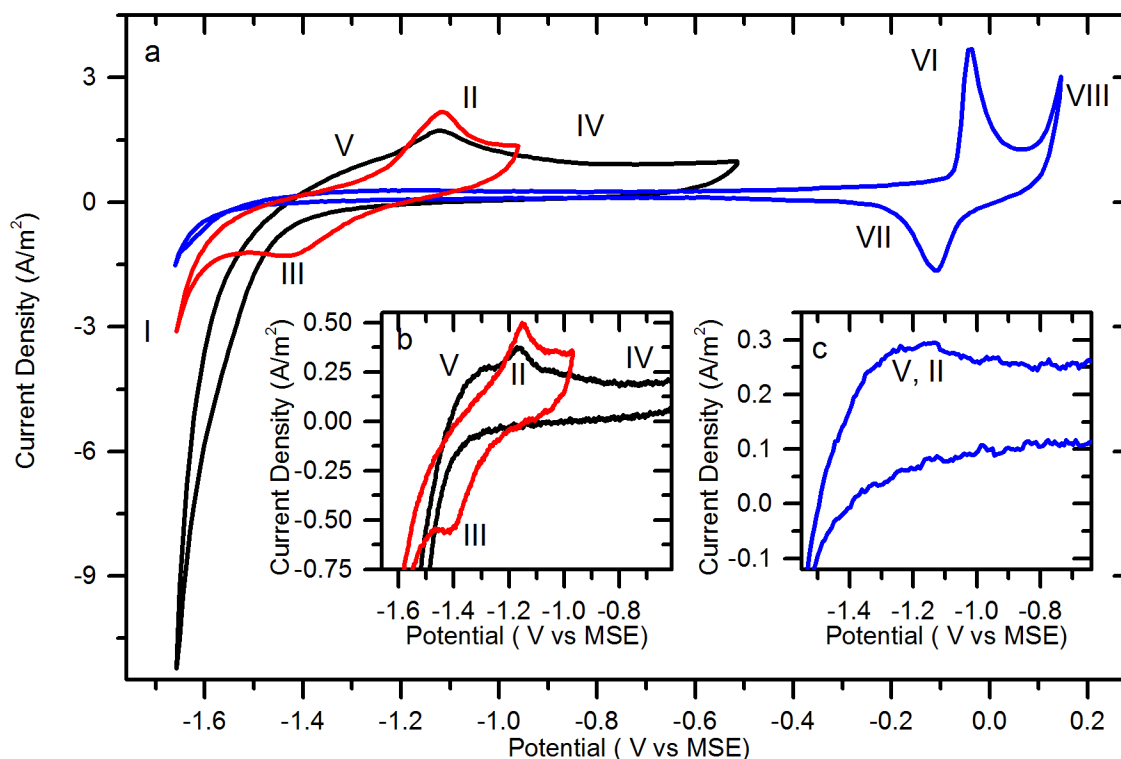
Figure 2.1: The (Cyclic voltammogram) CVs a nickel electrode in 1 M KOH. The main figure, a, shows three ranges of CVs, -1.66 V to -0.96 V, -1.66 V to -0.51 V and -1.25 V to 0.14 V al at 50 mV/s. The inset b shows a magnification of the anodic region, for a scan done at 10 mV/s to more clearly show II and V. The inset c shows a magnification of the same region as b, but after the electrode has been cycled past peaks VI and VII.

A CV of nickel in alkaline solutions is shown in Figure 2.1. The HER occurs at very cathodic potentials (region I, cathodic of -1.47 V vs MSE). The surface of the electrode is metallic nickel in this potential range. When the potential is scanned in the anodic direction, the surface is converted into $\alpha-Ni(OH)_2$ through peak II, which is a reaction with the OH⁻ ions:

$$Ni + 2OH^- \leftrightarrows \alpha - Ni(OH)_2 + 2e^- \,. \hspace{3cm} E^0\text{=-0.72 V [18]} \hspace{1cm} (2.6)$$

If the potential is inverted at a value cathodic of region IV (starting at about -0.96 V vs MSE) the reverse of reaction (2.5) can be seen in peak III. Since $\alpha-Ni(OH)_2$ is easily reducible (2.5) will reverse completely in this case [15]. If instead the potential is raised into region IV the surface starts to convert to $\beta-Ni(OH)_2$:

$$\alpha - Ni(OH)_2 \rightarrow \beta - Ni(OH)_2 \,. \hspace{6cm} (2.7)$$

The difference between the alpha and the beta forms of nickel hydroxide is that the alpha is more commonly amorphous, and when crystalline its layers are less densely packed and have

6

intercalated ions [19-22]. In fact, the dichotomy between these two forms of Ni(OH)$_2$ is a simplification, as forms that are neither are known [21]. Even if the dichotomy is false, it is still a widely used and useful classification. The conversion from the alpha form to the beta form occurs through a dissolution-redeposition process in alkaline media [19, 21] (note the lack of charge in the equation and corresponding current wave as this is a not an electrochemical process). In mildly alkaline to neutral solutions the aging still occurs, but through a topotactic anion leaching mechanism (the intercalated ions leaching out) [19, 20].

From region IV, if the potential is returned to the cathodic condition it started in, peak III can still be apparent. However, it is less distinct, having shifted cathodically and merged partly with the HER current. This is because β-Ni(OH)$_2$ is harder to reduce than α-Ni(OH)$_2$ [15, 23]. In fact, traces of β-Ni(OH)$_2$ are found on electrodes even after hours of reduction at highly cathodic potentials [24, 25]. The β-Ni(OH)$_2$ on the surface can also catalyse the hydrogen evolution [23], for reasons that are explained in section 3.4. The addition of β-Ni(OH)$_2$ to the surface also introduces peak V, which is associated with the hydrogen desorption [23].

Anodic of region IV is peak VI, and its inverse VII. These correspond to the oxidation of nickel hydroxide to nickel oxyhydroxide:

$$\beta - Ni(OH)_2 + OH^- \leftrightharpoons \beta - NiOOH + H_2O + e^- \qquad\qquad E^0\text{=0.49 V [26]} \qquad (2.8)$$
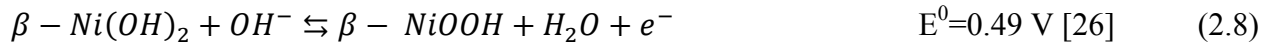
Similar to Ni(OH)$_2$ there are two different forms of NiOOH: β and γ. The γ phase will form at higher potentials (called "overcharging") [27]. It has higher spacing between layers and incorporates water coordinated with positive ions from the solution between the layers [27]. There are suggestions that α-Ni(OH)$_2$ oxidizes directly to the gamma form (because they are both the more disperse forms) [27, 28], but commonly one has to admit that the oxidation path of α-Ni(OH)$_2$ is still unknown [29]. It is however known that β-NiOOH only reduces into β-Ni(OH)$_2$ [29] (peak VII). This is why cycling over peaks VI and VII will produce a thick layer of β-Ni(OH)$_2$ [29, 30] with a NiO underlayer [29].

The final feature on the CV of the nickel electrode in alkaline solutions is region VIII, which is the Oxygen Evolution Reaction (OER) region. The OER is an electrochemical half-reaction that often makes up the other half of an alkaline electrolysis cell (opposite the HER). In alkaline solutions it combines OH$^-$ ions into H$_2$O and O$_2$.

After cycling the electrode from peaks VI and VII back to peaks II and III a large difference is seen. Peak II and peak V are no longer visible. In their place there appears a wide peak that is a combination of H-desorption and oxidation of the surface. Also, the activity of the electrode for the HER is seen to be reduced in the CV. These changes are a result of the entire surface becoming the slowly reducible β-Ni(OH)$_2$.

2.4.2 Weakly Acidic Solutions
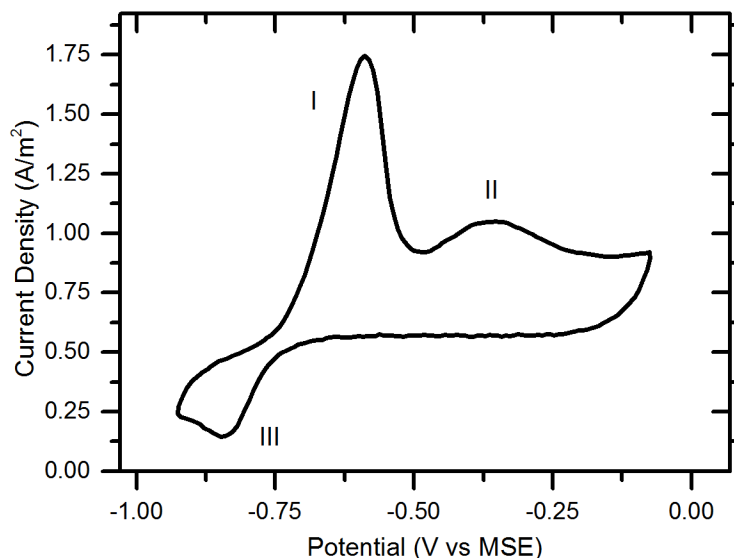
Figure 2.2 A CV from -0.93 V to -0.18 V at 50 mV/s in pH 2.8 sulfuric acid. The CV shows the principle reactions of concern here. Different inversion potentials and scan speeds would also include the OER, transpassive nickel dissolution to anodic potentials and Ni deposition and the HER to cathodic potentials.

In acidic conditions the oxidation mechanism of a nickel electrode changes due to the lack of OH$^-$ ions. According the Pourbaix (potential-pH) diagram of nickel, in acidic conditions Ni(OH)$_2$ or other oxidized states of Ni are not stable [31]. However, Pourbaix diagrams are computed at thermodynamic equilibrium, and that equilibrium will not exist at an interface. In fact, the nickel electrode will still form an oxidized layer even in acidic conditions, as described in this section.

Figure 2.2 shows a CV of Ni in acidic solutions. At very cathodic potentials, the surface is the same as in alkaline conditions. Despite the lack of OH$^-$ ions in the acidic solution, peaks I and II correspond to oxidation of the nickel surface to Ni(OH)$_2$, plus a NiO underlayer [32-34]. The overall process is summed up by:

$$Ni + H_2O \leftrightarrows Ni/NiO/Ni(OH)_2 \ . \tag{2.9}$$

8

The actual mechanism that leads to the layered NiO/Ni(OH)$_2$ is complicated. It is explained by Barbossa et al. [35], and the following is largely a summary of their reaction mechanism. The first step is the adsorption of water.

$$Ni_{(s)} + H_2O \leftrightarrows Ni_{(s)}H_2O_{ads} \tag{2.10}$$

This can occur at potentials just cathodic of peak I. The adsorbed water then splits into an adsorbed OH group and an H$^+$ ion:

$$Ni_{(s)} + H_2O_{ads} \leftrightarrows Ni_{(s)}OH_{ads} + H_{aq}^+ + e^- . \tag{2.11}$$

From this stage the reaction mechanism becomes more complicated, splitting into two paths. In one path the adsorbed OH forms a complex with a surface Ni, and further oxidizes to precipitate Ni(OH)$_2$ or an Ni^{2+} ion:

$$
\begin{aligned}
Ni_{(s)}OH_{ads} &\rightarrow Ni_{(s)}NiOH_{ads}^+ + e^- \\
Ni_{(s)}NiOH_{ads}^+ &\rightarrow Ni_{(s)} + NiOH_{aq}^+ \rightarrow Ni_{(s)} + H_2O + N_{aq}^{2+} \\
Ni_{(s)}NiOH_{ads}^+ + H_2O &\rightarrow Ni_{(s)} + Ni(OH)_2 + H_{aq}^+
\end{aligned}
\tag{2.12}
$$
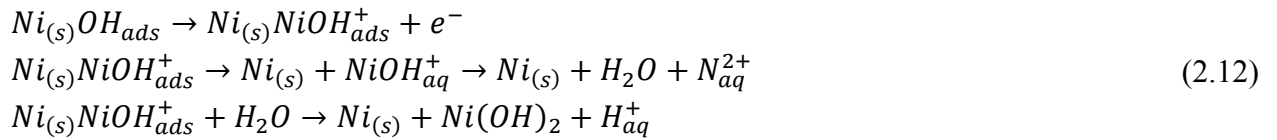
In the second path the surface accommodation process (also called "place exchange") causes OH group and a Ni to swap places:

$$Ni_{(s)}NiOH_{ads} \leftrightarrows Ni_{(s)}OHNi . \tag{2.13}$$

The buried OH group further oxidizes in place or releases a Ni^{2+} into the solution:

$$
\begin{aligned}
Ni_{(s)}OHNi + H_2O &\leftrightarrows Ni_{(s)}Ni(OH)_2 + H_{int}^+ + e^- \\
Ni_{(s)}OHNi &\leftrightarrows Ni_{(s)} + OH^- + Ni^{2+} + e^-
\end{aligned}
\tag{2.14}
$$
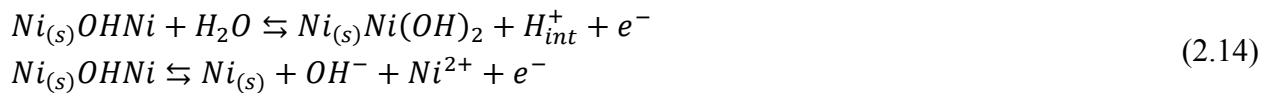
The Ni^{2+} from (2.12) and (2.14) can be combined with the OH$^-$ from reaction (2.14) to form Ni(OH)$_2$ on the surface:

$$Ni_{(s)} + Ni^{2+} + 2OH^- \rightarrow Ni_{(s)}Ni(OH)_2 . \tag{2.15}$$

Note that for (2.15) to work part of the surface must dissolve, because at most only one OH$^-$ is generated for every Ni^{2+}. As the potential is increased further (into peak II), the lower layers of the film convert to NiO through:

$$Ni_{(s)}Ni(OH)_2 \rightarrow Ni_{(s)}NiO + H_2O_{int} \qquad\qquad E^0 = 0.49 \text{ V [36]} \tag{2.16}$$

Peak II is thought to be largely made from (2.11) and (2.12), but direct dissolution of the nickel surface has been observed [33] and could play a part. Current in peak II is associated with (2.14). Peak III is much smaller than I and II because there is chemical dissolution of the Ni(OH)$_2$ layer in addition to the electrochemical dissolution. See Figure 2.3 for a diagram representation of the described reaction pathway.
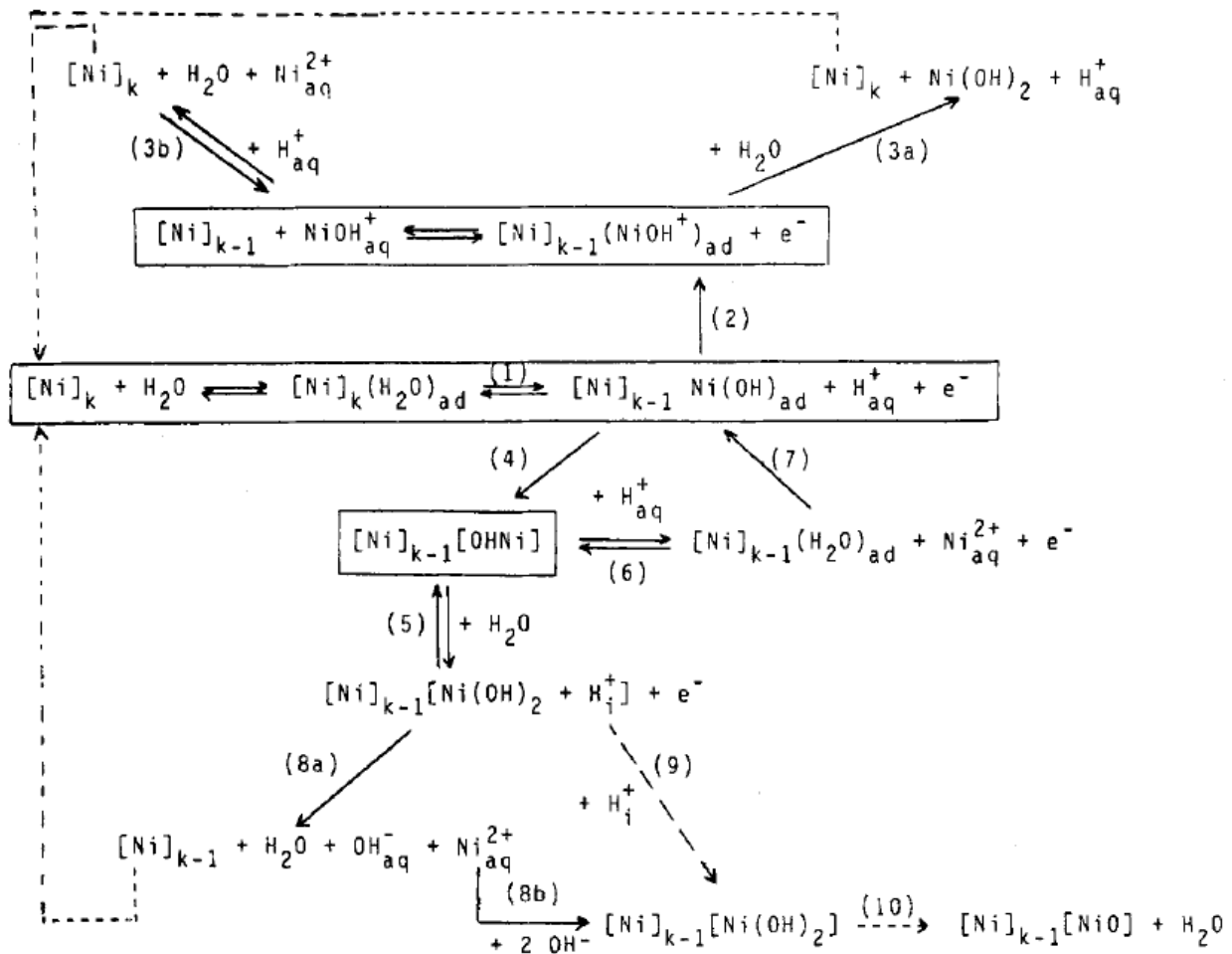
Figure 2.3: The pathway for the anodic oxidization of Ni suggested in Barbosa et al [35] (Reproduction by permission of the Electrochemical Society).

After the surface is well covered in the passive film (to several layers thick), a more specialized theory like the point-defect model may be more appropriate to describe the reactions which occur and the growth of the film [32]. One final important note is that all these mechanisms were determined in a sulphate solution, which has no special interaction with the Ni surface. There are certain ions that can disrupt this process. For example addition of Cl$^-$ to the solution is known to

promote dissolution of the surface, the surface develops pits, and then the solution can attack the surface through these pits [37].

2.4.3 Initial Surface Structures of Ni(OH)2

In the initial phases of growth in acidic solutions, experimental evidence shows $Ni(OH)_2$ grows as 3D islands [38, 39]. In weakly alkaline conditions the easily reducible α-$Ni(OH)_2$ can nucleate in a 2D form, but on conversion to β-$Ni(OH)_2$, 3D islands growth is apparent [25]. Growth in 3D islands can be described as a Volmer-Weber nucleation and growth mechanism, and is also how $Ni(OH)_2$ nucleates if it is deposited out of a solution [40, 41]. This is as opposed to a Frank–van der Merwe (layer-by-layer), Stranski–Krastanov (layer-by-layer followed by island growth) mechanisms, or formation of a surface alloy (mixing of the deposit and substrate to a depth of several atomic layers, occurs when a place-exchange reaction occurs quickly) [42]. Volmer-Weber growth occurs because the interaction between the new phase and itself is greater than the new phase and the substrate [42]. For this reason after the initial nucleation in the Volmer-Weber mechanism the islands will grow larger as more material is deposited (until the islands connect forming a full layer). These can be essentially hemispherical in nature [40, 41], or more complicated shapes are possible (discs [43], "flowers" [44, 45]) under specific conditions, but always the existing agglomerates are increased in preference to starting new ones.

An important consequence of the nucleation and growth mechanism of $Ni(OH)_2$, is that it leads to clumping of the $Ni(OH)_2$ which means that the creation of well dispersed $Ni/Ni(OH)_2$ structures is challenging. Such a structure would however, have important applications as an electrocatalyst for the hydrogen evolution reaction, as discussed later.

2.4.4 Practical Concerns

Pristine nickel surfaces exposed to air oxidize very quickly to a structure of 2-5 NiO layers, which is terminated with OH groups (it has also been described like the layered $Ni/NiO/Ni(OH)_2$ structure) if the air is humid [29, 46, 47]). Upon insertion into an alkaline solution these layers will grow, and the OH termination will become β-$Ni(OH)_2$ if the electrode's potential is left to float [46]. However, the air formed oxides can be reduced by applying a potential to the electrode in the HER region [29, 39].

Consistent experimental results are difficult to achieve with nickel electrodes. There are large drifts in current if the same electrode is continually used. This is attributed to the interstitial H^+ ions that are built up as a product of several of the surface oxidation or reduction reactions, or are inserted into the Ni matrix during HER [19]. For this reason, Hall et al. [19] recommend continually refreshing the electrode by cutting and/or ablating used material in order to get consistent results. This is very much in agreement with the author's personal experience, and was applied systematically in the present work.

2.4.5 Ni(I) Species

As seen in the proceeding section, Ni generally oxidizes to the 2nd oxidation state in both acidic and alkaline conditions. Stable Ni(I) compounds are rare but still know e.g. [48, 49]. However, there is very little mention of Ni(I) as a form of electro-oxidized Ni electrode in the literature (aside from the Ni(I) transition states seen above). It has been put forth that a species referred to as "reduced $Ni(OH)_2$" can be present on a Ni surface in alkaline conditions, in the HER region [23]. This could be a Ni(I) species if it exists.

2.4.6 HER activity

The Ni electrode is considered active for the HER, and is stable in severe alkaline conditions. For these reasons, and for the price, it is the preferred electrode material in alkaline water electrolysers for HER electrode (cathode) [5, 10]. Table 2.1 shows a selection of activity parameters measured for Ni from the literature.

Table 2.1: Activity of pure Ni. J_0 and b are the Tafel parameters, conditions shows what conditions the measurements were made in, and Intrinsic indicates if the j_0 parameter was normalized by geometric (no) or electrochemical active (yes) surface area.

Preparation/ Reference	J_0 (mA/cm^2)	b	Conditions	Intrinsic
Polished Ni plate [50]	6e-2	80	30% wt KOH, 28 °C	no
Deposited Ni [51]	1.1e-1	184	28% wt KOH, 25 °C	no
Polished Ni [5, 52]	1.1e-3	121	1 M NaOH, 20 °C	yes
Ni Foil [15]	3.3e-3	123	0.5 M KOH, 25 °C	yes

Ni Foil [15]	6.83e-2	136	0.5 M KOH, 70 °C	yes

3   Nickel as Electrocatalyst for the Hydrogen Evolution Reaction

Broadly speaking, Nickel based electrocatalyst can be dived into two categories. The first category contains catalysts that are active due to high specific surface area, and the second catalysts that are active due to a high intrinsic activity toward the HER.

Specific surface area is the true surface area divided by the geometric surface area (alternatively other normalization factors like mass are used). The concept of true surface area in electrochemistry is discussed in section 2.2. To create a highly active catalyst one aims to fabricate a material that has a large true surface area per geometrical surface area.

Intrinsic activity, on the other hand, is the true activity of the catalyst. It is the activity of a surface, divided by its true surface area. To explain how a high intrinsic activity is achieved one must understand why catalysts are active at all toward the HER. The general idea in heterogeneous catalysis is that the catalyst-reactant interaction must be not too strong, nor too weak. This is called the Sabatier principle, which is represented in the famous volcano curve [53]. In the case of the HER, the interaction between catalyst and reactant is historically taken to be the metal-H bond strength [54].
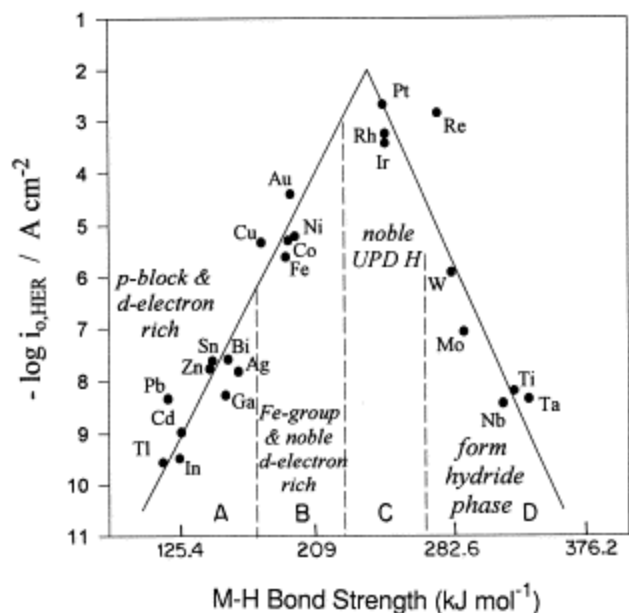
Figure 3.1 Volcano plot showing relation between metal-hydrogen bond strength and the rate of the HER. (Aside: If this is a volcano, where is the caldera?) (reprinted with permission from [55])

More recent works suggest that the character of the d-band of the catalyst's surface electronic structure is important [56, 57]. This is following similar work in gas phase heterogeneous catalysis where the d-band position relative to the Fermi level determines the bond strength [58] (and thus activity of a catalyst by the Sabatier principle). In electrochemistry the situation is more complicated. The Sabatier principle is still relevant and an optimized H bond strength is important. But having a d-band crossing the Fermi level and having a strong, long range, interaction with the orbitals of the H ion is equally important [56, 57].

In the following these two families of catalyst are described in more detail.

3.1 High Surface Area

High surface area Ni catalysts are grouped here by the strategy that is used to generate a high surface area. Each section explains the strategy, and briefly discuses the variations, if any, found within the group. Following this, activities of the catalysts are compared.

3.1.1 Raney Nickel and Raney Nickel-like

Raney Nickel was first developed in 1926 by Murray Raney by submerging a nickel-silicon alloy (and soon after a Ni-Al alloy) in a sodium hydroxide solution, for the hydrogenation of vegetable oils [59]. The alloying material in the nickel is leached out leaving a highly porous metallic

nickel material with a very high specific surface area (up to 100 m^2/g [60]). The methodology can be applied to a large variety of Nickel alloys. Catalysts like these are also referred to as sponge nickel, skeletal nickel, or sometimes just Raney nickel, after the first of the type. Originally Raney nickel was synthesized in powder form, a limitation for electrochemical systems, but this was addressed early. In terms of the hydrogen evolution reaction there have been several Raney nickel catalysts developed [61-65]. Other metals such as Cu [66], Zn [67-70], Mo [63, 65, 71], and Sn [64] have been used as the leeched material instead of, or in combination with, Al.

The primary effect, so far identified, on the activity toward the HER of Raney nickel catalysts is the ratio of material in the precursor alloy. A 1:1 ratio for Zn:Ni has been suggested as the optimum [68, 69]. However, various ratios of Ni to alloying material in the precursor have successfully generated high activity catalysts e.g. [69, 72, 73]. The trade off in terms of concentration of the leached metal in the precursor is that lower amounts produce a less porous surface, while high amounts produce no cracks in the structure [68]. Cracks are thought to be important because they facilitate access to inner layers of the catalyst [70].

3.1.2 Salt Melt

More recently sponge nickel catalysts have been fabricated by heating nickel salts under nitrogen for several hours. The result is a sponge-like metallic nickel structure like Raney nickel [74, 75].

3.1.3 Template Deposition

In template deposition a porous material is interposed between a surface and a deposition media. This leads to porous, high specific surface area catalysts. This technique has been used in a variety of ways to create high surface area nickel catalysts [76-81]. The templates can be made of a large variety of materials including plastics (pre-deposited on the surface [76], or co-deposited with the nickel [77]), liquid crystals [78], or alumina oxide [79-81]. The template can create stochastic surfaces [76-78] or regular patterns [79-81] (e.g. creating nanowires).

3.1.4 Deposition onto Pre-existing High Specific Surface Area

Another way to generate a high specific surface area nickel catalyst is to deposit nickel on to a substrate that already has a high specific surface area [82-88]. This has been achieved on conductive polymers [82-84], carbon nanotubes [87], and meso-porous-carbon [88]. Deposition

onto the conductive polymer can be onto pre-existing conductive polymer [83], or the polymer and the nickel can be co-deposited [84].

3.1.5   High Surface Area Performance

HER catalyst performance can be summed up in the Tafel parameters (exchange current density and Tafel slope), but not all studies measure the Tafel parameters. Other possible ways of measuring a catalyst's activity are the voltage required to attain a certain current (or visa-versa), or the total amount of H_2 produced over a period of time. Table 3.1 shows a comparison of the activity of several high surface area catalysts referenced here. It can be seen that in some cases it is difficult to compare the values in this table directly, since different measurements are listed. The measurements listed are those reported from the cited references. In fact, the difficulty in comparability of these values can be considered an issue with the way electrocatalysts are reported on in the literature. Interestingly, Raney nickel and Raney Nickel-like electrodes are clearly much better than the recent attempts at high surface area catalysts.

Table 3.1: Activity Comparison of Increased Surface Area catalysts. The table shows the activity of the best catalyst found in each listed reference. Each row shows, a short name for the catalyst, and a measure of the catalysts activity. This is taken to be preferentially exchange current density, but other reported values are also included.

Catalyst/ Reference	J_0 (mA/cm^2)	Alternate Activity Measurement	Conditions
Raney, NiZn/Ni, [67]		50.10mA/cm^2 @ -300mv , 83ml H_2 @ 3 V in 1h	1 M KOH @ 27 °C
Raney, NiAl, Pressed [61]		-211 mV @ 100 mA/cm^2	30% wt KOH @21 °C
Raney, NiZn, deposition [61]		-253 mV @ 100 mA/cm^2	30% wt KOH @21 °C
Raney, NiAl, ArcSpray [62]	0.727	-260 mV @ 250 mA/cm^2	1 M NaOH @ 25 °C
Raney NiAlMo plasma sprayed [65]	274	-67mV @ 250 mA/cm^2	1 M KOH @ 30 °C

Raney, NiAl Plasma Spray [63]		-82 mV @ 250 mA/cm^2	25% wt KOH @70°C
Raney NiAlMo, Plasma Spray [63]		-39 mV @ 250 mA/cm^2	25% wt KOH @70°C
Raney, NiAl, Melting [64]	4.02	-247 mV @ 250 mA/cm^2	1 M NaOH @ 30 °C
Raney, NiAlSn, Melting [64]	2.7	-150 mV @ 250 mA/cm^2	1 M NaOH @ 30 °C
Raney, NiCu deposition [66]	0.55		1 M NaOH, room temperature
Raney, ZnNi, Deposition [68]	1.58		6.25 M NaOH, room temperature.
Raney, ZnNi, Deposition [69]		-145 mV @ 400 mA/cm^2	10 M KOH @ 100°C
Raney, ZnNi, Deposition [70]		-150 mV @ 250 mA/cm^2	40% wt KOH @ 100 °C
Sponge NiMo (1:1) [71]	99	-311 mV @ 250 mA/cm^2	1 M NaOH @ 25 °C
Raney, ZnNi, Deposition [72]	30	-206 mV @ 250 mA/cm^2	1 M NaOH @ 25 °C
Salt Melt [74]		-360 mV @ 10 mA/cm^2	0.1 M KOH @ room temperature
Deposition through random template [76]		-300 mV @ 100 mA/cm^2	0.5 M NaOH @ 20 °C
Deposition through random template [77]		250 mA @ -1.66 V vs MSE	0.5 M NaOH @ 25 °C

Deposition through random template [78]		100 mA @ -1.64 V vs MSE	0.5 M NaOH @ room temperature
Nanowire array 20μm x 200nm [79]		30 mA @ -1.73 V vs MSE	1 M NaOH @ room temperature
Nanowire array 45μm x 400nm [80]		30 mA @ -1.63 V vs MSE	1 M Na$_2$SO$_4$ @ room temperature
Ni Deposit on high surface polymer [83]	0.047	-175 mV @ 1 mA/cm^2	0.5 M H$_2$SO$_4$ @ room temperature
Ni Deposit on high surface polymer [84]	0.239	-82 mV @ 1 mA/cm^2	0.5 M H$_2$SO$_4$ @ 25°C
Ni Deposit on C nanotubes [87]	0.011	-220 mV @ 20 mA/cm^2	1 M KOH @ room temperature

3.2 Intrinsic Increase in Activity

3.2.1 Alloys

Alloying a metal with low H binding energy to a metal with a high H binding energy is one of the first guiding principles for creating active alloy catalysts for the HER, and is often referred to as the Miles principle [89]. This principle is visualised by the so called volcano plot of the HER (see Figure 3.1) [55].

The Miles principle can be justified as the result of alloying hypo-hyper d-band metals [90]. This process should produce an alloy which has an H binding energy somewhere in between the two, which will be a better catalyst for the HER than the constituents. An alternate view to this is the "spillover effect", where the adsorption and desorption portions of the HER would happen on respectively the high and low H bond strength material [91]. Regardless, the guidelines to synthesize an active electrocatalyst for HER by following the Miles principle or the Spillover effect are the same. The Miles principle has been followed many times to produce active HER catalysts. Some of the most common elements alloyed with nickel for an HER electrode are

molybdenum [85, 92-98] and tungsten [95, 99-101], which both have complimentary h-binding energies to that of Ni according to the classic volcano plots for the HER [54, 55] (Figure 3.1).

It is apparent, however, that designing an alloy catalyst is not quite as simple as that. Several alloys that seem to violate the Miles principle have been reported [95, 96, 102-107]. Metals that, according to classic volcano plots, have similar H bond strength to nickel, including cobalt [102, 106-109], cadmium [96], zinc [106], copper [105], silver [104], iron [95, 102, 103], vanadium[101], and several rare earth elements [110]. A reason for this could be that the classic volcano curves appear to be incorrect according to more modern simulations of H-binding energy by ab initio methods [57, 111]. However, this only partially saves the Miles guideline, as there are still counter examples on revised volcano curves.

An issue with the Miles strategy is it does not address all three of the qualities thought to be relevant for highly active HER catalysts (the metal-H bond strength, having a d-band that crosses the Fermi level, and having a strong, long range interaction with the H^+ orbitals, as discussed in the opening of section3.2). There is some relation between the three (e.g. a surface that has an optimal H bond strength is more likely to have a d band that crosses the Fermi level), but they are not strongly correlated and sometimes the effects compete [57]. The interplay between the three qualities makes designing a high activity HER catalysts more complicated than if it were just the metal-H bond strength. So, although ideas like those suggested by Miles clearly have had their use, there is no easily understood explanation for what should produce a highly active Ni Alloy HER catalyst. The remaining solution is high throughput screening, where DFT and other computational techniques are used to evaluate potential catalysts before they are synthesized experimentally [112-114]. These have produced results with nickel, for example an AgNi catalysts [104].

A large variety of techniques for producing alloys exist, and several of them have been employed to create HER catalysts. The main one found in the literature is electrodeposition [95, 95-97, 102, 106]. Electrodeposition is preferred because it is an electrochemical fabrication technique that can produce a wide range of alloys with equipment that is readily available in electrochemical research laboratories. Other studies look at alloys that are alloyed mechanically by ball milling [93, 94, 98], thermal decomposing of salts [96], magnetron sputtering deposition [99], or by mixing at high temperature under inert atmosphere [92]. The fabrication technique

selected should make a difference in the final product. This can be inferred from the fact that even the catalytic properties of pure Ni are varied by these techniques (e.g. ball milling time of pure Ni effects activity [115]). However, there seems to be little consistent thought on why certain fabrication techniques are used beyond ease of use or novelty.

3.2.2   Long Term Stability

One possible issue with alloy catalysts, contrary to pure nickel catalysts, is that the alloying metal may not resist attack by the conditions in electrolysers, specifically known with Mo under industrial electrolyser conditions [96, 97]. Stability analysis of HER alloy catalysts is not always seen in the scientific literature (e.g. [99, 102]). However, more recent works with other alloying metals suggest that W and Co may not suffer from this problem [100, 106, 116]. In fact, long term polarization has been seen to increase the activity of some catalysts, in cases were initially low activity is caused by a substance that can be reduced in the HER region [106]. Deposition under increased gravity also seems to make a stable catalyst due to a difference in the crack structure of the films [100, 117]. These recent works do make the stability question look better for alloyed catalysts, but the lack of data from most reports leaves this as a mostly open question at best.

3.2.3   Nickel Nanostructures

Nanoparticles have been widely studied for catalytic applications (including the HER) in other metals with effects such as their size and shape coming under study [118]. For example, platinum nanoparticles with high miller index ((730), for example) facets have higher HER activity [119]. In pure nickel, indices this high have not been studied, but the (111) plane of bulk nickel is more active than other low index planes [120]. However, this does not seem to have been exploited explicitly. For nickel, in general, it has been recently (2013) noted that studies on nanoparticles as HER catalysts are rare [121], and this continues to be the case. There is some preliminary work, looking at how various qualities of their fabrication affect their activity (e.g. fabrication method, stabilizing agent etc.) [122, 123].

Lattice strain is a property nanostructures can alter that is not available in bulk nickel, and it is a property that theoretically affects HER activity [124]. The more recent effort to of Pătru et al. [121] has investigated Ni nanoparticles for this property, and produced positives results. This

work may also explain the older result that ball milling time (and the associated nanocrystaline structure changes) affects HER activity [115].

3.2.4 Performance of Intrinsic Catalysts

Due to the difficulty of measuring precisely the electroactive surface area, the quantitative evaluation of performances of intrinsic catalyst is challenging. In fact accurate measurement of surface areas is an important aspect to look at critically when attempting to compare the success of any study purporting to raise intrinsic activity. This is especially true when alloys often end up with roughened surface area. A not uncommon conclusion in Ni alloy studies is that HER activity is high mainly due to high specific surface area, but that there is still an intrinsic effect e.g. [95, 97, 102, 109]. Surface area is most commonly measured by EIS (Electrochemical Impedance Spectroscopy). One can also use deposition and stripping of $\alpha-Ni(OH)_2$ [15] or CO[125]. The two later techniques involve the charge required to electro- deposit or strip a monolayer of the species in question on a Ni surface. For $Ni(OH)_2$ this charge is found by CV in the range of peaks II and III in Figure 2.1, with an anodic inversion potential which is just cathodic of the potential of the formation of $\beta-Ni(OH)_2$.

EIS can, with a proper model, certainly give accurate surface areas (e.g. comparing rough and smooth Ni [126]). However, proper model selection is a major challenge in EIS [127]. It is dependent on several factors, including the features of the surface. Hence, one often faces the situation of trying to determine a property of the surface (the surface area) by a method that requires the knowledge of the surface's properties. In the main EIS surface area measurements are likely fine (and a full accounting of the quality of EIS data in studies is outside the scope of this review), but this wrinkle in comparing activities of catalysts is worth noting.

Table 3.2 shows the activity for several different Ni alloy electrodes. The issue discussed in section 3.1.5 of the incomparability of the reported activity measurements is again apparent, and compounded by the surface area measurement question. Quite frequently the activity shown in papers are not intrinsic (i.e. normalized by the electrochemical surface area). In those papers the value of the alloy as a catalyst is usually shown by comparison with some standard within the paper. Unfortunately, these practices make electrodes difficult to compare to one another, unless there has been some care taken to make a smooth surface. In sources where the electrochemical

surface area is taken in account, the exchange current density tends to be on the order of 10^{-3}-10^{-2} mA/cm^2. This is on the same, or one higher than that of pure Ni (Table 2.1).

Table 3.2: Activity Comparison of intrinsically active catalysts. Each row shows a short name for the catalyst, and a measure of the catalysts activity. This is taken to be preferentially exchange current density, but other reported values are also included. In the miscellaneous activities any potential which is not reference to a particular reference electrode is the overpotential. The last column "intrinsic" indicates whether the value has taken the true surface area into account directly (also noted if the surface was highly polished).

Catalyst	J_0 (mA/cm^2)	Misc. Activity Measures	Conditions	Intrinsic
NiMo arc melting then polished [91]	5e-2		0.5 M H2SO4, room temperature	n (but polished)
NiMo arc melting then polished [92]	7.9e-2		1 M KOH, 25 °C	N (but polished)
NiMo deposited[95]	5e-6	1.49e-2 mA/cm^2 @ -150 mV	0.5 M H$_2$SO$_4$, 295 K	y
NiW deposited[95]	3.1e-5	3.11e-1 mA/cm^2 @ -150 mV	0.5 M H$_2$SO$_4$,295 K	y
NiFe deposited [95]	5.6e-5	1.8e-3 mA/cm^2 @ -150 mV	0.5 M H$_2$SO$_4$, 295 K	y
NiMo deposited[96]		-1.66 V vs MSE @ -200 mA/cm^2	10 M KOH 25, 298 K	n
NiMoCd deposited[96]		-1.51 V vs MSE @ -200 mA/cm^2	10 M KOH, 298 K	n
NiMo thermal deposition[96]		-1.45 V vs MSE @ -200 mA/cm^2	10 M KOH, 298 K	n
NiMo depsited[97]	1e2	-1.769 V vs MSE @ -300 mA/cm^2	1 M KOH, 298 K	n
NiMo ball milled [98]	2.9e1	59 mV @ 250 mA/cm^2	30% wt KOH, 70 °C	n
NiW sputter deposited [99]	5.6e-2	172 mV/ dec (Tafel slope)	1 M KOH, 303 K	?
NiW deposited at high gravity[100]	2.94e-3 (7.5e-1)	0.32 mA/cm^2 (82 mA/cm^2) @ -150 mV	10% NaOH, room temperature	y (n)
NiW thermal decomposition		134 mV @ 1000 mA/cm^2	30% KOH, 70 °C	n

NiV thermal decomposition		120 mV @ 1000 mA/cm^2	30% KOH, 70 ∘C	n
CoNiFe electrodeposited [102]	4.43e-2		1 M NaOH, 298 K	n
NiFe deposited [103]	1.31e-1	265 mV @ 10 mA/cm^2	1 M KOH, 25 °C	n
NiAg E-beam deposited[104]		150 mV @ 0.15 mA/cm^2		n (but highly smooth)
NiCu, deposited[105]		-2 V vs SCE @ 130 mA/cm^2	6 M KOH, room temperature	n
NiCoMo, deposited [107]	4.6e-1	210 mV @ 300 mA/cm^2	30% wt KOH, 25°C	n
NiCo, deposited[108]	5e-2	275mv @ 100 mA/cm^2	30% wt KOH, 40°C	y
NiDy, arc melting, polished [110]	3.67e-3		8 M KOH, 25°C	n (but polished)
NiSm, arc melting, polished [110]	3.65e-3		8 M KOH, 25°C	n (but polished)

3.3 Combined Surface Area and Intrinsic Effect

For further increase in activity it is desirable to have methods combining both strategies: i.e. a high surface area catalyst with intrinsic activity. As already noted, alloyed catalysts tend to have high specific surfaces areas as a result of the alloying process. Additionally, nanoparticles will always have a high specific surface area. Finding scientific value in these is more challenging, since changing both the surface area and the intrinsic activity at the same time makes it more challenging to know where causes are, but the practical effects cannot be ignored. It should not be surprising that several studies have tried to optimise these aspects, for example by creating Raney nickel-like catalyst from Ni alloys [106, 109, 128]. From the other side, studies of Raney nickel note that having 5-6% Al remaining unleached produces optimal catalytic results [64], which could potentially be an intrinsic effect.

3.4 Bifunctional and Decorated Nickel

The principles discussed so far to create an active HER catalyst have not taken into account one important aspect and it is the main difference between the alkaline HER and acidic HER. That difference is that a water molecule must be split in (or prior to) the adsorption step of the HER (the Volmer reaction, reaction (2.3)). This leads to the activity of certain catalysts beings different in the two environments. It was recently noted by Subbaraman et al. [40] that while metal surfaces, such as Pt (and to a lesser extent Ni and other metals), show great efficiency at adsorbing and combining hydrogen atoms, they do not show good activity at cleaving a H-O-H bond (splitting water), while several metal hydroxides have this property [40]. This was shown initially by studying catalysts composed of a smooth surface of Pt decorated with islands of Pt or $Ni(OH)_2$. The surfaces with a higher ability to cleave H-O-H bonds perform better (Pt < Pt + Pt islands < Pt + $Ni(OH)_2$ islands). In fact it was shown later that this trend continues to varying metal hydroxide groups. Similar surfaces decorated with a metal hydroxides have HER activity as a function of the metal hydroxide's water splitting activity (which is itself a function of the metal hydroxide–OH bond strength, like metal–H bond strength for acidic HER) [129]. Knowledge that metal hydroxides could catalyse the HER is older than this [23], but the reasons were not appreciated. From the other direction, keeping the metal hydroxide a constant (as $Ni(OH)_2$), and varying the substrate metal recovers similar activity trends for the metals seen in acid, in alkaline solutions [41].

Bifunctional catalysts must work like regular catalyst, i.e. increases in the region where the reaction occurs cause the overall activity goes up (see section 3.1). Unlike traditional catalyst where the relevant area is the whole surface, the important area on bifunctional catalysts is the intersection of the component active for water splitting (the metal hydroxides) with the component active for the HER (the metal). In the present text it is called a triple phase boundary (TPB) in analogy to other types of catalysts (the third phase being the electrolyte). To maximize the TPB of a metal−'metal-hydroxide' should be the goal of any technique fabricating them.

So far, the fabrication procedure for decorating these bifunctional catalysts with metal hydroxides has been to deposit islands either potentiostatically or chemically, both from a bath of one of the metal's salts [40, 41, 129]. The resulting metal hydroxide islands are hemi-spherical, 10-50nm wide, and they cover 30-40% of the surface , depending on the substrate and metal

hydroxide. These islands are noted to grow by the Volmer-Webber nucleation and growth mechanism [40], as more fully explained in section 2.4.3. This island growth mechanism becomes a limiting factor of catalysts of bifunctionality kind. It limits how the TPB can be increased because some of the catalyst's surface must be used as $Ni(OH)_2$ islands.

There are alternate examples of bifunctional Ni HER catalysts. One alternative fabrication technique is to mix nanomaterials of the phases together, like Wang et al. [130] do with commercial nanoparticles and sheets of $Ni(OH)_2$. In principle this could overcome the difficulty discussed in the previous paragraph if the nanomaterials were of sufficiently small size, and well mixed. It is not clear that this was achieved. The results are difficult to interpret due to the choice of keeping the loading of Pt nanoparticles (NP) constant and varying the $Ni(OH)_2$ sheet loading (leading to a varying total amount of catalyst). Another bi-functional catalyst is made by creating Ni nanoparticles on carbon nanotubes (CNTs) from $Ni(OH)_2$ [131]. The authors of the study fabricated Ni nanoparticles partially covered by NiO. They suggested that these are bi-functional catalysts for the HER. This technique only works with CNTs as substrate, without CNTs a Ni nanoplate is formed instead. The need for CNTs during fabrication is not desirable. The clumpedness the NiO is, is not clear, but there is no reason to think it is well dispersed.

The stability of catalysts that use $Ni(OH)_2$ for the HER is questionable. As seen in section 2.4.1 $Ni(OH)_2$ will be reduced in the potential range of the HER. For β-$Ni(OH)_2$ the process is slow, happening over the course of hours, but it still happens. Contrary to this, there is still $Ni(OH)_2$ islands even after four hours at -100 mV overpotential HER [40], which reflects positively on the stability. However, this is the harshest stability test for these types of electrodes that the author is aware of, and it is in no way close to industrial conditions. Despite the slow reducibility of β-$Ni(OH)_2$, it must eventually reduce in alkaline electrolysers, which will reduce the activity the electrode.

3.5 Conclusions

Strategies of creating highly active Ni HER catalysts were reviewed. More traditional methods were broken down into those that had high specific surface area, and those that attempted to increase Ni's intrinsic activity.

The high surface area catalysts have a long and well developed history stretching back dozens of years, through Raney nickel catalysts. The pursuit of this goal is straight forward: increase the specific surface area. However, there are several fine points to consider, like the access to the inner layer of the catalyst. Beyond Raney nickel there are more recent methods (salt melt, nanowires etc.) that attempt to accomplish the same goal. Interestingly, these attempts could not get performances as high as Raney Nickel, which may indicate that it is very challenging to make any further significant improvement on this type of HER catalyst.

Studies that report on increasing intrinsic activity have a shorter history than in Raney nickel catalysts, but are still numerous. In terms of alloyed catalysts, it seems like every combination of metals and fabrication technique has a corresponding HER catalyst study. This is obviously a hyperbole (though not so far from the truth). The situation stems from the difficulty in understanding theoretically all involved effects. Indeed, unlike high surface area catalysts, the pursuit of intrinsic activity is much less clear. Although early strategies, like that of Miles, have produced valuable results, they do not mesh with all the research. To go further than the simply stated strategies one must consider all the effects on the electronic structure of the surface in the way only a computer simulation can. One of the major practical concerns of alloyed catalyst is its long term stability in the harsh environment of industrial electrolysers, although some work is beginning to address this concern. Nanostructuring seems to be a ripe field for investigating the basis of intrinsic activity in nickel, but nanostructured catalysts producing high activity (for example by selectively exposing appropriate facets, or other strategies) as in other metals are mostly unknown for nickel.

The newest strategy, the bifunctional catalysts, may be considered a new angle on increasing intrinsic activity. Those bifunctional catalysts highlight the importance of having a phase active for the water splitting reaction, which is a clear paradigm change. A very promising aspect of these catalysts is that they can potentially be combined with the very high surface area catalysts of the Raney type. However, bifunctional catalysts may only become interesting if one can address two major issues. First, because in this type of catalyst performance will be given by how large the TPB can be made, one must find ways to maximise the TBD. But, $Ni(OH)_2$, the preferred water splitting phase, grows by a Volmer-Weber mechanism, whether deposited from solution or oxidized directly on a Ni electrode. This mechanism directly causes clumping which

26

makes maximization of the TBD impossible. In fact, to develop a new methodology which could grow $Ni(OH)_2$ on Ni bypassing the Volmer-Weber mechanism would be a significant advance in the field. Second, the stability of bifunctional electrodes remains poorly addressed in the literature, and should be a concern due to its reliance $Ni(OH)_2$, which will eventually reduce if used as a cathode in the environment of an alkaline water electrolyser. Creating a bifunctional catalyst that is stable would be an important advance, and merely addressing the stability of electrodes like these would provide valuable information.

4 Objectives

Platinum is the best catalyst for the hydrogen evolution reaction as can be seen from Figure 3.1 [5]. However platinum is very expensive, additionally it is in very limited supply on earth, with the world's reserves in danger of running out if it is put to wide scale use [132]. Extra-terrestrial sources of Pt (from near-earth asteroids) are not currently economical, though may become accessible in the future [133]. In the meantime, other materials must be made do with for HER catalysts.

Nickel is generally the material made do with for commercial electrolysers. Increasing the electroactive surface area is currently the best method for creating a highly active nickel catalyst. However, the surface itself is not as intrinsically active as platinum by far (typically two orders of magnitude, as seen in Figure 3.1). To approach this ideal, a process is required that can modify a nickel surface to increase its activity. In this way, that process may be applied to a Raney-nickel electrode to obtain a high surface area catalyst with high intrinsic activity catalyst. Due to the recent advances in bifunctional catalysts these could be the way forward in this regard. However, these catalysts face two issues. First, they may not be stable at the cathodic potentials required for the HER. Second, there is the major issue of maximizing the TPB. As discussed in section 3.4 a major limiting factor is the nucleation and growth mechanism of $Ni(OH)_2$ which prevents the maximization of the TPB and therefore limits the activity of the catalyst. Both aspects must be solved in order to get the most out of bifunctional catalysts.

In fact, the overall objective of this work is to develop a new type of nickel based electrocatalyst in the novel paradigm of bifunctional HER catalysts that solves the issue of maximising the TPB. It will do this by the development of a strategy to side step the nucleation and growth problem, which is the main aim of this thesis. Essentially, Ni must be forced to oxidize in a wholly different manner, whereas opposed to the hydroxide phase clumping naturally it will spread out as it does in platinum. When platinum is oxidized the OH groups, which are incorporated into the surface after adsorption through place exchange, are in regularly spaced arrays [134]. To fulfil the aim of this thesis, nickel will be forced to oxidize in a manner similar to Platinum. This will be achieved by encouraging it to oxidize through the place exchange (reaction (2.13), section2.4.2), as opposed to any of the other mechanisms. As will be further explained in

Chapter 5 and 6, the trick is to exploit the fact that that the place exchange is not electrochemical, so its rate is independent of potential.

4.1 Contributions

The contributions of this thesis are

1) **Strategy**: a strategy for the modification of a metal surface, Ni or others, to force it to oxidize in a different manner, similar to Pt. The strategy is specifically developed for Ni where it produces a structure called $Ni(OH)_x$, but similarities with other metals may allow its extension. The strategy calls for use of a non-constant voltage waveform to regulate the rate of a non-electrochemical reaction step compared to other steps.

2) **HER Treatment**: The application of 1) to develop a treatment for Ni which results in a highly intrinsically active and stable, bifunctional HER catalyst. The characterizations of these treated electrodes show not only both their stability and activity, but also that validity of 1).

3) **Urea Electrooxidation Treatment**: The application of 1) to develop a treatment for Ni which results in a highly active Urea oxidation catalyst. The developed treatment is the same as 2), but with adjusted parameters for the different requirements of the Urea oxidation.

4.2 Thesis Organization

Following this chapter the main work of this thesis begins, starting with three chapters which are presented as manuscripts (chapters 5-7). Chapter 8 is a normal chapter, and is followed by the conclusions and outlook, chapter 9.

Chapter 5: The first manuscript is a case study of the treatment of contribution 2, the HER treatment. In this chapter the characteristics of treated electrodes are seen to be consistent with contribution 1. Also, treated electrodes are seen to be very active and stable for the HER.

Chapter 6: The second manuscript further investigates the HER treatment in a function of its parameters.

Chapter 7: The third manuscript discusses the details of treatment of contribution 3, the urea oxidation treatment. An electrode which is very active toward Urea oxidation is seen. How the treatment parameters must be adjusted to create active urea oxidation electrodes is presented.

Chapter 8: This delves into the practical elements of using the HER treatment. It addresses issues of cost and consistency that application as an industrial process must need care about.

Chapter 9: The conclusions of this thesis are presented, and an outlook on the future paths of research which may be inspired by this work is given.

5 Platinum-like Oxidation of Nickel Surface by Rapidly Switching Voltage to Generate Highly Active Bifunctional Catalysts

5.1 Forward

In the paper presented in this chapter a case study of the effects of an electrochemical square wave treatment on Ni with parameters that produce a highly active catalyst for the HER is presented. This paper was published in Electrochemistry Communications [135]. It is important to note that this limited the length of the paper. The afterward (Section 5.3) contains some elaborations on the concepts presented. The following chapter (6) contains also contains a fuller development of some concepts (e.g. parameter selection), than found in this chapter.

5.2 The Paper

Platinum-like Oxidation of Nickel Surfaces by Rapidly Switching Voltage to Generate Highly Active Bifunctional Catalysts

Andrew R.T. Morrison,

Seyed Schwan Hosseiny,

and Rolf Wüthrich

5.2.1 Abstract

Recently the importance of catalyzing the water splitting step of the hydrogen evolution reaction (HER) was highlighted. We demonstrate here a treatment to modify a nickel surface into a highly effective bifunctional HER catalyst ($i_0 = 0.18$ A/m^2, Tafel Slope = 106 mV/dec) that has a good distribution of both water splitting sites and H_{ads} combination sites. The resulting surface is characterized electrochemically, and with SEM, EDX, XPS and AFM. The data is found to be consistent with the treatment oxidizing the Ni surface in a novel way creating the hypothesized "Ni(OH)$_x$" structure (x between 0 and 2).

5.2.2 Introduction

The world is expected to transition to a renewable energy economy in the future [6, 7]. The Hydrogen Evolution Reaction (HER) is expected to play a role in this, but new materials are required for catalysts [6]. The most common type of electrolyser for HER today is alkaline [9].

The accepted mechanism of the alkaline HER consist of two steps: the "Volmer" step (water splitting in alkaline media) resulting in adsorbed hydrogen H_{ads} ($H_2O + e^- \rightarrow H_{ads} + OH^-$), followed by the combination step via either the "Heyrovsky" reaction, a second electron transfer reaction ($H_{ads} + H_2O + e^- \rightarrow H_2 + OH^-$), or the "Tafel" reaction, a chemical recombination reaction ($2H_{ads} \rightarrow H_2$). The importance of the water splitting step in this reaction was recently highlighted, in addition to the previously-known H_{ads} combination step [40, 41, 129]. To achieve a high reaction rate both steps must be catalyzed [40].

With the knowledge that two different types of surface sites are important for catalysing the HER, the challenge of developing HER electrodes is to maximize the triple phase boundary (TPB) between electrolyte, water splitting, and hydrogen recombination site. In previous work, $Ni(OH)_2$ was used to catalyse the water splitting, and a bifunctional catalyst was synthesized by covering a metal with nano-sized islands of $Ni(OH)_2$ [41, 129]. To realize a better catalyst a larger TPB is desirable, which implies a more uniform mixture of sites is necessary. However, obtaining a good dispersion with $Ni(OH)_2$ is challenging, because it forms via a Volmer-Weber nucleation and growth mechanism, resulting in the formation of islands [38, 136].

In the present paper we propose a novel surface: $Ni(OH)_x$, with x varying between 0 and 2, as an inherently bifunctional structure that sidesteps the nucleation and growth problem. Such a structure could be created by forcing a nickel surface to oxidize more like a platinum surface. Platinum oxidizes by incorporation of OH groups through place-exchange [136]. Place-exchange still occurs on nickel, but it is slow compared to nickel's other oxidation mechanisms. Nickel oxidation in weakly acidic solutions results in a $Ni/NiO/Ni(OH)_2$ structure [38, 39, 46] but start with the quick adsorption of OH groups. At the potentials where OH groups adsorb, there are two subsequent paths between a metallic nickel surface and the layered $Ni/NiO/Ni(OH)_2$ structure [35]. The first is through continued oxidation of $NiOH_{ads}$ groups, and the second is through the place-exchange process of $Ni/NiOH^+_{ads} \rightarrow Ni/OHNi$, which is a slow reaction compared to the other pathways [35].

Application of a square wave potential is used in this work to oxidize a Ni surface. It is hypothesized this will cause it to progressively form the targeted $Ni(OH)_x$ structure by exploiting the slow place exchange. During the anodic portion of each cycle a few OH groups will be buried in the electrode by place-exchange. Then, during the cathodic portion, all newly oxidized

32

species will be reduced except the buried OHs. This is because the place-exchange is not electrochemical, so is slow in both directions. With each subsequent cycle more OH groups will be buried. With properly selected parameters, the end result could be the proposed $Ni(OH)_x$ structure. This work explores the results of such a square wave treatment on Ni, especially for HER activity.

5.2.3 Materials and Methods

Experiments were performed using an AMEL 7050 potentiostat, using a standard three electrode cell [13]. Potentials are with reference to the $Hg/HgSO_4$ electrode in saturated K_2SO_4. Solutions were prepared using ultrapure deionised water (18 MΩ·cm).

Nickel wire (99.98% purity, Alfa Aeser) of 0.5 mm diameter was used for the electrode preparation. Before each experiment an unused segment of wire was polished using 600 grit abrasive paper (Mastercraft), followed by rinsing with ultrapure deionised water (fresh polished wire avoids drift [29]). A 2 mm portion of the wire was exposed to the solution (remainder wrapped in Teflon tape). Unless otherwise noted, the pre-treatment surface area, measured by the method explained in [15], is used throughout as it is challenging to measure the surface area of Ni electrodes with high coverage of hydroxides [137]. Using the pre-treatment surface area is justified by the similar roughness before and after treatment.

The treatment was done by applying a square wave (frequency 8 Hz, high voltage of −125 mV and low voltage of −770 mV) for 40 minutes (longer times produce no further effects, shorter times produce proportionally less effect) in a 24 mM ascorbic acid and 0.2 M Na_2SO_4 solution. The counter electrode was a high surface area nickel wire coil.

The electrochemical characterization of the sample consists of cyclic voltammograms (CVs), chronoamperometry (two step polarizations, Tafel plots), and chronopotentiometry (stability test in the hydrogen region). Each point in the Tafel plot is from a 2 minute polarization at a given potential. For the two step polarization, the initial potential was −1.7 V, the first step was to a varied potential, and the second step was back to −1.7 V. The electrode was held at each potential for five minutes. All electrochemical characterizations were done in a degassed (by nitrogen bubbling for 15 minutes prior to each experiment and throughout) solution of 1 M KOH (Fischer, ACS grade). The counter electrode was a high surface area platinum coil.

XPS spectra were taken on a Thermo Scientific Theta Probe instrument. The X-ray source was monochromatized Al K (1486.7 eV). The X-ray beam size was 400 μm and the energy resolution corresponds to Au3f7/2. XPS spectra were analyzed according to Biesinger [138] where only the Ni 2p3/2 region was fit, with the background line covering the entire Ni 2p region, and an offset added according to the iterative fitting method.

AFM micrographs were taken on a Multimode 5.3 with NCHR tools. The SEM micrographs were taken on a Hitachi S-3400N SEM. The EDX spectroscopy was performed in the SEM using an Oxford EDS & WDS elemental Analysis Unit. For the AFM and SEM characterization, samples were prepared by e-beam deposition of Ni onto glass, instead of nickel wire samples.

5.2.4 Results and Discussion

SEM micrographs (Figure 5.1 A, B) reveal black spots, possibly pits, formed post-treatment, indicating dissolution. However, the natures of such features are difficult to determine by SEM micrograph. Further analysis by atomic force microscope (AFM) of the surface roughness of the treated (Ra 2.17 nm) and untreated surfaces (Ra 2.20 nm) shows that they are almost identical (Figure 5.1 C, D) while the surface chemistry has changed after treatment (oxygen content increased as seen by EDX analysis from 3.7 wt% to 21.7% wt%). XPS data of the surface was best fit with a $Ni/NiO/Ni(OH)_2$ model [138]. This analysis indicates an increase in $Ni(OH)_2$ content (untreated: 62% Ni, 14% NiO, 24% $Ni(OH)_2$; treated 10% Ni, 27% NiO, 63% $Ni(OH)_2$;Figure 5.1e, f). The XPS spectra of $Ni(OH)_x$ is unknown, but it is surmised to be similar to $Ni(OH)_2$. Also, the wide range XPS scan shows no activation of trace elements.
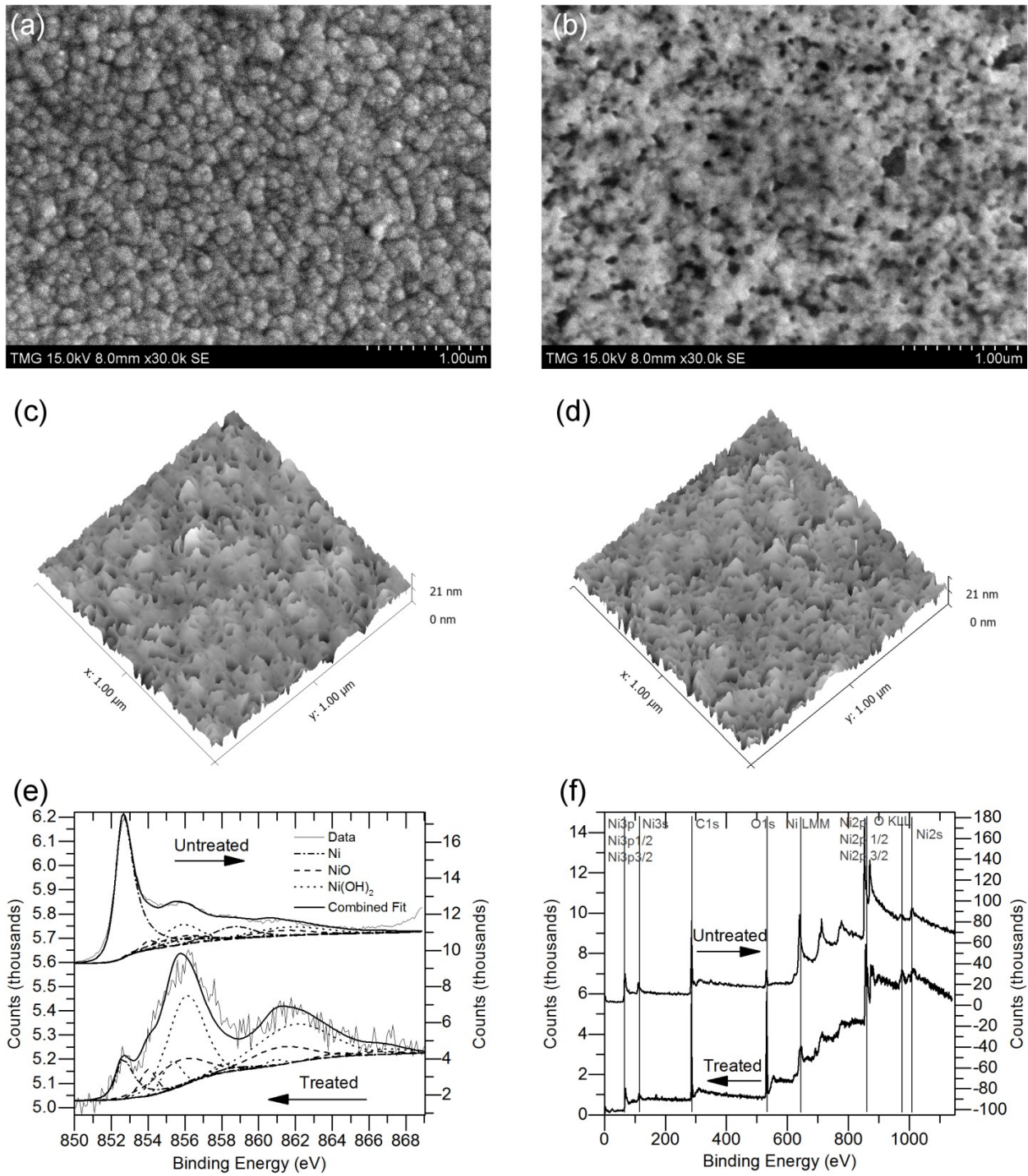
Figure 5.1: Microscopy of samples. a) untreated Ni SEM b) treated Ni SEM c) Untreated Ni AFM (Ra 2.20 nm), d) Treated Ni AFM (Ra 2.17 nm). e) XPS 2p data fit to Ni/NiO/Ni(OH)$_2$ model [16]. f) Wide range XPS data.

Figure 5.2a compares the CVs of untreated nickel with treated nickel. The single anodic peak in nickel (III) is attributed to the oxidation of Ni to α-Ni(OH)$_2$, the cathodic peak IV is its reverse

and wave V is the HER [15, 29, 139]. After the treatment, peak III and Peak IV are still present, but two new anodic peaks are visible. Peak I corresponds to the hydrogen desorption, and can be observed in untreated nickel, if β-Ni(OH)$_2$ is present [15, 23]. The yet unexplained peak has no analogue in untreated nickel to the authors' knowledge (peak II). Peak II is anodic of peak I and cathodic of peak III. This indicates an oxidation of a species that is easier to oxidise than metallic nickel, which would be consistent with the oxidation of the proposed Ni(OH)$_x$ structure. The continued presence of peak III either indicates that the treatment does not exclusively create the Ni(OH)$_x$ structure, or it may be due to the areas of the surface where x=0.
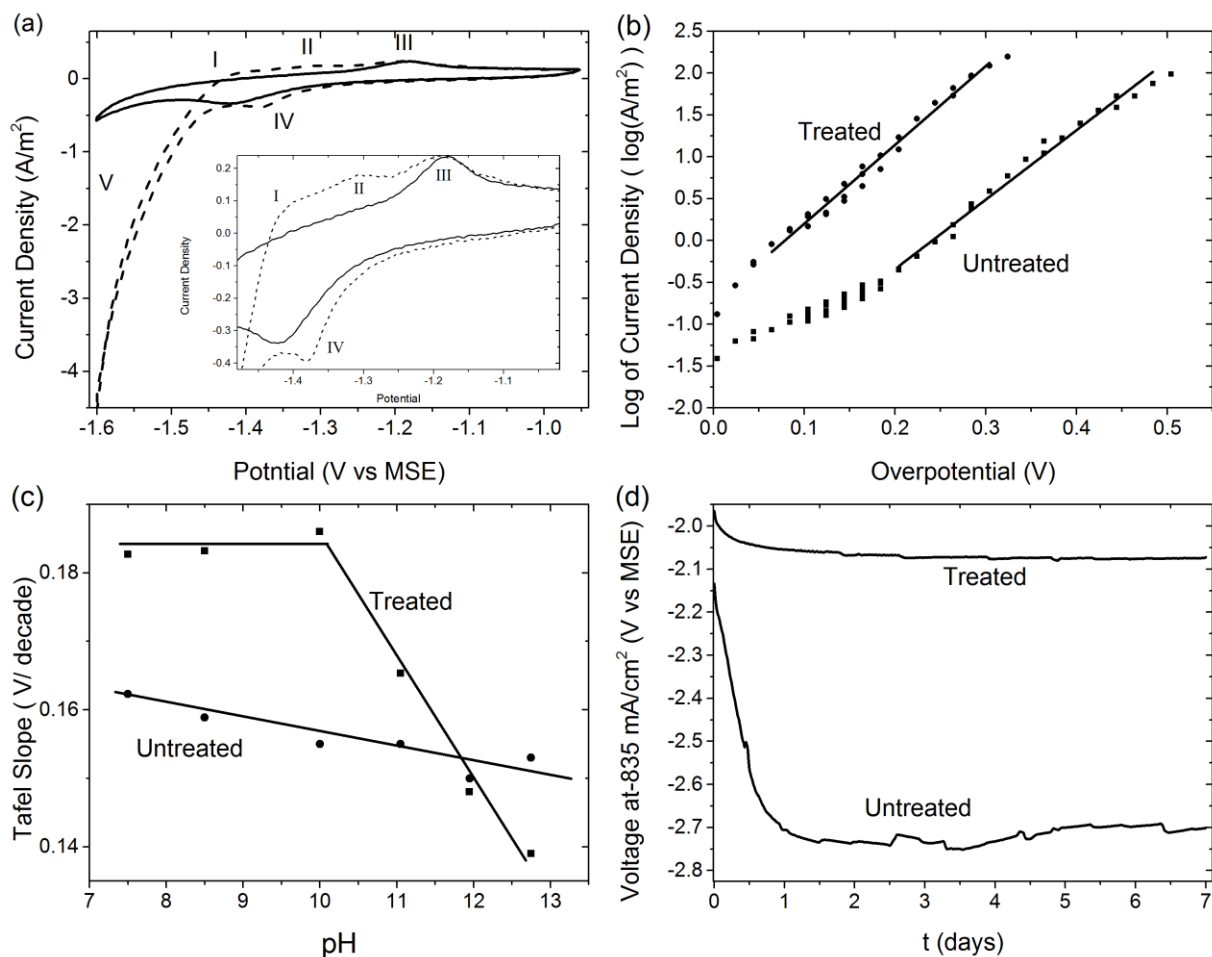
Figure 5.2: Electrochemical characterization: a) cyclic voltammograms of untreated (solid) and treated nickel (dashed) wires where the roman numerals indicate different areas of interest; inset: magnification showing the main anodic peaks b) Tafel plot of the treated and untreated nickel for the HER region; for untreated nickel a Tafel slope of 121 mV/dec and exchange current density of 0.01 A/m^2 was found, which is in close agreement with other work [19, 20]. For the treated electrode a Tafel slope of 106 mV/dec and an exchanged current density of 0.18 A/m^2 was found. c) Relationship between

37

Increased HER activity is already seen in the CVs. To further investigate the activity, the kinetic behavior of the catalysts was evaluated by Tafel plots (Figure 5.2b). The Tafel parameters measured for untreated nickel agree with the literature [5, 52] while the Tafel parameters for the treated surface show the higher activity, with an increase in exchange current density of more than one order of magnitude, and a lower Tafel slope. These results are also in agreement with the catalytic performance in the CVs. Additional polarization curves were done in solutions of various pHs (Figure 5.2c). The treated electrode demonstrates a strong dependence of Tafel slope with pH in contrast with the untreated electrode. This dependence is expected as the treated electrode derives its high activity from a bifunctional effect, the importance of which will decrease with pH (water splitting is only important for alkaline HER [40, 41, 129]).

Since the stability of HER catalysts is important, the treated electrode was tested at high current density of −835 mA/cm^2 (geometric area) for seven days (Figure 5.2d). At the start, the overpotential of the treated electrode was of 0.25 V lower than that of the untreated nickel, which widened to 0.6 V at the end of the experiment. Both treated and untreated stabilized 3 days and little loss of activity was seen after that.

To further investigate the modified Nickel surface, a series of double potential step experiments were undertaken. The aim was to identify the potentials at which there are reactions that modify the surface and affect the rate of HER. Therefore we use the ratio $I(E_2)/I(E_i)$ of sampled currents from the double step experiment. Figure 5.3a shows that when the first step potential E_1 is anodic of −1.3 V the ratio $I(E_2)/I(E_i)$ sharply decreases, indicating loss of activity relative to the start of the double potential step experiment. The value of −1.3 V is just cathodic of the new peak (II) in Figure 5a, indicating that the species oxidised at peak II is responsible for the increase in activity. For values of E_1 cathodic of −1.3 V, there is no significant change in $I(E_2)/I(E_i)$, indicating reduction has no effect on the activity of the electrode. This is consistent with the stability of the treated electrode in the hydrogen region over 1 week in Figure 5.2d as reduction does not affect activity.
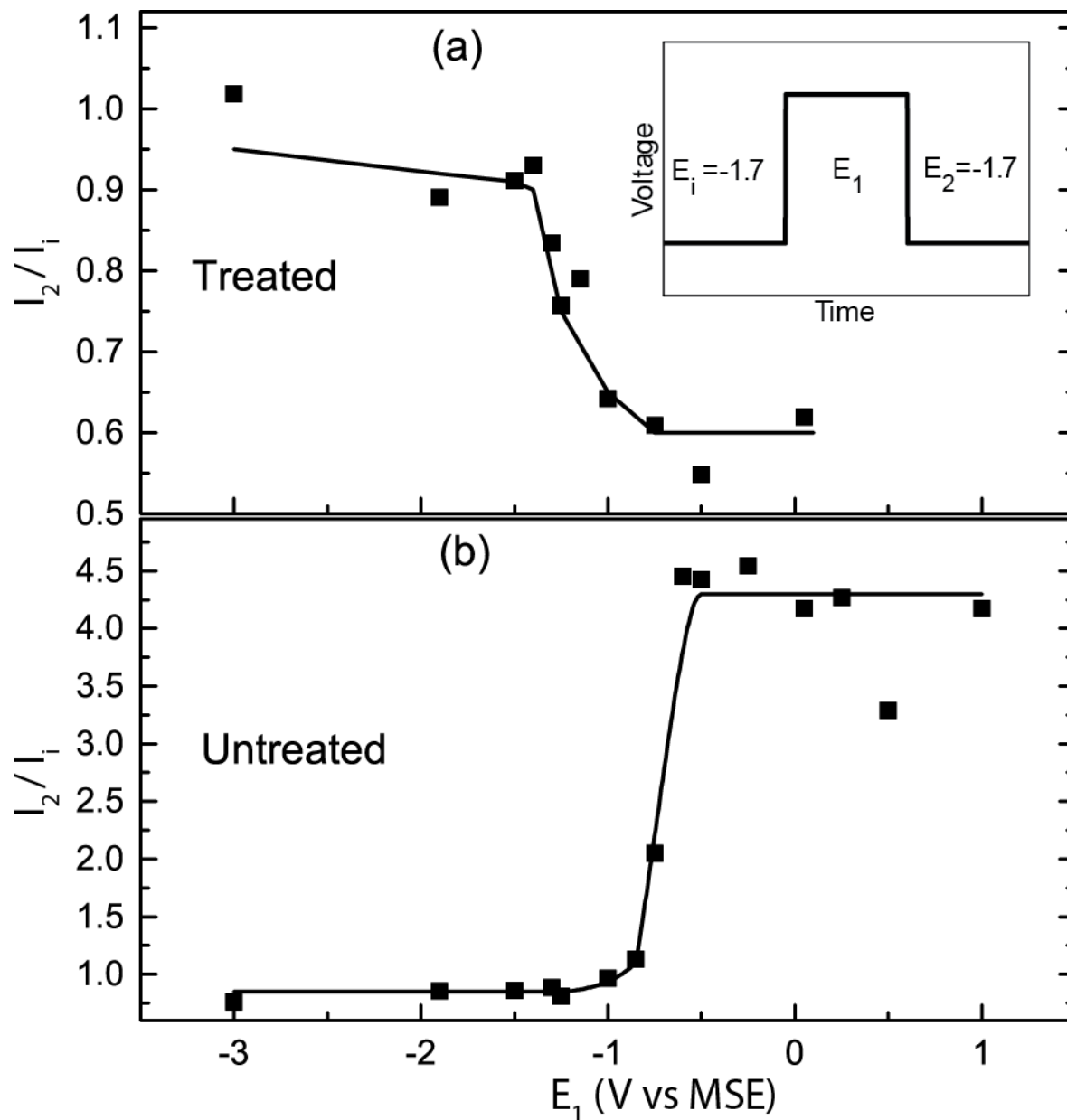
Figure 5.3: Summary of a series of double potential step experiments. The potential begins at $E_i= -1.7$ V, then is stepped to a variable value E_1 where the current is sampled after five minutes, and finally to $E_2= -1.7$ where the current is sampled after five minutes. The ratio of initial to final current, $I(E_2)/I(E_i)$, is plotted along the y-axis against the different values of E_1 (x-axis). The inset shows the voltage waveform.

Untreated nickel shows a totally different pattern. Unlike the treated electrode, nothing significant happens for E_1 anodic of -1.3 V. In fact, in contrast with the treated electrode, there is an increase in the ratio $I(E_2)/I(E_i)$ at E_1 anodic of -0.85 V. Potentials anodic of -0.85 V are the range in which β-Ni(OH)$_2$ forms on Ni [15]. The increase in activity due to the formation of β-Ni(OH)$_2$ has been previously observed [23], and is consistent with the more recent results noted

above from Danilovic [41]. Importantly, this increase in activity is minor compared to the effect of the treatment (40 times the current at -1.7 V vs 4 times). Re-examining Figure 5.3a, E_1 values anodic of -0.85 V have no effect on the treated electrode. If the treated electrode were being modified by the generation of β-Ni(OH)$_2$ some evidence of this should be seen in the ratio I(E_2)/I(E_i) at E_1 values anodic of -0.85 V. This indicates the surface is in a state where β-Ni(OH)$_2$ cannot be formed, such as Ni(OH)$_x$.

5.2.5   Conclusions

We have shown a method to create a highly active and stable HER catalyst from a nickel surface. The method presented is based on our hypothesis of exploiting the slow place-exchange process to create a good dispersion of sites for both the water splitting and combination steps of the HER. Based on SEM and AFM images, the treated surface displayed morphology similar to the untreated material, while at the same time having a significantly higher activity toward the HER (increasing the exchange current density by more than an order of magnitude, and decreasing the Tafel slope). The Ni shows an electrochemical difference post-treatment by the appearance of a new CV peak (peak II in Figure 5.2). Double step polarizations identified this peak as related to the surface species that increased the activity, hypothesized to be a Ni(OH)$_x$ structure. Further work is suggested to fully elucidate the treatment mechanism and resulting surface, and also to investigate other applications: to other reactions that require bifunctionality (e.g. [140, 141]), and to other metals that have place-exchange reactions [134, 136, 142].

5.3   Afterward

5.3.1   Anodic CV

For completion, the anodic side of the CV of the treated electrode is examined here. Figure 5.4 reveals that peaks VI and VII, corresponding to the oxidation of Ni(OH)$_2$ to NiOOH and the reverse [139], completely disappear in the first cycle post-treatment. The shoulder VIII seems to take their place, but after cycling several times the peaks re-appear, and the shoulder remains. Since the surface is expected to be in the proposed Ni(OH)$_x$ phase, there would be no Ni(OH)$_2$ to oxidise to NiOOH, and the reappearance of the peaks indicates that on cycling the electrode will slowly revert to the more traditional hydroxide. Thus, the shoulder VIII is attributed to further oxidation of the Ni(OH)$_x$ structure.
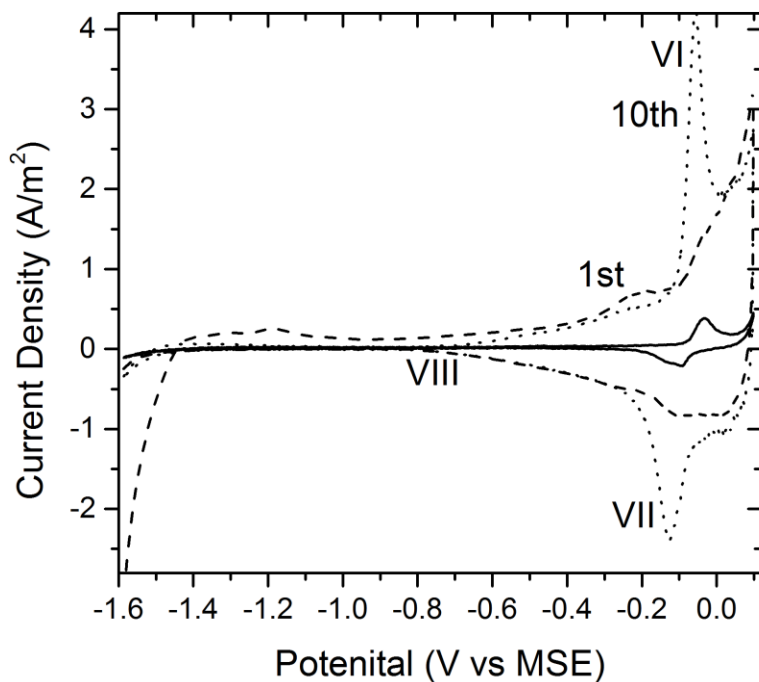
Figure 5.4 CVs going to the anodic side showing untreated Ni (solid), and the first and tenth scan after treatment (dashed and dotted, respectively).

5.3.2 XPS Spectra

Additionally, for more detail, the XPS spectra mentioned in the paper is shown in Figure 5.5. The usual course of analysing XPS data holds that each atom on the surface in a certain chemical state will have a single Gaussian peak associated with it, and the binding energy the peak is at determines what the chemical state is, while the magnitude determines how much of that state there is. To analyse an XPS spectra it is fit to a sum of Gaussians by adjusting their magnitude. However, the fitting the Ni 2p 3/2 region is not quite this text book procedure, as was shown by Biesinger et al [138] where the spectra of Ni, NiO, and $Ni(OH)_2$ are identified. Unlike the described case, the Ni in each of these states actually corresponds to a sum of Gaussian peaks, not a single one. So, the fit is done by adjusting the magnitudes of these sums of peaks, instead of peaks individually. As mentioned in the paper a model for the XPS spectra for $Ni(OH)_x$ is not known (it is novel phase). This is why it cannot be accounted for directly in the analysis, but it can be surmised that the spectra must be similar to $Ni(OH)_2$ Which is why the fit was done for substances which are known, but similar to $Ni(OH)_x$.
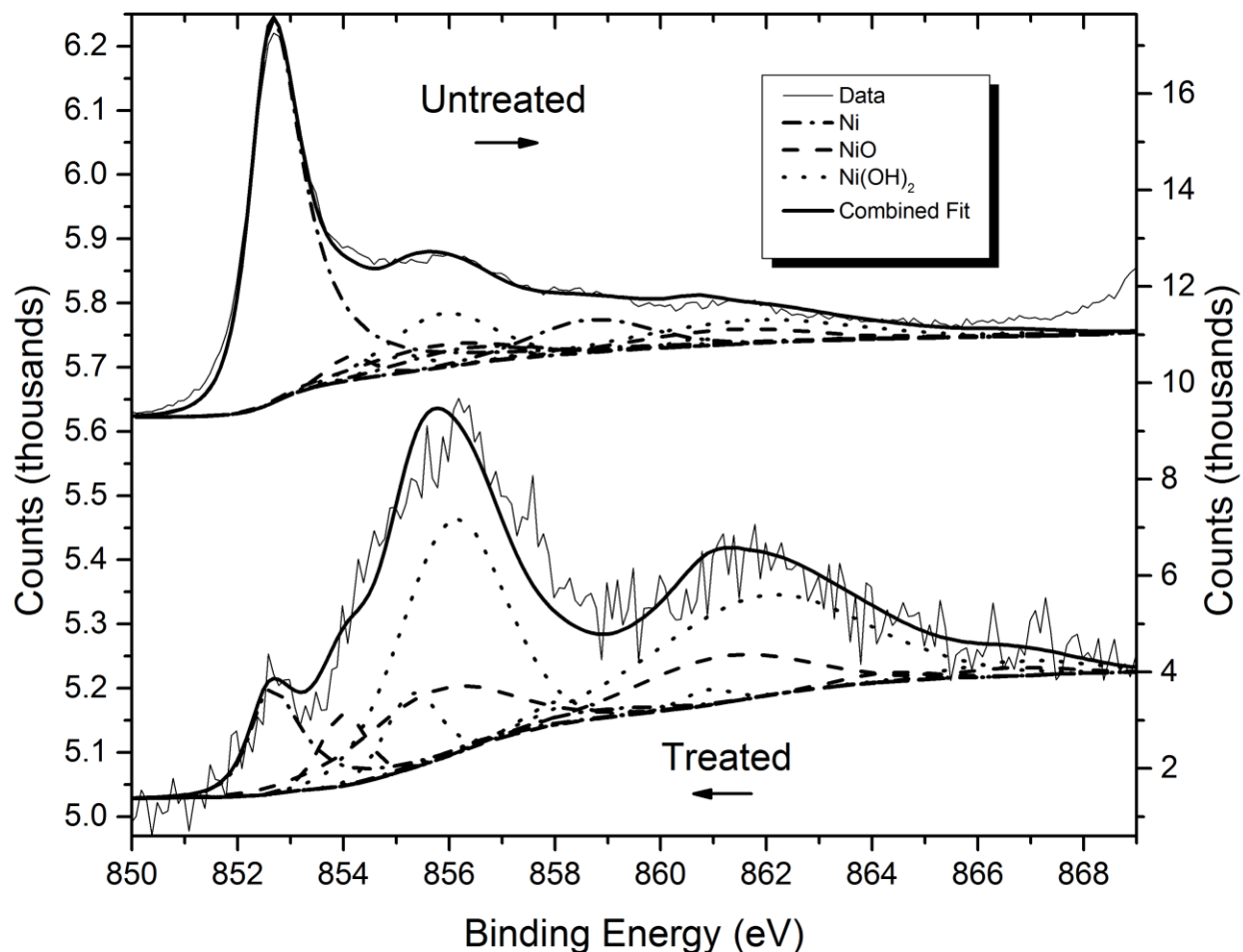
Figure 5.5: The XPS spectra fit as described in the paper presented in this chapter. The percentage of each phase given in the paper corresponds with the percentage the curves for that phase make up in the plot. The lower curve is the treated electrode with 10% Ni, 27% NiO, 63% Ni(OH)2 and the upper curve is untreated nickel with 62% Ni, 14% NiO, 24% Ni(OH)2.

5.3.3 SEM and AFM Images

As mentioned in the article the Ra of the pre and post-treatment surfaces are very similar. The AFM data was analysed using the software Gwyddion [143]. The Ra is the average roughness. Essentially, it is the standard deviation of the height. Higher order statistics such as the skewness (3rd order statistic) or kurtosis (4th order statistic) can also be used to compare surface in quantitative ways. In the case of the AFM data presented in Figure 5.1 the treated surface has a skewness of -0.706 and the untreated has -0.842. Since they are negative the surface has more extreme low values than high values, but there is not much to separate the two. The kurtosis of the treated surface is 0.113 and 0.916 for the untreated. These numbers were computed using the standard that a Gaussian distribute surface would have kurtosis of 0. Positive kurtosis indicates

that the roughness is due to peaks more so than bumps. This parameter shows the largest difference of any of these stats, but they are still very close together. The final statistic that can be interesting is the estimated surface area based on creating triangular polygons out of the points measured by the AFM [143]. In this analysis the 1x1 µm area the treated surface had 1.18 µm^2 of area and the untreated 1.15 µm^2 of area (a 2% difference). So, even in the high order statistic no or little change in morphology can be detected.

5.3.4   The Ni(OH)$_x$ Structure

In the manuscript the Ni(OH)$_x$ structure is described as having x vary from 0 to 2 across the surface, this will be elaborated slightly here. The treatment is burying OH groups at random. In some locations there will be no buried OHs (x=0), and the surface will be metallic nickel. In some locations only a few will have been buried (0<x<2), while in others the saturated amount will be buried (x=2). Values greater than 2 are not considered likely because as more OH groups are added past this it should cause a usual Ni(OH)$_2$ structure to spread, rather than increase the density of OH groups.

5.3.5   Context

The success of the treatment in creating an active and stable HER catalyst is clearly seen in this paper. The treatment increases the exchange current density to 0.18 mA/cm^2 and the Tafel slope is decreased. The evidence also ties the characterization of the treated electrode to the general strategy, and the Ni(OH)$_x$ structure. As noted in the conclusion, the double polarization experiment links the new peak in the CV to the change in the surface which increases the electrode's activity, and this is hypothesised to be Ni(OH)$_x$ because it oxidizes easier than a metallic Ni surfaced. There is also the fact that activity of the treated electrode depends on the pH, which was not directly mentioned in the conclusion of the paper. This is exactly what you would expect from a bifunctional catalyst because bifunctional catalysts are only important for the HER in alkaline solutions.

6 Optimization of the Square Wave Treatment of Nickel to Produce Highly Active Bifunctional Catalyst for the Hydrogen Evolution

6.1 Forward

Although examining one case did provide important and interesting data, the question rises about how to tune the treatment parameters for a given application. Obviously left out of the paper in chapter 5 was the selection process of the parameters for the treatment. In this paper that optimization process is detailed, some of the effects of the treatment at non-optimal parameter are seen.

6.2 The Paper

Optimization of the Square Wave Treatment of Nickel to Produce Highly Active Bifunctional Catalyst for the Hydrogen Evolution

Andrew R.T. Morrison,

Louis Juillac,

Sébastien Guyomart,

Rolf Wüthrich

6.2.1 Abstract

The hydrogen evolution reaction (HER) is important both for its relevance to current industrial electrochemical process and for its potential future use in a renewable energy economy. Recently an electrochemical treatment was reported that modifies a nickel surface to create an electrode that is highly active toward the HER. The treatment was hypothesized to oxidize the nickel in a platinum-like manner creating a $Ni(OH)_x$ surface. Herein the method used to optimize the parameters of the treatment for the resulting electrode's HER activity is presented. The dependence of the activity of the treated electrode surface is very sensitive to the parameters: each parameter has a narrow range from which a highly active surface will result, and the transitions into these ranges are sharp. This offers insights into the mechanism of the treatment. Electrodes treated with optimal and other parameters are analysed electrochemically. The optimally treated electrode is shown to maintain its high activity over the course of long

polarization in more severe conditions (high current density, high concentration, and in a two electrode cell).

6.2.2 Introduction

Alkaline water electrolysis is a mature technology relevant in several industrial fields [9, 11, 12]. Alkaline water electrolysers break water down into hydrogen gas and hydroxide ions at the cathode, the hydrogen evolution reaction (HER). At the anode hydroxide ions are combined to form oxygen gas and water, the oxygen evolution reaction (OER). Industrial electrolysers most often use nickel as a cathode material [5, 10]. Electrolysers' efficiency can be improved by providing a better catalyst for the half reaction that occurs at either electrode. Thus, the industrial relevance of increasing the activity of nickel toward the HER is seen. Further, in the coming years the world will be expected to make a transition to an energy economy based on more renewables [6, 7]. The exact form this future economy will take is still an open question [6], but production of hydrogen via water electrolysis can be expected to play a role if some important challenges are overcome [8]. The creation of cheap (i.e. noble metal free) and effective electrocatalysts has been identified as among the major challenge [6]. Thus, a way to increase the activity of nickel based electrodes towards the HER while avoiding the addition of expensive noble metals would not only benefit a present industry, but could contribute to solving the problem of arranging the future's energy economy.

A significant amount of research has gone into finding highly active nickel based HER catalysts. Traditionally two paradigms are used. The first approach aims to increase the specific surface area of the catalysts. High specific area catalysts can be made by selectively leaching nickel alloys, originally aluminium [59] (Raney Nickel), but later with other metals like zinc [67] or molybdenum [71]. Other examples of high specific surface area electrode fabrication methods are deposition of nickel through a template [78, 80] or onto an already high specific surface area substance [88], but they do not reach Raney Nickel levels of specific surface area. The second approach focuses on attempts to optimise the hydrogen-metal binding energy by alloying Nickel with other metals (originally suggested by Miles et al. [89]) such as Mo [85, 95-97, 144, 145] or W [95, 99, 117]. More recently the importance of having a bi-functional catalyst, favouring the water splitting step in alkaline media, has come to be highlighted [40, 41, 129, 130, 146], particularly the use of $Ni(OH)_2$ as a catalyst for the water splitting step. Within this optic, an

electrochemical treatment for generating a highly active, stable, bi-functional catalyst on nickel was designed [135]. The treatment was developed to generate a catalyst with a high dispersion of the two functional phases. Before that work, high dispersion was challenging as Ni(OH)$_2$ is grown by a Volmer-Webber nucleation and growth mechanism, tending to form islands rather than a high dispersion of phases [38, 136].

Here, the parameter space of this novel treatment is explored. Optimal values are found, and the implications of the form of the parameter space are discussed.

6.2.3 Theory of the Treatment

The treatment aims to create a surface of Ni(OH)$_x$, where x varies across the surface from 0 to 2. Creating this surface with a static polarisation is not possible because oxidation of a nickel surface under a static polarisation creates a layered Ni/NiO/Ni(OH)$_2$ structure [38, 39, 46]. The mechanism for the growth of this structure follows two main paths [35]. In both paths, when anodic polarization begins, the nickel surface Ni$_{(s)}$ is quickly covered with OH$_{ads}$ in

$$Ni_{(s)} + H_2O \leftrightarrows Ni_{(s)}OH_{ads} + H^+_{aq} + e^- \ . \tag{6.1}$$

In the first path the OH$_{ads}$ groups and a surface Ni oxidize into NiOH$^+$$_{ads}$ groups, transitioning to Ni(OH)$_2$ either directly on the surface (by adsorbing another OH$^-$), or via creation of a Ni^{2+} ion and further oxidation in solution. This side of the reaction is formalized by the equations

$$\begin{aligned} Ni_{(s)}OH_{ads} &\rightarrow Ni_{(s)}NiOH^+_{ads} + e^- \\ Ni_{(s)}NiOH^+_{ads} \leftrightarrows Ni_{(s)} + NiOH^+_{aq} &\leftrightarrows Ni_{(s)} + H_2O + N^{2+}_{aq} \\ Ni_{(s)}NiOH^+_{ads} + H_2O &\rightarrow Ni_{(s)} + Ni(OH)_2 + H^+_{aq} \end{aligned} \tag{6.2}$$

The second pathway begins with the OH$_{ads}$ groups participating in the non-electrochemical place-exchange reaction of

$$Ni_{(s)}NiOH_{ads} \leftrightarrows Ni_{(s)}OHNi, \tag{6.3}$$

and is followed by further adsorption of OH$^-$ progressing toward the Ni(OH)$_2$ structure. Eventually the lower layers are converted to NiO (leaving interstitial water as well) via.

$$Ni_{(s)}Ni(OH)_2 \rightarrow Ni_{(s)}NiO + H_2O_i \tag{6.4}$$
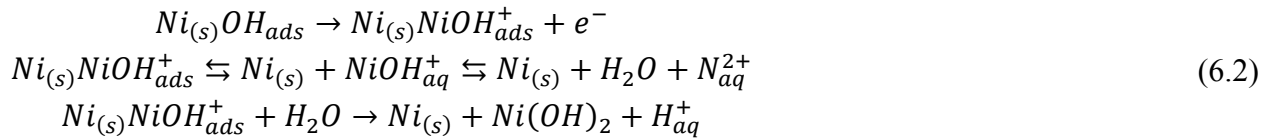
To prevent creation of the usual layered structure, the non-electrochemical nature of reaction (6.3) is exploited by switching the potential quickly. The rate of reaction (6.3) does not depend on the electrochemical potential contrary to (6.2). Thus, applying a reducing potential to the surface after oxidation will eliminate the intermediaries from (6.2), but not the buried OH groups from (6.3) [135].
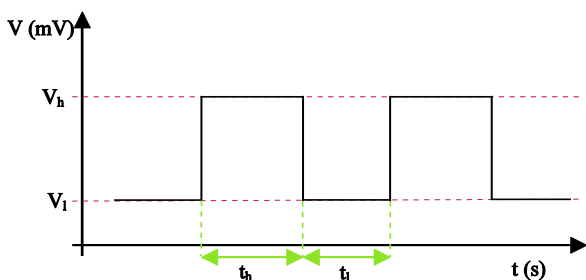
Figure 6.1: Labeled form of a square wave.

Guided by these remarks, a treatment applying a square wave potential (Figure 6.1) is used to create a $Ni(OH)_x$, structure. In each cycle, during the high potential, a few OH groups are buried via the second path of oxidation. During the low portion of the cycle all of the intermediaries from (6.2) are reduced. Thus each cycle adds buried OH groups to the surface. In this way the $Ni(OH)_x$ structure is built successively, each cycle moving the surface a small step toward the proposed structure [135].

6.2.4 Experimental

Experiments were done using an AMEL 7050 potentiostat. Potentials are with reference to the $Hg/HgSO_4$ electrode (MSE) in saturated K_2SO_4. Solutions were prepared using ultrapure deionised water (18 MΩ·cm).

Nickel wires (99.98% purity, Alfa Aeser) of 0.5 mm diameter were used for the working electrode. Before each experiment, the wire was polished using 600 grit abrasive paper (Mastercraft) followed by cleaning with ultrapure deionised water by rinsing. Only a small portion of the wire is exposed to the solution by wrapping all but the tip in PTFE tape. For the initial set of optimization experiments the exposed portion is 4.3mm±0.7mm. For the second set (and all other experiments), the tolerance and length are decreased and a 2mm ± 0.05mm portion of the wire is used. A fresh portion of wire is used for each experiment (to encourage consistent results [29]). Surface area is measured by an electrochemical method based on the charge

47

associated with the formation of a mono-layer of α-Ni(OH)$_2$ on the surface [15]. Surface areas used are always pre-treatment surface area throughout this article, as it is challenging to measure the surface area of Ni electrodes with high coverage of hydroxides; values for surface area measure with high coverage of hydroxides have high error values [137]. This simplification is justified as according to AFM and SEM images of treated surfaces the morphology does not change [135].

The electrode treatment was performed using a variety of parameters of square wave and concentrations of ascorbic acid (C$_{AA}$) and sodium sulphate (C$_{SS}$). The parameters of a square wave are high potential V$_h$, low potential V$_l$, high time t$_h$, low time t$_l$, and duration (L) (as shown in Figure 6.1). Alternately, the time parameters may be expressed as period (T) and duty cycle (D=t$_h$/T). The treatment was performed in a 100ml beaker, always filled with 40ml of solution. In the first set of experiments the electrode positions were not accurately controlled. In the subsequent experiments the working electrode was always placed 5mm below the surface of the electrolyte, the reference electrode within 1mm the working electrode, but not touching. The counter electrode, a high area nickel wire coil, was positioned at the bottom of the beaker, at least 30mm away from working electrode. The working electrode was well rinsed with de-ionized water prior to, and following each treatment.

The primary mode of electrochemical characterization was a polarization at -1.7 V for 5 minutes before and after a treatment. The results of these measurements are summarized in this work by plotting the ratio of current at -1.7 V before to current at -1.7 V after treatment. This is taken to be a measure of the activity. The higher the ratio, the more active the electrode has become following the treatment. This measure of activity is used to optimize the parameters of the treatment. Further electrochemical characterization of the sample consisted of cyclic voltammograms, two step polarizations [13], Tafel plot (chronoamperometry), and long term stability tests in the hydrogen region.

For all further characterization a pre-polarization of −1.7 V for five minutes was applied. For the two step polarization the initial potential was −1.7 V, the first step was to a potential which was varied, and the second step was back to the initial potential at −1.7 V. The electrode was held at each potential for five minutes. The Tafel plots were done by polarizing at each potential for 2 minutes and sampling the current at the end of that 2 minute polarization. A fresh electrode was

treated for every five points on the Tafel plot (to minimize drift from long polarization), and the plots represent a combination of several such experiments. The long term experiments were done in a two electrode cell. All electrochemical characterizations were performed in a solution of 1M KOH (degassed by nitrogen) except the long term polarizations, which were done in 5M KOH. The counter electrode was a high surface area platinum coil, except for the long term polarization, where it was a nickel wire with 10x the geometric surface area as the electrode under study (but otherwise polished and wrapped with Teflon as other electrodes).

6.2.5 Results and Discussion

The results of the first set of experiments, with the aim to explore the parameter space of the treatment, are shown in Figure 6.3 (an example of the chronoamperometry that each point in the figure represents can be seen in Figure 6.2). This first set varied each parameter in the order listed in Table 6.1, starting with the values stated there. Based on the graphs in Figure 6.3, the optimal values within the explored parameter space were determined and are listed in Table 6.2 (referred to throughout as "optimal", though they are only the best found so far, not *strictly* globally optimal). Selection was based on how effective the treatment was, except for duration. For the duration 40 min was selected, as only marginal gains are seen above this value.

Parameter	Initial Value
V_h	−150 mV
V_l	−810 mV
t_h	50 ms
t_l	50 ms
C_{AA}	30 mM
C_{SS}	100 mM
L	40 min (19200 cycles)

Table 6.1 Initial parameters for treatment. The parameters are listed in the order which they are varied during the initial set of experiments.

Parameter	Optimal Value
V_h	−125 mV
V_l	−770 mV
t_h	41.25 ms

t_l	83.75 ms
C_{AA}	24 mM
C_{SS}	200 mM
L	40 min (19200 cycles)

Table 6.2: Optimal parameters, as determined by the initial run of optimization (Figure 6.3) (note: these are not necessarily the globally optimal values, just the best found)
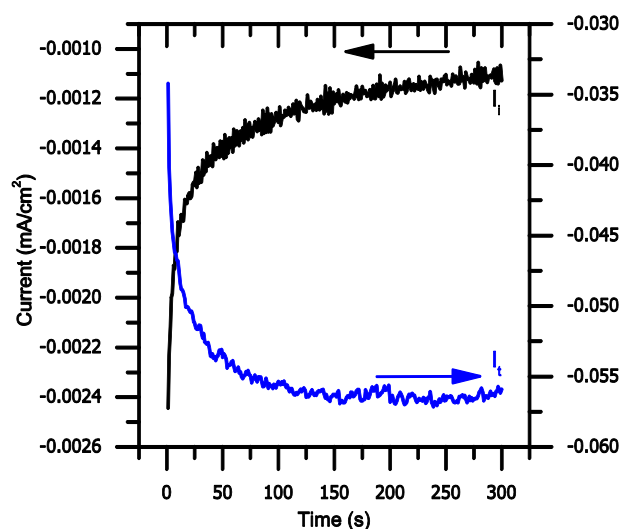
Figure 6.2: An example of a five minute polarization before (black) and after (blue) treatment. (note the different scale on the y-axis) Each point on Figure 6.3 and Figure 6.4 represents an experiment like this, and the treatment in-between. The parameters used for this example were the optimal ones.

There are additional aspects of interest to these initial experiments than the optimal parameters, such as the narrow range of values that produce the optimum for most parameters. For example, for V_h (Figure 6.3 b) the optimal parameter is around -125mV, but just 125mv anodic or cathodic produces an electrode that is at least seven times less effective. The same is true for V_l, the optimal value is -770mV but ±125 mV away results in at least five times less activity (Figure 6.3 a). In fact, a similar pattern can be seen throughout all the parameters studied, except duration and Na_2SO_4 concentration.

To investigate this pattern further a second set of experiments was conducted for selected parameters. In these experiments one or two treatment parameters are tuned away from their optimal values, keeping all other parameters optimal. These experiments also served to indicate that no subsequent improvement to the optimal parameters would be readily found.
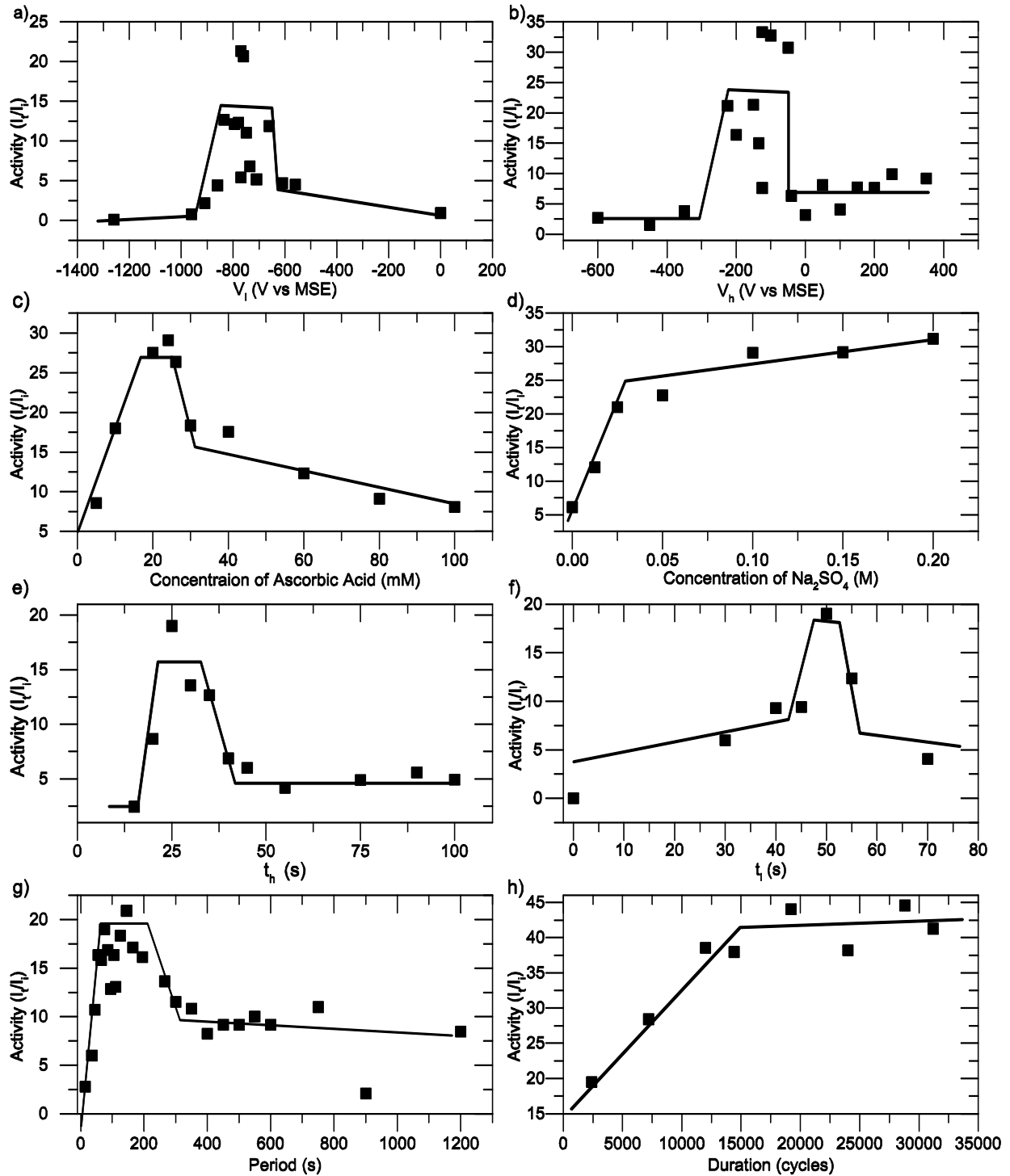
Figure 6.3: Initial pass of parameter exploration. Freely drawn trend lines were added.

The additional set of experiments confirmed the observation that generally each parameter has a narrow range of values for which the treatment produces results near the optimum. In fact, the additional experiments show how sensitive the effectiveness of the treatment is to the

51

parameters. For example, in terms of T, the effectiveness of the treatment rises sharply from T = 0 ms till it reaches a maximum at T = 50ms (Figure 6.4 c). The activity continues at the maximum until T = 175 ms, and then falls to a small value. A similar pattern is seen in the graphs for duty cycle (Figure 6.4 d & e), t_l (Figure 6.4 a) and V_h (Figure 6.4 b). All three graphs have sharp edges between the maximum value attained and surrounding values. The exception is duration (Figure 6.4 f) which has the same continually growing pattern observed in the initial pass of experiments. Figure 6.4 d &e additionally show plots of activity versus duty cycle, but with different values of period for comparison. These graphs illustrate that the parameters are not independent of one another; change the period and the range of values of duty cycle that produce highly active electrodes also changes.

The sensitivity to parameters is expected based on the understanding of the treatment mechanism explained in section 2. In each cycle of the almost 20k cycles that comprise a treatment, a step is taken toward the final structure. If the parameters are such that the step taken is not in the correct direction the surface will never progress toward the structure. Thus the sensitive and binary nature of the activity is explained in a general manner. Explanations for the specifics are discussed below.
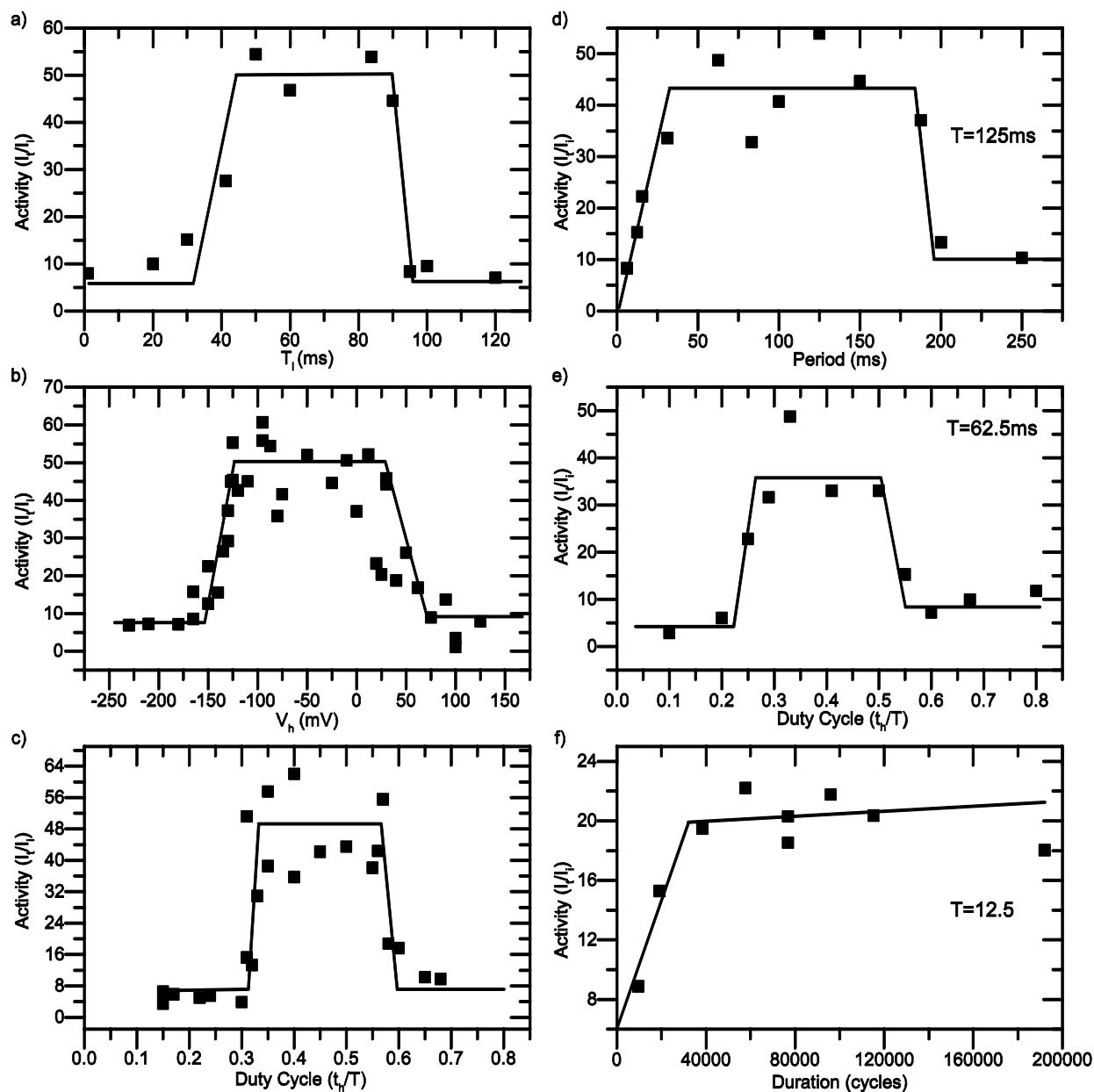
Figure 6.4 The effect of adjusting several parameters away from the optimum parameters a) The effect of low time on the treatment effectiveness (Vh=-125 mV, Vl=-770, t_h= 41.25ms, CAA=24mM, Css=200mM, L=19200 cycles). b) The effect of High Potential on the treatment effectiveness (Vl=-770, D= 33%, T=32.25 ms CAA=24mM, Css=200mM, L=19200 cycles). c) The effect of period on the treatment effectiveness (V_h=-125 mV, V_l=-770, D=33%, C_{AA}=24mM, C_{ss}=200mM, L=19200 cycles). d) and e) The effect of Duty Cycle on the treatment effectiveness (Vh=-125 mV, Vl=-770, T= as labeled in figure, CAA=24mM, Css=200mM, L=19200 cycles). f) The effect of Duration on the treatment effectiveness (A: Vh=-125 mV, Vl=-770, D= 33%, T=(A:32.25 ms ,B: 12.5ms), CAA=24mM).

To start, the reasons why certain parameters result in poor increase of catalyst activity are broadly divided into two categories: oxidation biased (e.g. V_h too high, t_l too low, etc.) and reduction biased (e.g. t_l too high, V_h too low etc.). Interpreted through the theory in section 2, it can be seen that when the treatment parameters are oxidation biased the unwanted

53

intermediaries, from reaction (2), are allowed to build up cycle to cycle. This inexorably leads to a Ni surface with a traditional hydroxide structure on it. For reduction biased parameters all, or too many, of the OH groups are removed during the low portion of a cycle. Further, keeping the surface free of hydroxides should promote the dissolution of the nickel [147]. If the surface is dissolving fast enough, the $Ni(OH)_x$ structure cannot develop as the surface is continually stripped away. To probe this further, the radius of the electrode was measured before and after a treatment for different parameters using a 36 hour treatment duration. It was found that reduction biased parameters dissolve the electrode (decreasing the radius by 0.15 mm in 36 h), while optimal and oxidation biased parameters do not have a measurable effect on the radius in that time.

Categorizing poorly performing parameter sets into oxidation or reduction biased only accounts for parameters that directly affect the amount of oxidation or reduction occurring in a single cycle. Parameters that do not have this direct effect are the concentration of Na_2SO_4, cycle period, and treatment duration. The treatment duration is the simplest to explain. For short durations, the structure has not completely covered the surface. For long durations there is no observed decrease in effect because the treatment reaches equilibrium once the structure is fully built.

The effect of the concentration of Na_2SO_4 is discussed next. First note that since the treatment is sensitive to the parameters, non-uniform electric fields over the surface of the electrode will also reduce the effectiveness of the treatment. This is because only a portion of the electrode surface will actually be subject to the specified parameters. A higher conductivity of electrolyte will increase uniformity of field due to reduced electrical resistance of the solution and consequently improve the treatment efficiency. Since Na_2SO_4 does not interact with the electrode surface at these potentials [35], no further effects are expected from the concentration of Na_2SO_4. Indeed this is seen in the results, when the concentration of Na_2SO_4 is increased, the effectiveness of the treatment increases (Figure 6.3 h). The effect can also be seen when treating large nickel electrodes where the field is less likely to be uniform over the entire surface. Experiments showed that the treatment on longer wire electrodes was less effective.

Cycle period is the only one of the three non-categorized parameters that shows poor performance for both too high and too low values. For very short periods, the problem is that

there is not enough time for any relevant reaction to occur on the surface, except double layer charging and discharging. For long periods, the surface will start to take on its steady state structures. During high potentials islands of standard $Ni(OH)_2$ will form. They will be reduced (fully or partially) at the low potential, but the damage will have been done. Any location where an island forms will have its $Ni(OH)_x$ structure converted to $Ni(OH)_2$. The nucleation sites of these islands will move cycle to cycle, so no location will have time to develop the $Ni(OH)_x$ structure.

A final interesting observation from all these experiments is that, even for parameters that show poor treatment results, there is still an apparent increase in nickel activity. Nickel naturally forms a $Ni(OH)_2$ layer under multiple conditions. It is reasonable to suggest that when the treatment does not have the desired effect, a $Ni(OH)_2$ layer still forms. Thus, the mild increase in activity is consistent with the increase in activity that is expected for the presence of $Ni(OH)_2$ as noted in[23] and expected from [41].

Properties of the optimal parameter treated surfaces were further examined. First polarization curves (Figure 6.5) were recorded. The treated electrode was found to be a substantial improvement on the untreated, both in terms of exchange current density (18 times higher), and a lower Tafel slope. The lower Tafel slope indicates a change in the mechanism of the HER. This was expected due to catalysis of the water splitting reaction. As the potential is increased outside of the Tafel region, the difference between the treated and untreated catalysts becomes less pronounced, but is still significant. This is important for practical applications where the current will generally be higher than the Tafel region.
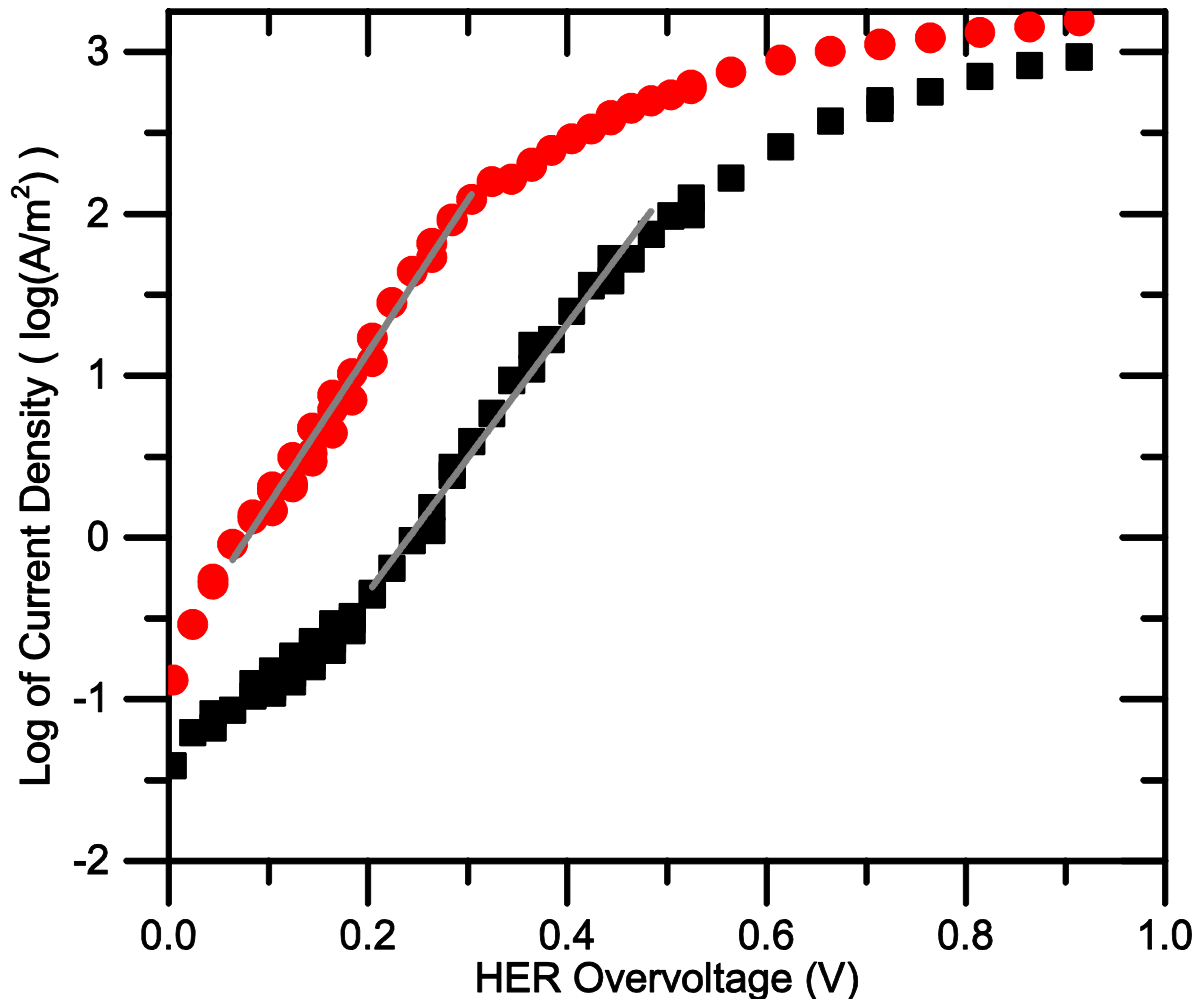
Figure 6.5: Polarization curve of treated (red) and untreated nickel (black), with fits of the Tafel region shown (blue). For untreated nickel a Tafel slope of 121 mV/dec and exchange current density of 1e-2 A/m^2 (which is in close agreement with [5, 52]). For the treated electrode a Tafel slope of 106 mv/dec and an exchanged current density of 0.18 A/m^2.

The cyclic voltammogram (Figure 6.6 a) for the treated electrode was explained in previous work [135]. Peak I represents the hydrogen desorption (which is visible in untreated nickel, with β-Ni(OH)$_2$ present [23]), peak II is unique to the treated electrode, peak III is oxidation of Ni to Ni(OH)$_2$, peak IV is the reduction of Ni(OH)$_2$ to Ni, and current wave V is the hydrogen evolution. Figure 10b shows CVs for two other electrodes, one treated with oxidation biased parameters (V_h=75 mV), and one treated with reduction biased parameters(V_h=-175 mV). The electrode treated with reduction biased parameters has a CV that is essentially identical to untreated nickel. This is unsurprising, the treatment at these parameters is dissolving the surface, and keeping the surface free of hydroxide build up, hence no new reactions. The CV for

oxidation biased parameters on the other hand show the emergence of peak I. This is expected on an electrode that has a hydroxide layer, as noted above [23].
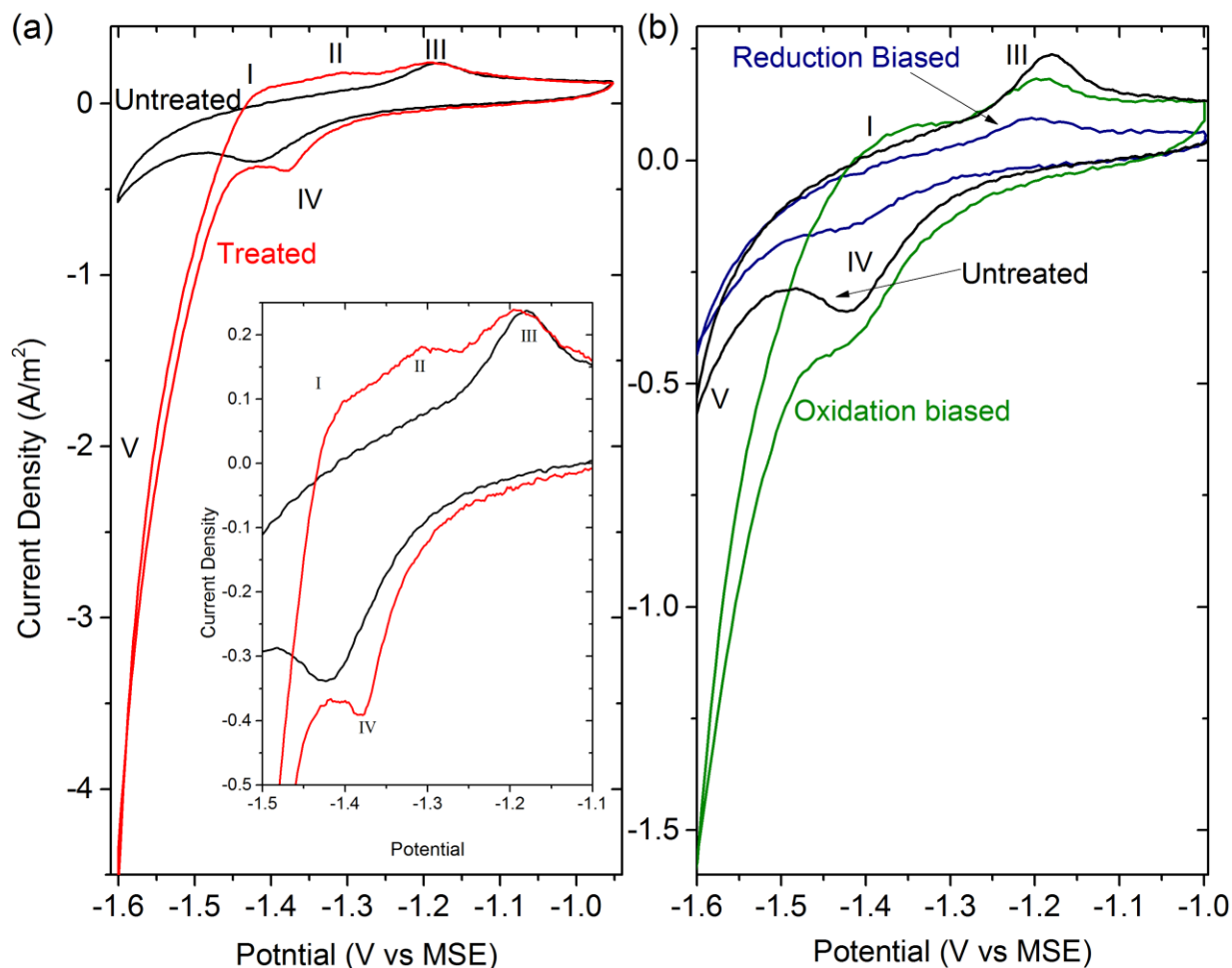
Figure 6.6 a) CV of nickel electrode treated with optimal parameters (red) and an untreated nickel wire (black) b) CVs of nickel electrode treated with oxidation biased (red) and reduction biased(black). Scan speed in both 10 mV/s.

To further elucidate peak II observed in previous work [135], double potential step experiments were done with parameters that are on the edge of being optimal (V_h=50mV; Figure 11). The double potential step experiment for these parameters shows a combination of the features from the treated and untreated electrodes. There is the decrease in the $I(E_2)/I(E_i)$ ratio for E_1 anodic of -1.4 V that corresponds with the oxidation the $Ni(OH)_x$ structure. There is also the increase in the ratio for E_1 anodic of -0.8V that is seen in untreated nickel, corresponding to the creation of β-$Ni(OH)_2$. This is consistent with the hypothesis that the structure on the surface of catalysts treated with parameters that are on the edge of the optimal region is both traditional Ni and the $Ni(OH)_x$.
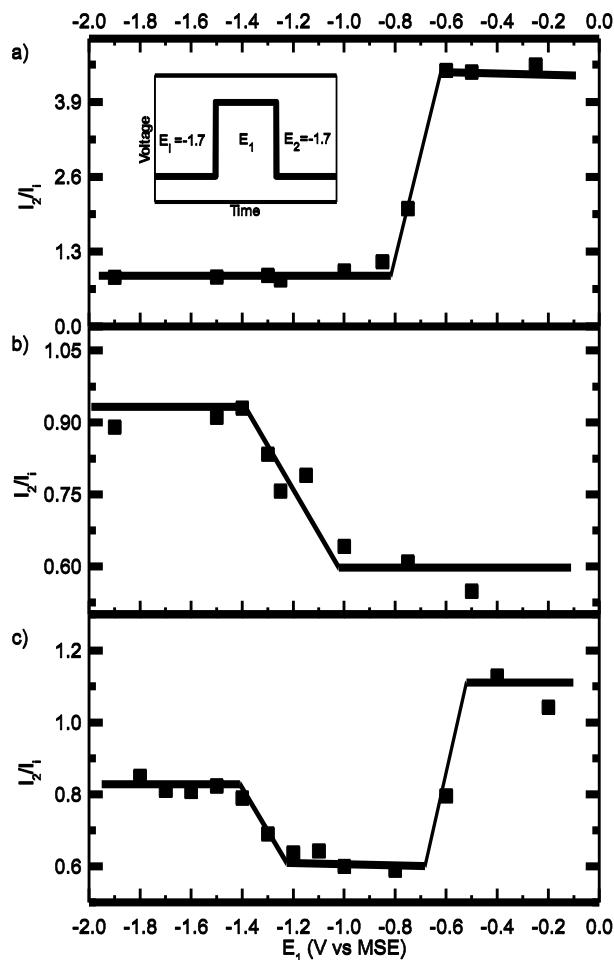
Figure 6.7 Summary of double potential step experiments (the inset shows the potential profile for this experiment), normalized as explained in the experimental section: A: Untreated Nickel, the edge at 0.7 V corresponds with creation β-Ni(OH)$_2$ [15, 23] B:Treated nickel, the edge is thought to correspond with the oxidation of Ni(OH)$_x$ [135] C: Off-standard parameters, note how they are a combination of treated and untreated (V$_h$ = 50 mV all other parameters standard).

Finally, to see treated electrodes in more realistic conditions, long term polarizations at high current densities were done (Figure 6.8). Note that a two electrode cell was used for this experiment, so part of the potential comes from the counter electrode (i.e. part of the loss of activity will be on the anode). The untreated electrode loses activity rapidly over the course of 2 days increasing the cell voltage by 0.3 V to stabilize at 3 V. The treated electrode loses activity quickly for half a day increasing by 0.125V to stabilize at 2.65V. This experiment was also done on electrodes treated with oxidation and reduction biased parameters. For oxidation biased parameters the cell voltage starts lower than the untreated electrode, but within a day it increases to a level similar to the untreated electrode and stays there for the duration. This could be because the hydroxide layer created by the oxidation biased parameters (hypothesized to be β-Ni(OH)$_2$) is totally reduced within a day, while the Ni(OH)$_x$ layer is more stable. The electrode

58

treated with reduction biased parameters shows a very similar pattern to the treated electrode, except shifted up by 175 mV. This could be because small islands of Ni(OH)$_x$ on the surface are sufficient to have some effect on cell voltage, these islands could exist for reduction biased parameters close to the active region.

The treated electrode gains 14mV/day of cell potential. This gives stability of a level to be useful above an untreated electrode for multiple weeks at this current density (and perhaps longer at lower densities). Importantly, the treatment process is repeatable on the same electrode. After 12 days of polarization, the treated electrode was retreated with the same parameters, and returned to the two-electrode cell. The cell potential of the retreated electrode was very similar to the activity of the first experiment for that electrode.
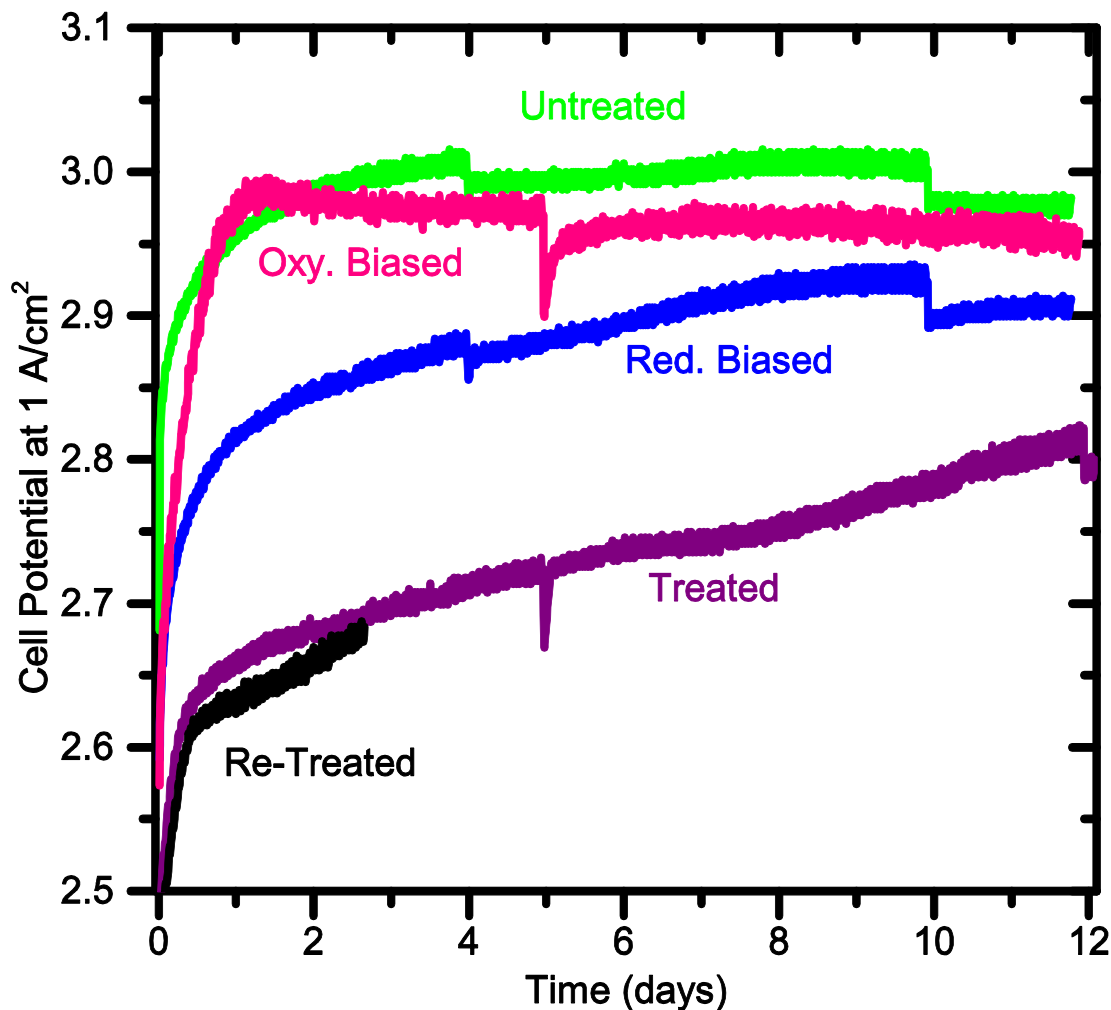
Figure 6.8 Long term stability in 5 M KOH at 1A/cm^2 (geometric) with curves from a treated wire, an untreated wire, a wire treated with oxidation biased parameters (oxy. biased), a wire treated with reduction biased parameters (red. biased), and the treated wire re-treated (all labeled on plot). The discontinuities are from the introduction of fresh KOH into the cell. Note that the cell potential is a two electrode potential.

6.2.6 Conclusions

An efficient experimental method was used to explore optimum parameters for use during the square wave treatment of nickel for increasing its activity toward the hydrogen evolution. Optimal parameters were determined. These values produced a stable, highly active HER catalyst (an order of magnitude increase). Additional exploration of the parameter space failed to find better values than the initially determined optimal parameters.

Further, the optimization procedure yielded valuable evidence for the nature of the treated surface. Most parameters have a narrow range where the treatment yields results comparable to the optimized results. Further investigation in some parameters showed that there are sharp edges

60

to the ranges where good results can be obtained (producing a nearly binary plot of effectiveness vs treatment parameter). This sensitivity to the parameters supports the previously hypothesized mechanism of the treated which results in the $Ni(OH)_x$ structure where OH groups are incorporated cycle by cycle. The hypothesised mechanism was also used to explain the effect of parameters being out of the acceptable range primarily by considering the ratio of oxidation to reduction occurring.

6.3   **Afterward**

6.3.1   **Context**

The process by which the optimal parameters were determined was presented, and further evidence on the stability of the treated electrode was seen. The stability was seen to be imperfect, but still good, lasting several weeks. However, treated electrodes may be re-treated to recover their activity, which is relevant to considerations of their stability. The selection process for the parameters of the treatment was simple brute force optimization. The initial parameter selection was an educated guess based on the reactions required to occur during the treatment. However, the overall parameter-activity space takes a shape consistent with the theory of the treatment strategy. The activity of treated electrodes was seen to be very sensitive to treatment parameters, and have quite narrow ranges of parameter values that produce high activities. Additionally, the characterization of electrodes treated by oxidation or reduction biased parameters was seen to be quite different than electrodes treated with optimal parameters, which is expected since their surface chemistry is changing (or not changing) in different ways.

6.3.2   Other Reactions and Metals

As mentioned in section0, the applicability of the treatment to other metals and reactions would be not be surprising. However, finding the correct parameters would be required (as was done for the HER in this chapter). In fact some limited success has been obtained with the treatment on Co, as can be seen in Figure 6.9. Not unexpectedly, the parameters needed to treat Co are very different from Ni.
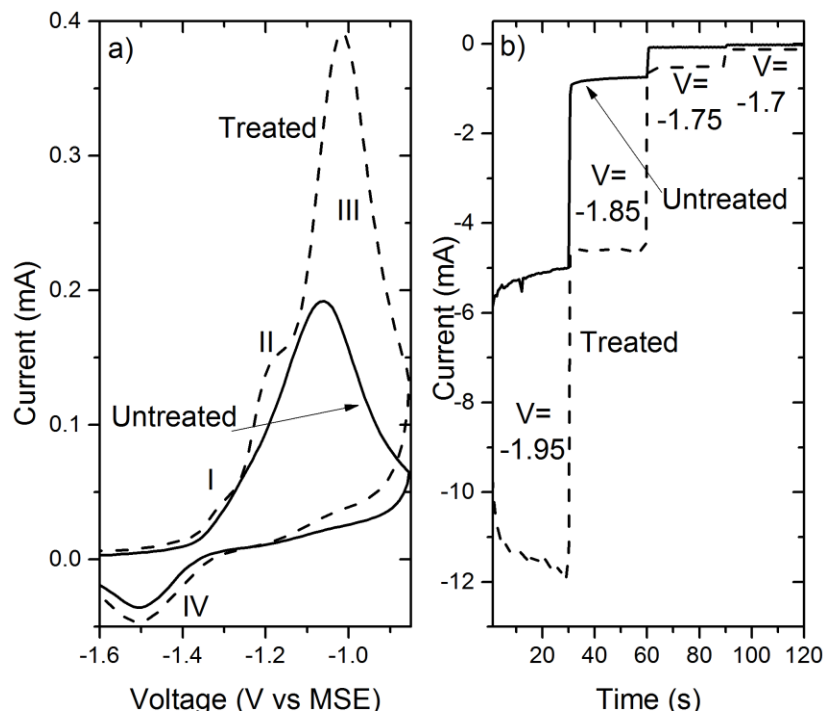
Figure 6.9: The effect of using a square wave treatment on Co in 1 M KOH. The solid line is before treatment, and the dotted line after. There chronoamperometry clearly shows increased activity, and the CV shows a new peak (II). The treatment parameters were: V_h=-850 mV, V_l=-1600 mV, T=125, Duty Cycle=33%, L= 5760000 cycles.

This represents only initial results, as a proof of concept. More may be possible especially when combined with on-line monitoring (see section 8.3). Another proof of concept is seen in Figure 6.10, the results of an optimally treated Ni being used as a nitrate reduction electrode (along with an untreated electrode for comparison). There is a clear benefit to using the treated electrode, but again this is simply a proof of concept. It is expected that further improvement is possible.
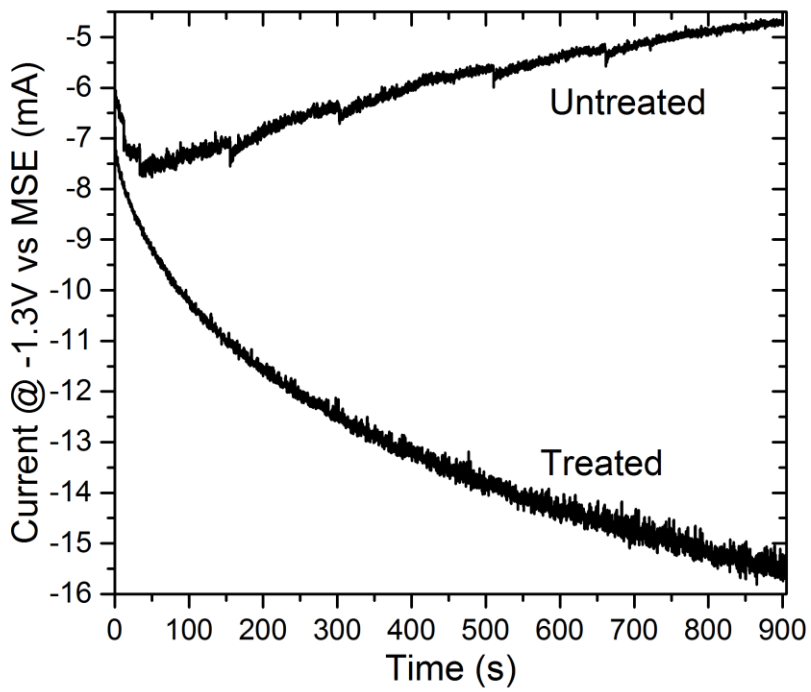
Figure 6.10: A comparison with an optimally treated electrode and an untreated electrode for the nitrate reduction.

7 Electrooxidation of Urea with Square Wave Treated Nickel Catalysts

7.1 Forward

In the afterward of the previous chapter (chapter 6), the applicability of the treatment toward a non-HER reaction is shown: the nitrate reduction. The nitrate reduction is similar to the HER in one respect, they are both cathodic reactions. This chapter more fully explores the possibility for using a treated electrode as an anode, specifically for the Urea electrooxidation.

7.2 The Paper

Electrooxidation of Urea with Square Wave Treated Nickel Catalysts

Andrew R.T. Morrison,

Rolf Wüthrich

7.2.1 Abstract

Urea is a harmful pollutant found in the wastewater of some industry and common sewage. In the past few years there has been interest in the urea electrooxidation reaction (UOR) because it not only addresses the pollutant problem, but could also allow the more efficient production of hydrogen through electrolysis. A recently designed electrochemical treatment for creating highly active hydrogen evolution electrodes is tuned to create high activity catalysts for the UOR. The properties of these catalysts are examined, and it is found that their high activity toward the UOR is due to fast regeneration of the sites active toward the UOR. This fast regeneration is hypothesized to be due a surface structure where highly active sites are surrounded by areas for urea and products to adsorb, preventing them from blocking the active sites.

7.2.2 Introduction

The urea electrooxidation reaction (UOR) has a wide variety of applications among them wastewater treatment. Urea makes up a large portion of wastewater coming from industrial Urea production plants, as well as common sewage [148, 149]. Urea naturally slowly breaks down into CO_2 and Ammonia [150, 151]. Ammonia is undesirable in the environment [152]. Urea containing waste water can be treated electrochemical, to prevent the production of Ammonia, and also to produce hydrogen gas at the same time [153-160]. In fact, urea rich alkaline solutions

can be used in an alkaline water electrolyser to reduce the cell potential required for electrolysis, therefore improving the efficiency over tradition alkaline water electrolysers [161]. UOR also plays an important role in urea sensors [162], artificial kidneys [163], and urea fuel cells [164].

The overall UOR on nickel in alkaline solutions is [158-160]:

$$CO(NH_2)_{2(aq)} + 6OH^- \rightarrow N_{2(g)} + 5H_2O_{(l)} + CO_{2(g)} + 6e^-. \qquad\qquad E^0 = -0.46\ V \qquad\qquad (7.1)$$
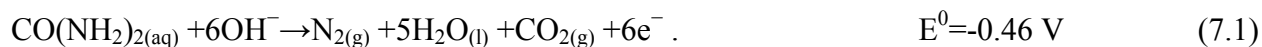
Other reaction products are possible, producing nitrates and ammonia, depending on the electrode material, current density and solution composition [153-155], but these products are not seen on nickel [161]. Nickel based catalysts for UOR has been studied in several different forms, and have seen a surge in interest in recent years. There have been several studies on UOR electrodes including on electrodeposited layers of nickel and Ni-Co alloys [160, 165], $Ni(OH)_2$ powders and nanostructures [157, 166, 167], multi-metallic catalysts[156, 160], Ni deposited on grapheme [168], nickel with other metallic deposits or nanostructures [156, 169].

In addition to different catalysts, the details of the mechanism on nickel have also been investigated. The UOR on nickel has been known to be catalysed by the generation of the NiOOH on the surface [161]. In fact, it has been shown that this overall reaction likely goes by an indirect route and can be broken down into two steps [158, 159]. The first step is the electrochemical oxidation to nickel oxyhydroxide. This is followed by the chemical oxidation of the urea, the by-product of which is reducing the surface back to $Ni(OH)_2$. The $Ni(OH)_2$ is again electrooxidized, and the process repeats:

$$Ni(OH)_{2(s)} + OH^- \rightleftharpoons NiOOH_{(s)} + H_2O_{(l)} + e^- \qquad\qquad (7.2)$$

$$6NiOOH_{(s)} + CO(NH_2)_{2(aq)} + H_2O_{(l)} \rightarrow 6Ni(OH)_{2(s)} + N_{2(g)} + CO_{2(g)} \qquad\qquad (7.3)$$
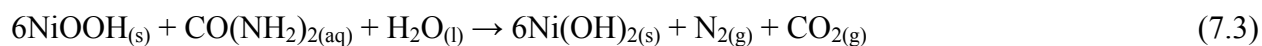
The regeneration of $Ni(OH)_2$ to NiOOH is an important step in the reaction. A limiting factor may be the blocking of these sites by Urea, or UOR products [158, 159], possibly CO [156, 169, 170], which makes the regeneration step the limiting step of the reaction. Promoting the regeneration step, by preventing or limiting blocking of the active sites, explains the effectiveness of catalysts comprised of Ni combined with other materials (e.g. bimetallic catalysts or Ni on graphene [165, 168]), and the higher activity seen when potential cycling [171]. However, a pure nickel catalyst that is capable of this has never been reported so far.

65

Recently, an electrochemical treatment has been demonstrated to increase nickel's activity toward the hydrogen evolution [135]. The effect of the treatment is primarily an electrochemical surface modification. It yields a surface that is a well-mixed, bifunctional catalyst for the HER [135]. The structure of the treated surface is thought to be a novel $Ni(OH)_x$ structure (with x varying between 0 and 2). The treatment itself consists of rapid cycles of oxidation and reduction, applied to the surface as a carefully tuned square wave voltage waveform. The treatment shows great sensitivity toward the parameters of the square [172]. The UOR concerns potentials more anodic to those of the HER, but the initial impression that thus it would be unuseful for the UOR is not correct. The bifunctional nature of the treated nickel surface will tend to prevent blocking of active sites, so the treated surface should show a much faster regeneration of these sites. Second, the treated surface is active toward water splitting (indeed this is what makes it an active HER catalyst), and equation (7.3) shows this is a required part of the UOR. In this paper the use of square wave treated electrodes for the UOR is investigated by synthesising treated nickel wires, and performing electrochemical characterization in the UOR region.

7.2.3   Methods

Experiments were done using an AMEL 7050 potentiostat. Potentials are with reference to the Hg/HgO electrode in 1 M KOH, except the potentials of the treatment which are with reference to $Hg/HgSO_4$ electrode (MSE) in saturated K_2SO_4. Solutions were prepared using ultrapure deionised water.

Electrode preparation was done following our previous work [135, 172]; described here again for connivance. Nickel wires (99.98% purity, Alfa Aeser) of 0.5 mm diameter were used for the working electrode. Before each experiment the wire was polished using 600 grit abrasive paper (Mastercraft) followed by cleaning with ultrapure deionised water by rinsing. Only a small portion of the wire is exposed to the solution by wrapping all but the tip in PTFE tape (2mm ± 0.05mm). A fresh portion of wire is used for each experiment. Surface area is measure by an electrochemical method based on the charge associated with the formation of α-$Ni(OH)_2$ [15]. Surface areas used are always pre-treatment surface area throughout this article as it is challenging to measure the surface area of Ni electrodes with high coverage of hydroxides [137].

This simplification is justified as according to AFM and SEM images of treated surfaces the morphology does not change [1st].

The square wave treatment was performed using the procedure explained in our previous work [135, 172] with the parameters of the square wave being high potential V_h of -200 mV, low potential V_l of -770 mV, high time t_h of 41.25 ms, low time t_l of 83.75 ms, and duration L of 40 min (19200 cycles). The treatment was performed in a 100ml beaker, always filled with 40ml of solution. The solution was 24 mM of ascorbic acid and 200 mM of sodium sulphate. The working electrode was always placed 5mm below the surface of the electrode, the reference electrode within 1mm the working electrode, but not touching. The counter electrode, a nickel wire coil, was positioned at the bottom of the beaker, at least 30mm away from the working electrode. The working electrode was well rinsed with de-ionized water prior to, and following each treatment.

The electrodes were characterized by cyclic voltammetry, sampled current voltammetry, and chronoamperometry. For sampled current voltammetry the current was sample after 30 s at a given potential. Two types of chronoamperometry were done, a long term stability test of 12 h, and a short term experiment of 5 minutes. The short term polarization were used as in previous work [172]to get a measure of activity increase toward the reaction by dividing current before by current after the square wave treatment at the potential of interest. The potential of interest for UOR is -0.05 V. Similar experiments for the HER are presented as comparison, and for those the potential of interest is -1.7 V. Electrochemical characterizations were performed in a solution of 5M KOH (degassed by nitrogen) with and without sometimes 0.33 M urea, which is the same concentration as in urine (where one possible application for this study lies [161]). The counter electrode was a high surface area platinum coil.

7.2.4 Results and Discussion
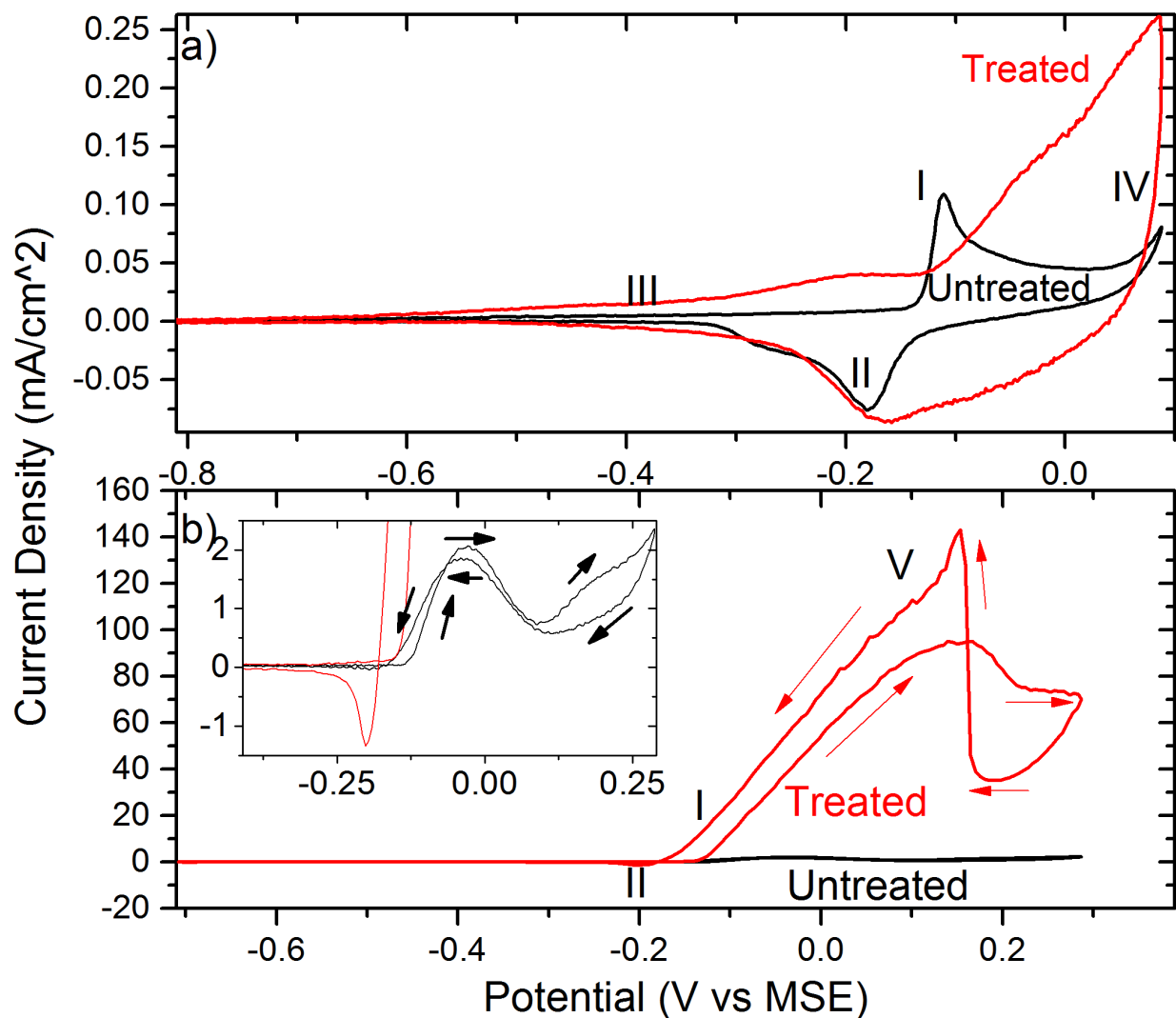
Figure 7.1: CVs of treated (red) and untreated nickel wires (black) in a solution of 5 M KOH (a) and in a solution of 5 M KOH and 0.33M Urea (b).

Figure 7.1 shows the cyclic voltammograms for a nickel wire of treated/untreated with and without urea. In the urea-free solution for untreated nickel, peak I is the conversion of nickel hydroxide to nickel oxyhydroxide, and the reverse reaction is peak II. At IV the oxygen evolution reaction (OER) occurs. This reaction is enhanced on the treated electrode. Also, on treated nickel there is an additional shoulder/peak combination in the CV at III that is not as well understood as the traditional nickel CV peaks, but is proposed to be the further oxidation of the $Ni(OH)_x$ structure. As the treated electrode is cycled in the KOH solution peak I and II will re-grow.

There are several differences for the CVs conducted in electrolyte with Urea. In the forward scan (cathodic to anodic) there is a much larger anodic peak at I that is associated with the UOR [161]. The current then decreases before increasing again for the OER. This behavior occurs because the UOR and the OER compete for the same active sites on the electrode (through the competition between OH^- and urea [170]). In the reverse scan there is again an anodic peak at I, which is the UOR. Finally, there is a lessened cathodic peak at II. The cathodic peak is still the reduction of NiOOH to $Ni(OH)_2$, but in the presence of Urea the peak magnitude is lowered. This is because as part of the UOR NiOOH is constantly being reduced to $Ni(OH)_2$ (equations 7.2 and 7.3). When the potential is decreased only those sites going through the NiOOH part of the reaction will contribute to the peak's current.

The most obvious difference between the CV for the treated and untreated electrodes in the presence of urea is that the treatment does indeed significantly increase the current in the UOR region. As noted, the UOR has an onset potential corresponding with the peak I, and this does not change for the treated electrode. This indicates that III is not associated with a reaction forming NiOOH on the surface, or the Urea oxidation should begin sooner. Thus, the treated nickel partially oxidizes into a unique state which is not NiOOH (emphasizing that $Ni(OH)_x$ is unique from $Ni(OH)_2$).

Comparing the relative magnitude of the forward and reverse anodic peak in the treated and untreated electrode provides a significant clue for determining why the treated electrode has such a higher activity toward the UOR. Note the fact that for untreated nickel the anodic peak in the forward scan of the CV (anodic to cathodic) is higher than the peak in the reverse scan. This is consistent with other studies, and is explained by the blockage of the active sites by adsorbed Urea or products of the electrooxidation [159]. The blocked sites are unable to re-oxidize to NiOOH, and so are unable to catalyse the UOR. The regeneration of active sites could also be a limiting step for the electrooxidation reaction itself. The relative magnitude of peaks is inverted in the treated electrode with the reverse scan peak having a significantly higher magnitude than the forward scan. The peak also has a much sharper rise than the reverse scan anodic peak does for untreated nickel. In the literature such a sharp rise is only seen on Ni deposited on a high surface area carbon foam for high NaOH concentration (4 M and above). It was attributed to fast oxidation of compounds blocking the active sites due to increased OH^- concentration [173]. In

the case for Figure 7.1 b there is no difference in OH⁻ concentration between the two CVs, so a different explanation is required. The sharp rise occurs at the point when the UOR outcompetes the OER for the active sites, and indicates the treated electrode's active sites for the UOR are being regenerated more quickly than the untreated electrode. In the untreated electrode the current rises slowly as the sites are re-activated. This behavior can indicate either that the active sites are not being blocked, or the blockage is removed significantly faster. Either would be accomplished by highly active sites for the UOR surrounded by areas where the reaction does not occur as readily, giving space for the Urea and the products to adsorb without blocking. This interpretation explains both the higher activity and the high magnitude of the anodic peak in the reverse scan.
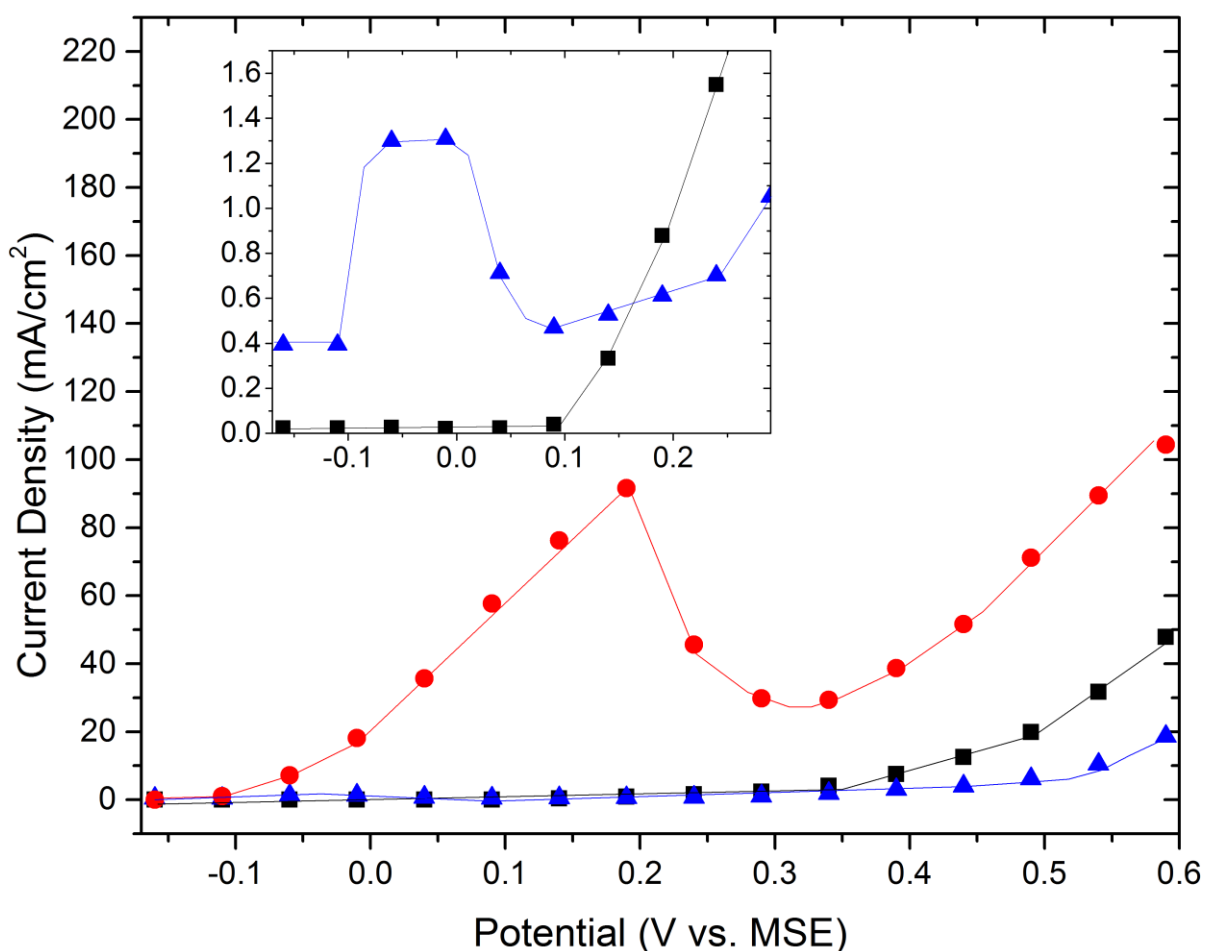
Figure 7.2: Sampled current experiment in 5 M KOH. The potential is held for 30 seconds then the current is sampled. The figure shows the experiment for untreated with 0.33M Urea (triangle), untreated without Urea (square), treated (circle). The inset shows the lower currents magnified to show where the untreated electrode oxidized Urea.

Sampled currents methods were used to further investigate the properties of the catalysts. Although the patterns of the CVs are largely repeated, there are interesting differences since the sampled current method filters out some transient elements of the signal. Without urea the current is negligible until the point where the oxygen evolution begins at 0.35 V (peaks I and II, being purely surface dynamic, do not show up in sampled current experiments). With Urea the current increases for both treated and untreated at the potential of peak I, and then decreases due to the competition with the OER, and increases again when the OER starts winning the competition. For the treated electrode this decrease occurs at the potential of the sharp rising edge of the reverse scan of peak I. This voltage was hypothesized, from the CV, to be where the transition between UOR and OER takes place. The maximum seen for the UOR in the treated electrode is also anodic of that for the reaction on an untreated electrode by 200 mv. This difference has a practical effect. Treated electrodes will be able to run at a higher cell voltage than untreated electrodes in an electrolyser containing urea. It also indicates that the treated electrode surface is better at regenerating the active sites for the UOR than the untreated electrode, as suggested in the introduction.
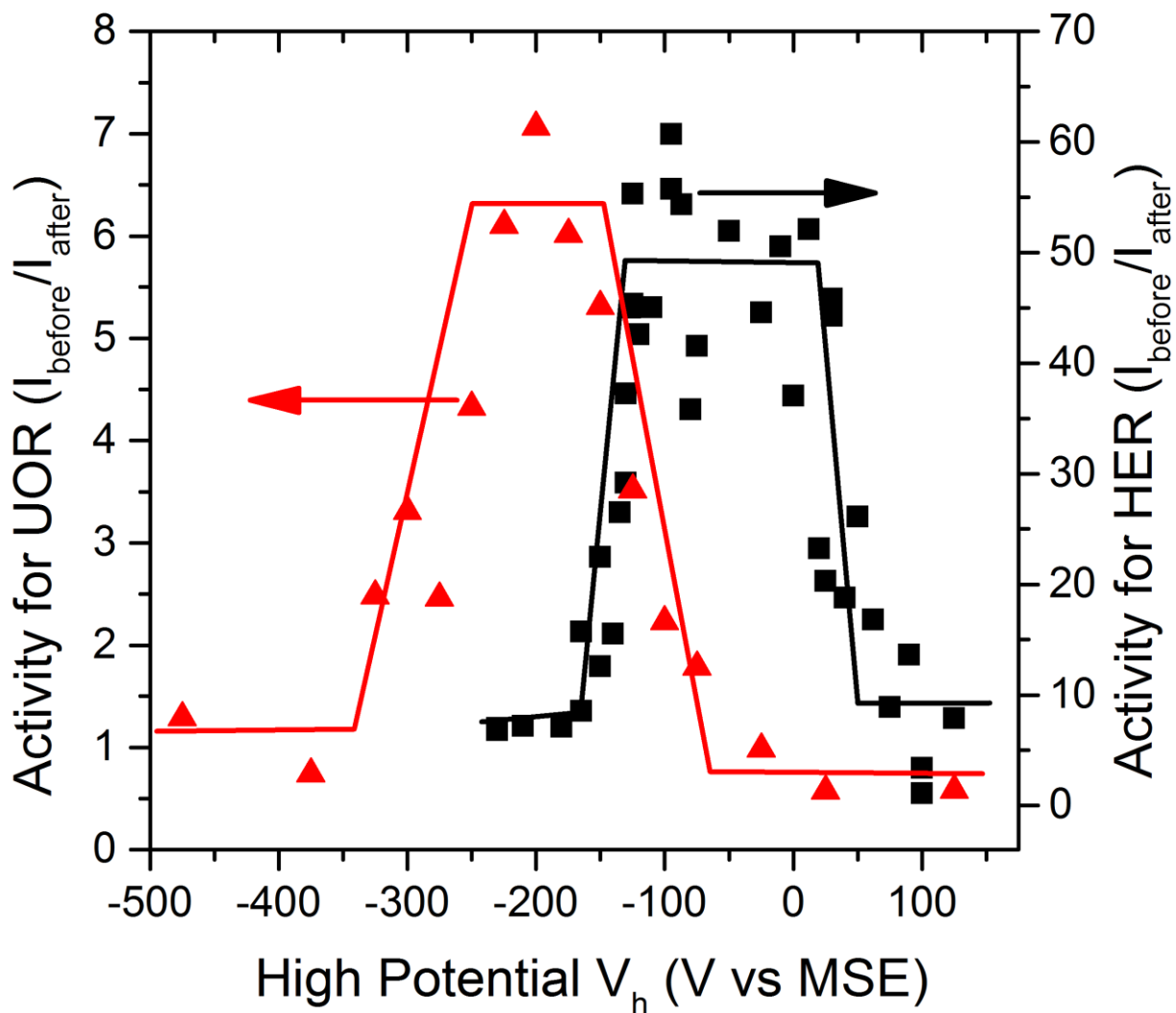
Figure 7.3: Effect of the high potential V_h during the treatment on activity of the treated electrode toward both the UOR and the HER. Triangles and the left axis are for the UOR, while squares and the right axis are for the HER.

The activity of treated electrodes towards the HER is known to be very sensitive with respect to the parameters of the treatment [172]. It is interesting to see if this sensitivity is also true for activity toward the UOR. Figure 7.3 shows that UOR activity is highly dependent on V_h (in fact it is similarly dependant on the other parameters, but V_h is used an example herein) as in the case of the HER. However the location of the region that produces an increase in activity is shifted slightly negative of the active region for HER. The positive half the UOR active region in Figure 7.3 overlaps he negative edge of the HER active region.

This shift between the optimum parameters for the HER and UOR can help to explain why the electrodes are active for the UOR. The range of V_h resulting in high activity for UOR is slightly

reduction biased, in terms of the HER. For the HER, reduction biased parameters produce poor results because they have a tendency to dissolve the surface, but for values close to the ones yielding high activity small islands of active $Ni(OH)_x$ are thought to exist [172]. The $Ni(OH)_x$ islands are expected to be highly active sites for the UOR, because of their water splitting properties [41, 135]. Isolated islands that are highly active for the UOR surrounded by less active areas, is exactly the interpretation given for the CV data in Figure 7.1. The active sites are then $Ni(OH)_x$ islands, which are dispersed on the surface with space between them.
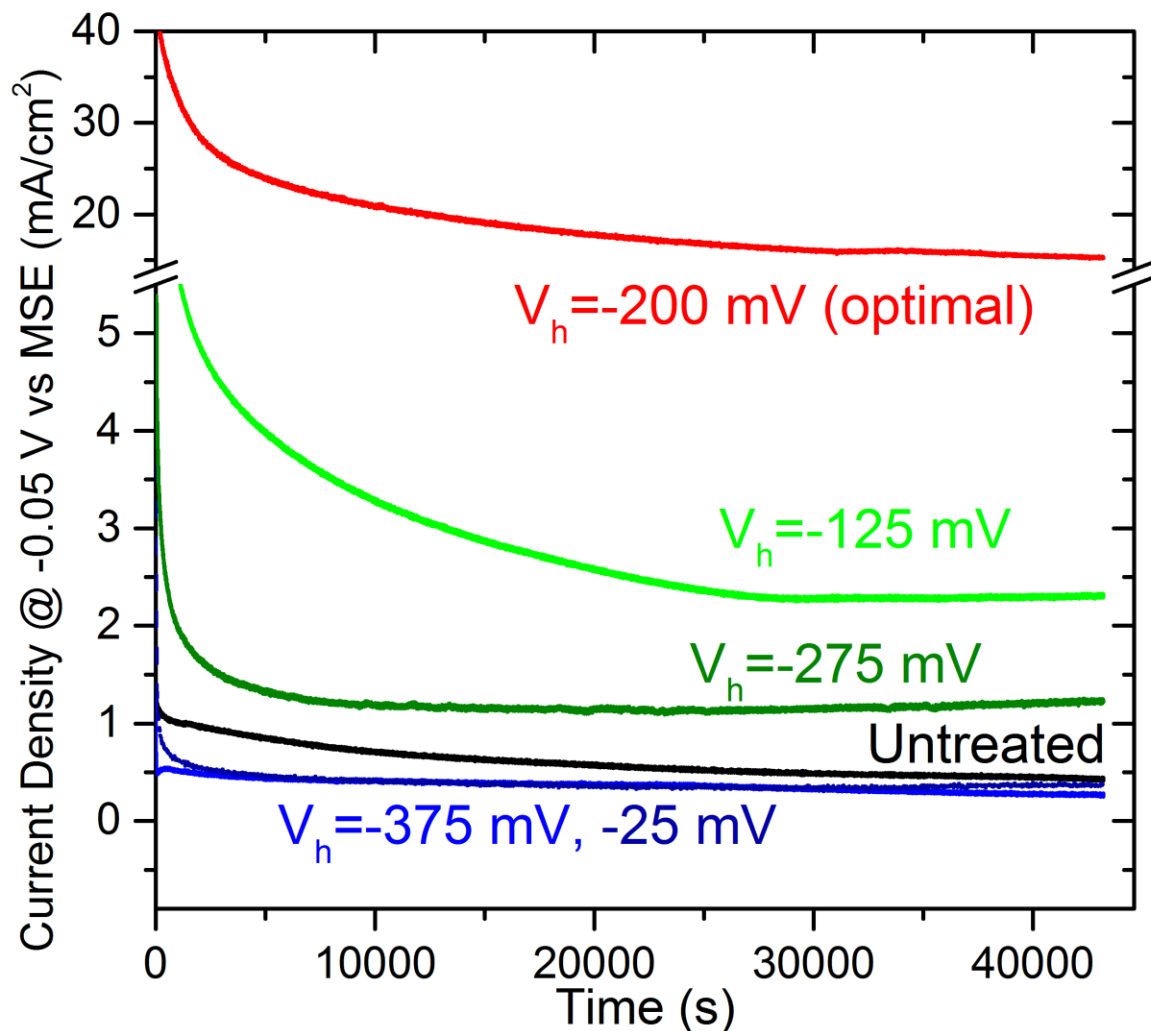
Figure 7.4: Twelve hours polarizations in a solution of 5 MKOH and 0.33 M Urea. Voltage applied is -0.05 V vs MSE.

Long term polarisation experiments (Figure 7.4) were conducted in order to evaluate stability of the treated electrodes under reaction condition. The polarization was selected to be at -0.05 V,

which is close to the optimum voltage for the untreated electrode, but not the optimum voltage for the treated (Figure 7.2). This choice should show the treated electrode in the least favorable light. Despite this, the treated electrode's current stabilizes at a significantly higher current than the untreated electrode (while the untreated electrode is still trending slightly downward). At 12 h the treated electrode's current density is 15.3 mA/cm^2 while the untreated electrode only has 0.42 mA/cm^2.

Figure 7.4 also shows curves for electrodes treated with non-optimal parameters, in two categories. The first category is for V_h close to the optimal value (V_h=-125 mv and -275 mV). These data show higher current density than an untreated electrode, but still significantly lower than the optimally treated electrode. This is consistent with the interpretation that the UOR activity comes from small islands of Ni(OH)$_x$. According to this interpretation one should expect a minor increase in activity for square wave parameters producing some islands, but not the optimal concentration. The other category is for V_h far from the optimal value (V_h=-25 mV and -375 mV), outside the range of values that have a positive effect on the UOR activity according to Figure 7.3. In this case one expects to form surfaces with either a fully formed Ni(OH)$_x$ layer or no Ni(OH)$_x$. In both cases this is not beneficial for the UOR and indeed the data show very low current, even slightly lower than an untreated electrode.

7.2.5 Conclusions

An electrochemical square wave treatment that is known to increase the activity of nickel electrodes toward the HER has been shown to significantly increase the activity of nickel electrodes toward the UOR. This importantly shows the wider application of the previously reported on electrochemical square wave treatment of nickel [135] for developing catalysts.

The increase in activity is due to the treated nickel electrode regenerating the sites active for the UOR very quickly. This likely comes from the surface having a dispersion of islands which are active for UOR with room between. The active sites are thought to be the Ni(OH)$_x$ structure which should catalyse the water splitting portion of the UOR. The electrode treated with the optimal value of V_h was found to be stable, maintaining significant higher activity over the course of 12 hours than nickel untreated or treated with non-optimum parameters.

7.3 Afterward

7.3.1 Context

In this paper a treatment to create a very active electrode for the UOR was reported on. The treatment is an adjustment of the treatment for HER electrodes, to slightly more reduction biased parameters. The fact that making an active UOR electrode requires different parameters than making an active HER electrode should not be surprising. It is a different reaction, and so has different requirements of the surface chemistry. More interesting is how the parameters are different: the parameters required to produce active UOR electrodes can be justified in terms on the theory of the $Ni(OH)_x$ electrode as presented in the previous two chapters. Another note on the UOR treatment is that it opens the possibility of using two treated nickel electrodes in an alkaline water electrolyser, with the addition of urea.

It is also interesting to note here that the elbow at VIII in Figure 5.4 is not associated with the onset of the UOR. The UOR onset is associated with the creation of NiOOH, it is sacrificially reduced (and then re-oxidized) in the UOR. The fact that VIII does not correspond with the UOR onset signifies that the structure of the hypothesized oxidized state of $Ni(OH)_x$ created at VIII is not like NiOOH.

7.3.2 Electrooxidation of Other Organics

There are inherent similarities between the electrooxidation reactions of Urea and some other organics, such as Ethanol and Methanol [174, 175]. Indeed, using the UOR treatment parameters produces electrodes which are also good for their electrooxidation, as can be seen by the preliminary data shown in Figure 7.5.
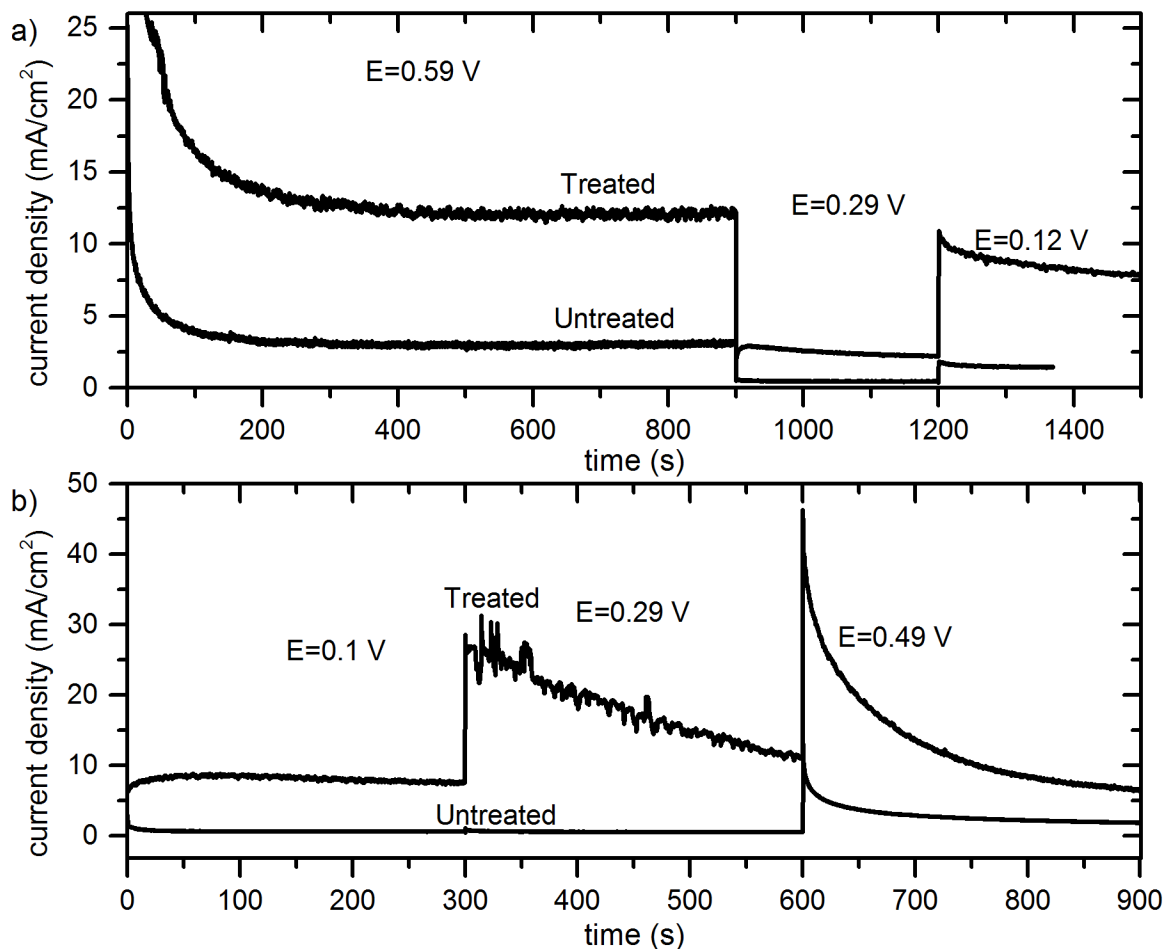
Figure 7.5: Polarizations of Ni electrodes treated with the optimal UOR parameters used as anodes for a) methanol electrooxidation, and b) ethanol electrooxidation. The polarizations are at the voltages listed in the graphs vs the MSE electrode

8 Practical Elements

In this chapter different practical concerns for implementing the treatment will be discussed. First, the cost of maintaining the treatment's electrolyte quality will be addressed. Then, the energy and equipment requirements of the treatment are considered. Also, a method to deal with the sensitivity to treatment parameters noted in chapter 6 is proposed. Finally, the application of the treatment to metals other than nickel is addressed. The scientific importance of the data examined here is also discussed.

8.1 Composition of the Solution

Throughout the preceding chapters the solution used to treat electrodes has been a combination of 200 mM sodium sulphate and 24 mM ascorbic acid. The use of ascorbic acid was originally

motivated by thoughts of its antioxidant properties. However, ascorbic acid decomposes in solution significantly over the course of a few days. In fact solutions more than three days old do not produce highly active catalysts. This is no doubt linked with the noted sensitivity of the treatment to its parameter noted in chapter 6. Practically, a solution that changes properties to the detriment of the relevant process is not desirable. Luckily, it appears that ascorbic acid is not an essential ingredient in the treatment. The treatment also performs well with a wide variety of combinations electrolytes (listed in Table 8.1), as long as the conductivity is 30mS and the pH is 2.95. The only exception to this that was found was solutions containing chlorine. This is likely because chlorine attacks the passive layer on nickel electrodes, which is the kind of layer the treatment forms.

Table 8.1: Salts and acids used to make solutions to treat Ni electrodes, combinations of all the items used here experimented with.

Salt Used	Acids Used
Monosodium Phosphate	Acetic Acid
Disodium Phosphate	Sulfuric Acid
Sodium Ascorbate	Hydrocholric Acid
Sodium Nitrate	Phosphoric acid

Another important factor of the solution is its cost. Since the concentrations are fairly small the cost of the solution will be very low. For example, using a sulphuric acid and sodium sulphate treatment bath the cost of the bath would be less than a dollar litre even if the reagents were bought at laboratory supply prices [176]. Further the solution would be good for several treatments before it needed renewing. On the other side of the operation there is the cost of waste disposal. Since the pH is greater than 2 the solution is not considered a hazardous corrosive [177]. The other concern for waste treatment is the amount of nickel, if any, is left in the treatment solution. Although Ni is a serious waste product, treating waste water for heavy metals like Ni is costed in the dozens of dollars per 1000 gallons [178]. Thus the cost of the treatment solutions from purchase to treatment should not be significant.

8.2 Power Use and Peak Current

A portion of the expenses to treat an electrode will come from the power consumption. Figure 8.1 shows typical current data and cell voltage of a single cycle of the treatment. Cell voltage V and charge Q is enough to calculate the energy E consumption of a single cycle according to E=QV. Since the energy required will scale linearly with surface area (along with the peak current) a value given in energy/surface area is an appropriate metric. The energy per cycle is approximately 40 μJ/cm^2/cycle. This comes out to about 1 J/cm^2 to treat a catalyst (with 19200 cycles, the number of cycles used with optimal treatment parameters). This translates to on the order of $1e-8 /cm^2 at $0.1/kwh, a quite insignificant cost.
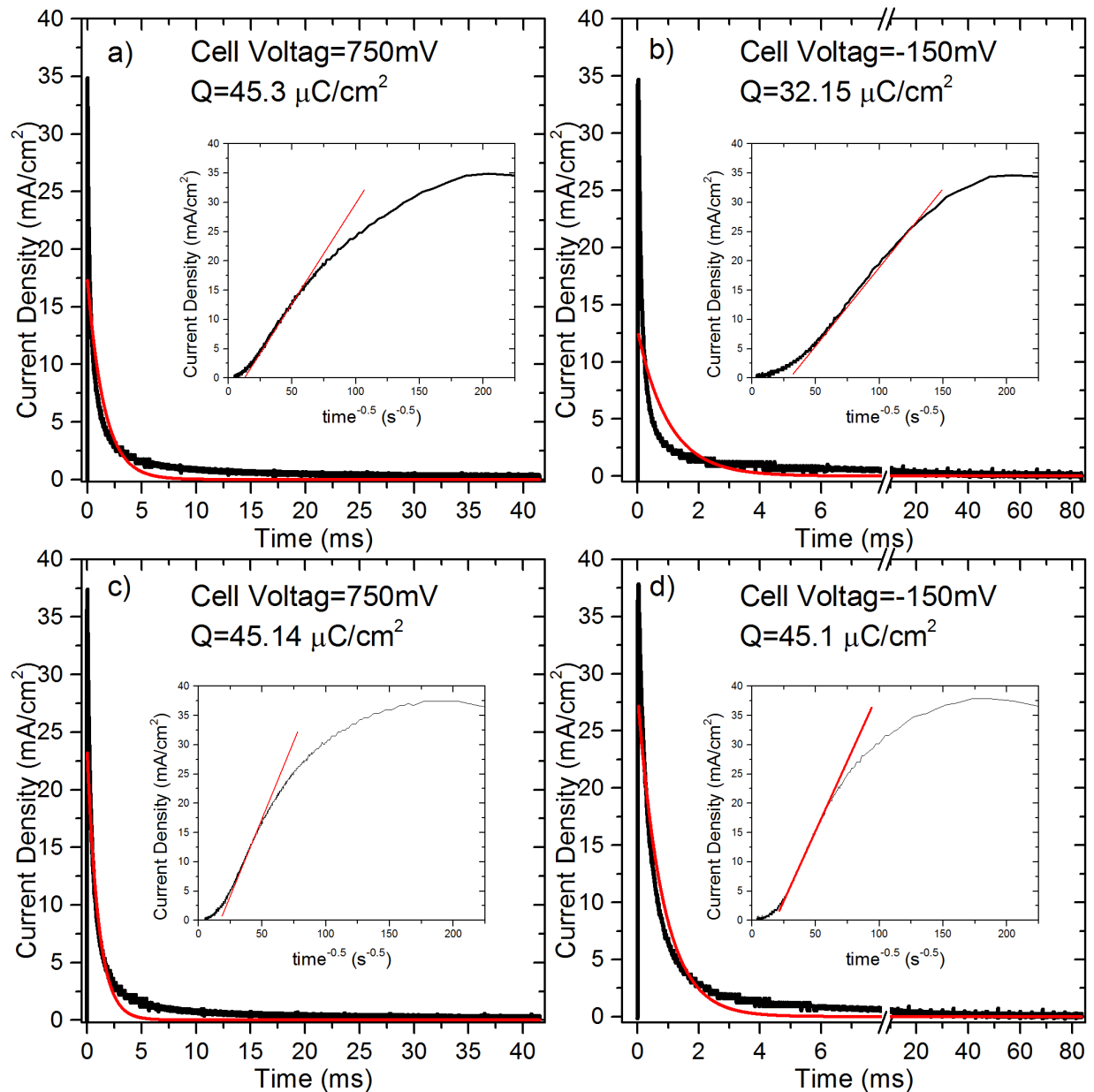
Figure 8.1 Typical examples of current density during a single cycle of the treatment with optimal parameters, for the anodic (a and c) and cathodic (b and d) current. a and b are from the initial portion of the treatment (30 seconds in) and c and d are from the end (2250 seconds). A best fit exponential curve is shown simply as a point of reference for the shape of the curve (clearly, these curves are not purely exponential).

Another related cost will be the equipment used to apply the treatment, and in general the cost of this equipment will go up with peak current required. Typical peak current density required for optimal treatment parameters are, as seen in Figure 8.1, around 50 mA/cm^2. To evaluate the requirements of the power supply able to apply the treatment on commercial electrodes, one has to know the typical size of used electrodes in industrial electrolysers. This type of information is

not published widely. However references can be found to 300 cm^2 and 1000 cm^2 size electrodes in the form of the IMET stack from Hydrogenics [179]. While it is not clear what type of area this is (geometric, etc.) it still gives an initial idea.

Sizes up to 100cm^2 (corresponding to currents on the order of 5 A) can be dealt with easily by several bench top power amplifiers. More specialized high-current supplies are available up into the thousands of amps peak current (for example those from Magna-Power [180]), but often with low bandwidths (~60hz). Low bandwidth may jeopardize optimal working conditions for the treatment. It is therefore very likely that custom electronics would be required for high surface areas (>1000cm^2).

Another way to deal with the treatment of high surface area electrodes consists in trying to optimize the treatment in order to minimise the peak current. Double layer charging contributes significantly to the peak current, but is not significant to the mechanics of the treatment. The peak current from the capacitive charging can be reduced by making the change in voltage less sudden. This suggests rounding off the edges of the square voltage wave as in Figure 8.2, which results in a reduced peak current.
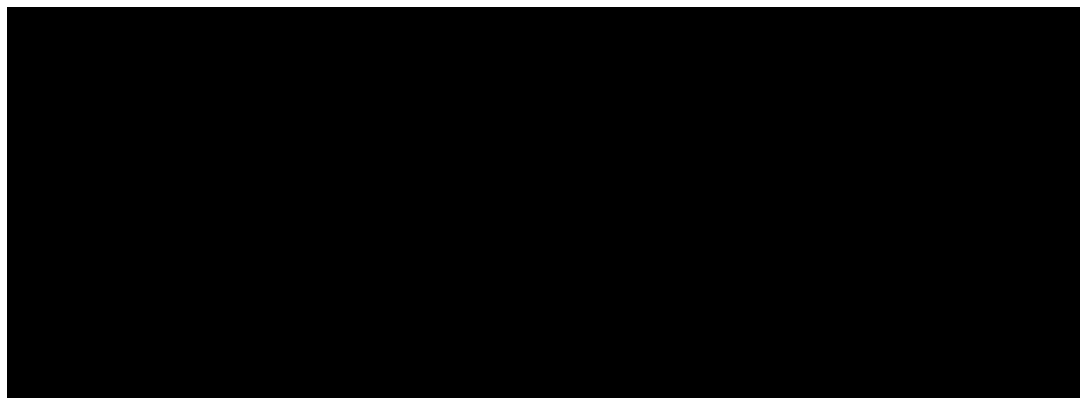
Figure 8.2: A diagram of a comparison between the standard treatment, and the treatment with the corners rounded off to reduce peak current, while keeping the same activity.

Characterization of this treated electrode shows that the treatment still produces similar results to those from the optimum parameters. This is likely not the limit of how far the peak-current can be reduced while maintaining the activity of the treated electrode. If very large surface area electrodes need to be treated, this could be a promising way to minimise the currents required.

8.3   On-line Monitoring

In chapter 6 it was noted that the results of the treatment are very sensitive to the parameters of the treatment. In fact, altering the geometry of the cell can sometimes de-tune the parameters. This potentially presents practical issues. The first is consistency. The sensitivity may make achieving a consistent result at an industrial scale challenging. The second is adaptability. It is desirable to be able to apply the treatment to any form factor of electrode easily, not after days of optimizing parameters. Both issues would be mitigated by having very precisely controlled conditions. However, the ideal is to have a signal that can be monitored during the treatment, which indicates status. The only signal that is readily available during the treatment is the current.
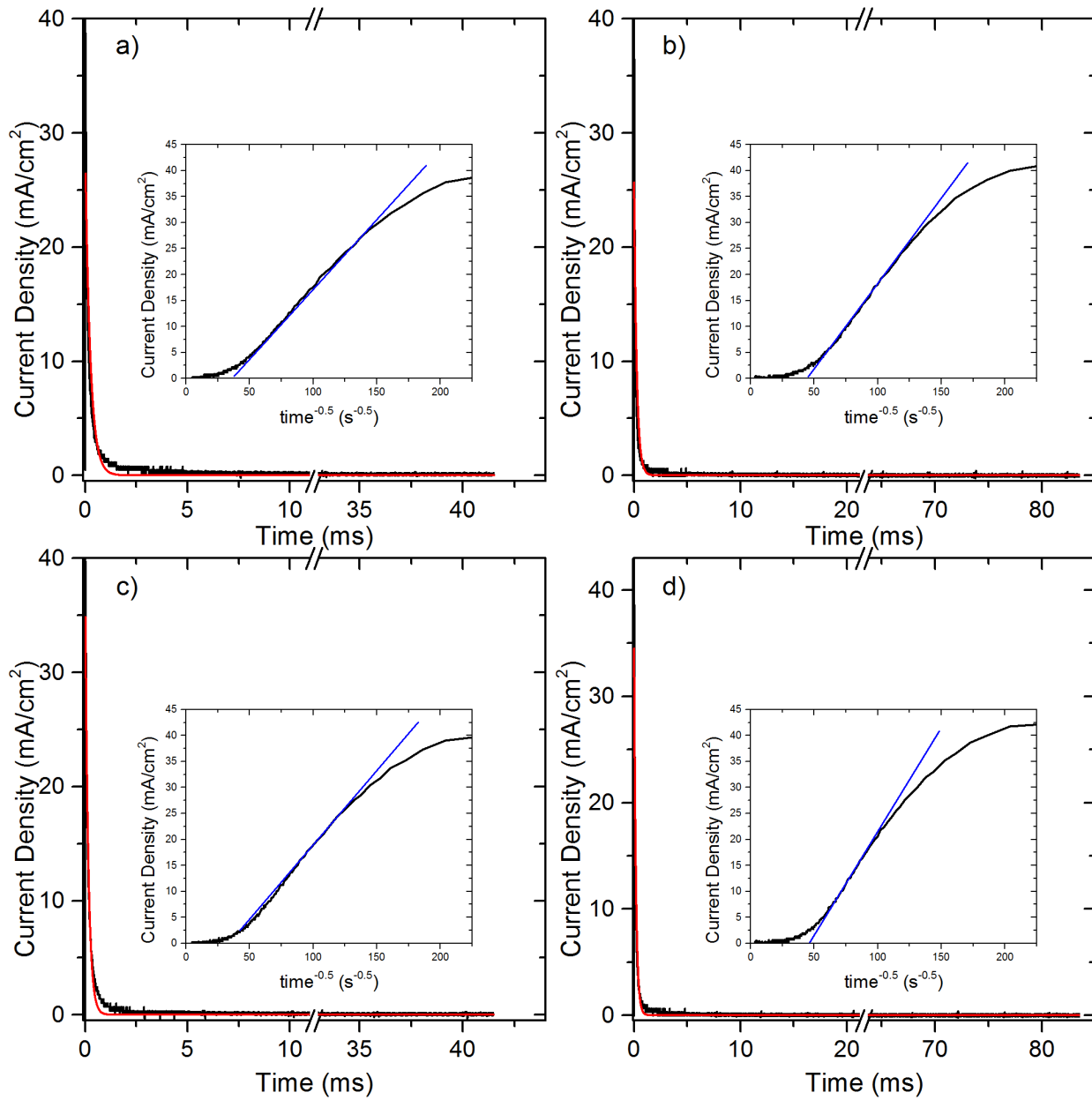
Figure 8.3 Typical examples of current density during a single cycle of the treatment with oxidation biased parameters (Th=120 mV, all else optimal), for the anodic (a and c) and cathodic (b and d) current. a and b are from the initial portion of the treatment (30 seconds in) and c and d are from the end (2250 second in). A best fit exponential curve is shown simply as a point of reference for the shape of the curve.
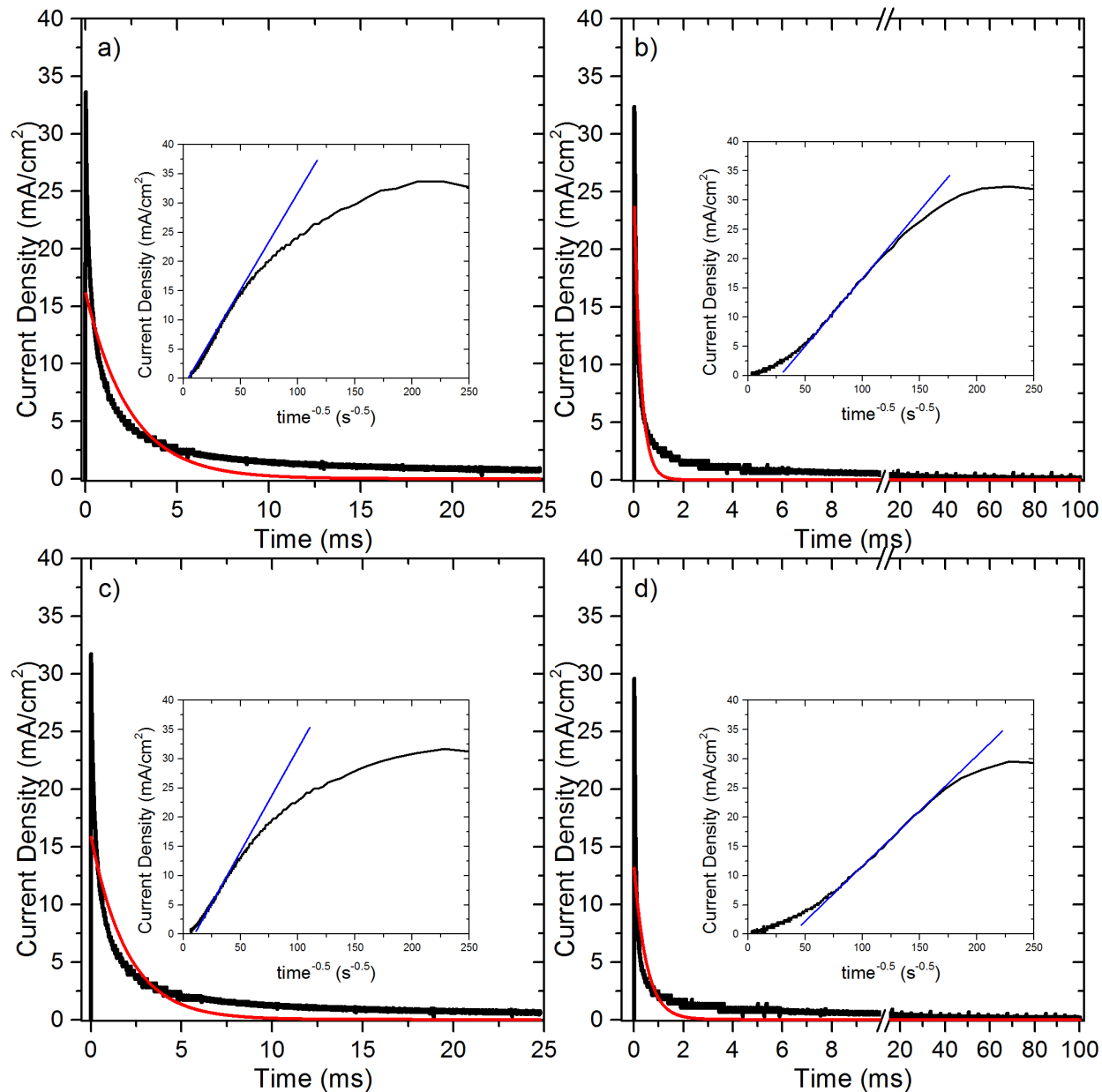
Figure 8.4 Typical examples of current density during a single cycle of the treatment with reduction biased parameters (Duty Cycle=20%, all else optimal), for the anodic (a and c) and cathodic (b and d) current. a and b are from the initial portion of the treatment (30 seconds in) and c and d are from the end (2250 second in). A best fit exponential curve is shown simply as a point of reference for the shape of the curve.

The current signal during the treatment using optimal (Figure 8.1), oxidation biased (Figure 8.3) and reduction biased (Figure 8.4) are examined. The total current is the sum of several contributions. First, there is the double layer charging. In fact, the double layer charging is a significant portion of the total current. To see this, the order of magnitude of the time constant of an RC circuit with double layer capacitance C is analysed. We estimate the resistance R from the

83

peak current (which is ~10 mA given a surface area of 0.3 cm^2) and peak to peak applied voltage (which is approximately 1 V). This gives R on the order of 100 ohms. The double layer capacitance of these electrodes is estimated to be 0.6 to 12 μF (specific capacitance of 2-40 μF/cm^2 [181] and surface area of 0.3 cm^2). It follows a time constant of 1/RC between 0.1 to 1 ms. This is comparable to the time constant of the decays seen for the current signal during the treatment.

The second kind of contributions to the total current are the currents associated with the actual reactions. They will exhibit some form of exponential decay (possible with an offset in the case of dissolution reactions) [13]. It may be tempting to analyse these reactions as if they were diffusion controlled (or partially diffusion controlled). However, it is not entirely clear that the standard forms for analysing diffusion controlled reactions would be applicable (looking for linear relations in current density and t$^{-0.5}$) as the electrodes are not shaped for such an analysis [13]. In any case, as can be seen in insets in Figures 8.1, 8.3 and 8.4 there is generally no such linear relationship. Another difficulty to be accounted for is that the significant double layer charging. Electrochemical reactions that take place while the double layer is charging (which is a non- negligible amount of time in each cycle) are not taking place under the same conditions as a fully charged double layer, which can affect the kinetics of the reaction.

In summary, it appears that analysing the current signal during the treatment directly is a challenging prospect, and not appropriate for an on-line monitoring solution. Instead, a simplified quantity will be considered here.

A convenient quantity to investigate is the charge transferred during a single cycle, split into the anodic and cathodic charges. The charge transfer will be correlated with the number of individual electrochemical reactions that occur. A large part of the charge will be due to double layer charging, but in each part of the cycle this component will be constant throughout and the anodic and cathodic double layer charge components of the signal must balance.

Figure 8.5 shows the graphs of charge transfer per cycle.
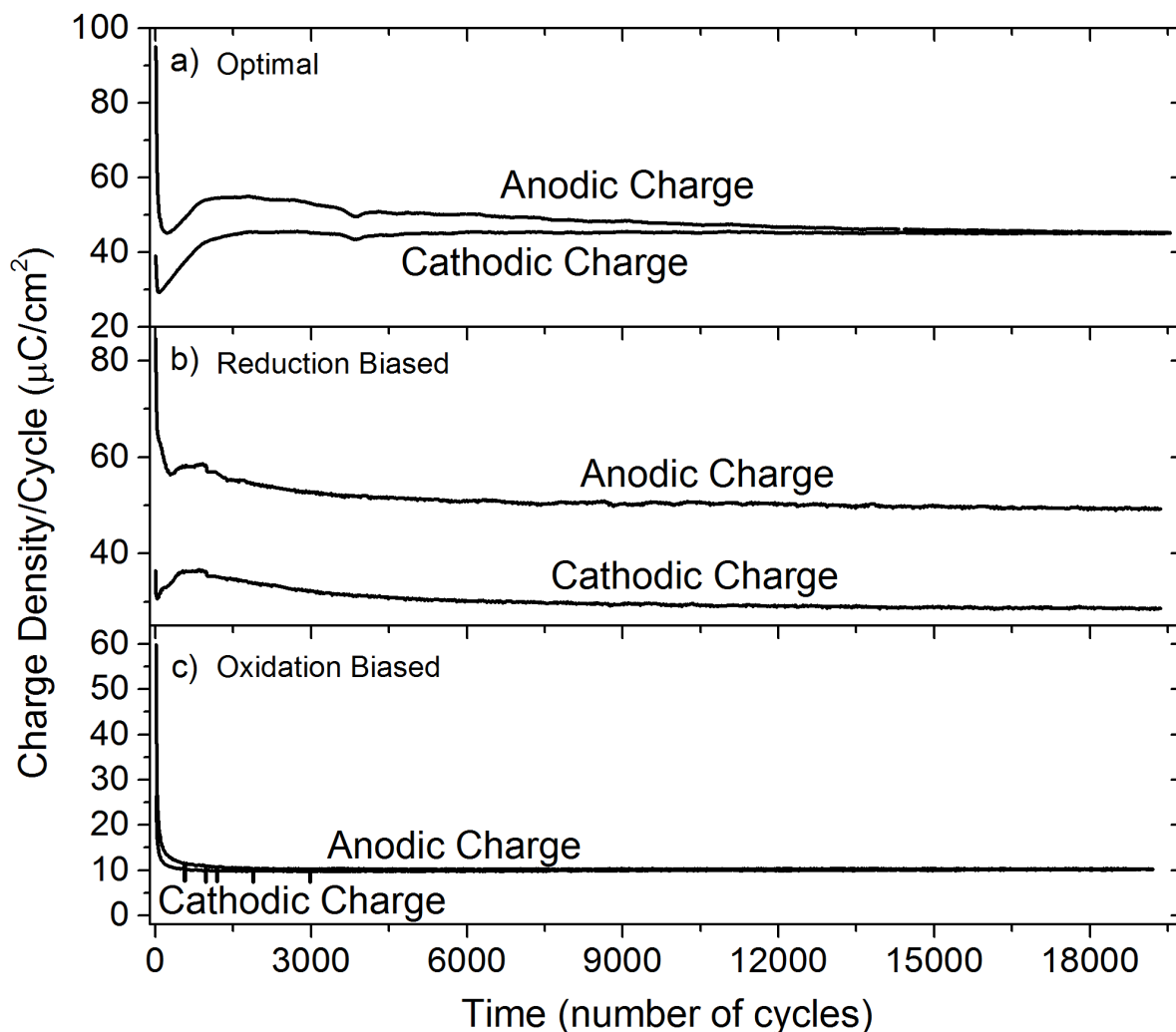
Figure 8.5: Charge per cycle during the treatment for three different parameter sets. a) Optimal, b) reduction biased (duty cycle=20%) c) oxidation biased (Vh=120 mV).

The three classes of signal are distinctive. The difference between the three is that in the optimal case the anodic and cathodic charge will tend toward balance, but not actually balance till the last third of the treatment. However, for the non-optimal cases, after about 3 minutes, the difference between the two charges will remain constant. Therefore, the different cases can be identified within the first five minutes (and often much faster). This is very encouraging as it can cut down the amount of time needed to tune parameters. The time to test a single parameter set would go down from an hour to something like ten minutes (depending on fixed times associated with replacing the electrode in the cell).

85
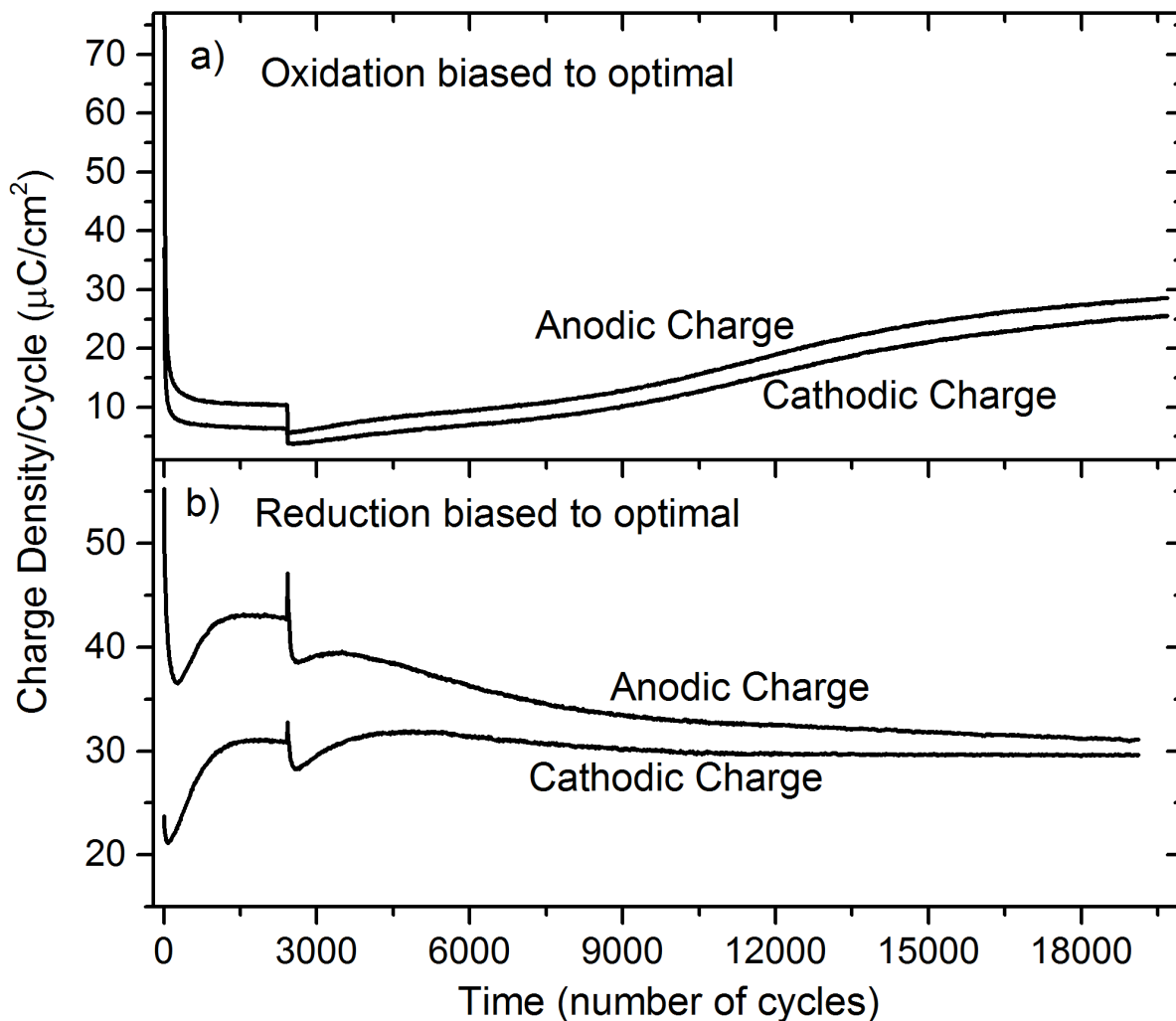
Figure 8.6: Charge per cycle for when the parameters of the treatment are changed 5 min into the treatment. a) From oxidation biased (Vh=120 mV) to optimal. b) From reduction biased (Vh=-180) to optimal.

An even better solution would be the ability to automatically tune parameters on-line. To do this the parameters need to be altered online. Going from reduction or oxidation biased parameters to the optimal parameters within the first ten minutes does not affect quality of catalyst. That is to say that for initial parameters within the ranges explored in Chapter 6 that are switched into optimum parameters in the first 10 minutes show characterization is identical to optimally treated electrodes   Figure shows the charge per cycle for changing parameters into the optimum range.

From the five graphs of charge per cycle (Figure 8.5 and Figure) a simple online tuning heuristic can be stated:

1. Identify which category the parameters are currently in. If in the optimal category, stop.

2. Pick one parameter that affects the bias (V_h, V_l, duty cycle, etc.) and tune it a small amount toward the optimal zone. (see Table 8.2 for possible actions)

3. Repeat 2 until the charge per cycle graph looks like one of the transition examples. (Figure 8.6)

4. If charge per cycle graph starts to look like the opposite non-optimal condition, reverse the tuning slightly.

Table 8.2: Control action to be taken based on the condition seen. Table built based on findings from chapter 6

Condition	Possible Actions
Oxidation Biased	• Decrease V_h • Decrease t_h • Increase V_l • Increase t_l . • Decrease duty cycle
Reduction Biased	• Increase V_h • Increase t_h • Decrease V_l • Decrease t_l • Increase duty cycle

This is clearly not an exact procedure, but a skilled operator can follow this heuristic to find the optimal zone of a purposefully detuned parameter set with some success. Implementing this heuristic as an automatic control algorithm is not addressed here, but this is a proof of plausibility of such an algorithm.

An explanation of the three different types of signals seen in Figure 8.5 is now discussed. For reduction biased parameters there is a large amount of net charge flowing in the anodic direction. By combining this with the knowledge from chapter 6 that reduction biased parameters promote dissolution of the electrode, it becomes clear that the net anodic charge is associated to the electrode dissolution.

For oxidation biased parameters the zero net charge flowing is attributed to the reduction and oxidation of the same amount of the passive film. In other words, the passive film does not grow after the initial formation. The charge per cycle is additionally quite low compared to the other two states, suggesting that the passive film built in this case is difficult to grow or reduce passed a certain point.

The most interesting of the three graphs is that of the optimum parameters (Figure 8.5 a). It can be seen as a combination of the two non-optimal cases. There is a significant net charge flow over the first portion of the treatment till approximately 30 minutes (14400 cycles). This time frame is the minimum treatment duration required to obtain optimal results (see section 6.2). In the first 30 minutes of the treatment the surface is converted to the $Ni(OH)_x$ structure. Once the final structure is reached there is a dynamic equilibrium, much like the case in the oxidation biased parameters. The progression toward a dynamic equilibrium when using the optimum parameters, is also supported by the experiments were the parameters were changed mid-treatment. The previous non-optimum modification of the surface was able to be overwritten by the optimum parameters. This is a consequence of the step by step nature of the treatment. Each cycle of an optimal parameter treatment the surface take a step toward the desired $Ni(OH)_x$ state. This happens regardless of the state of the surface before the optimum parameters are applied. If the surface is heavily oxidized, then the treatment will tend to reduce the surface in net. If the surface is reduced, it will oxidize it. The step by step nature itself can be seen in the net charge transferred per cycle, which is never higher than a few dozen $\mu C/cm^2$ (vanishing near the end, Figure 8.7).This level of charge transfer is much less than even the charge required for a single electron process which is 257 $\mu C/cm^2$ [182].
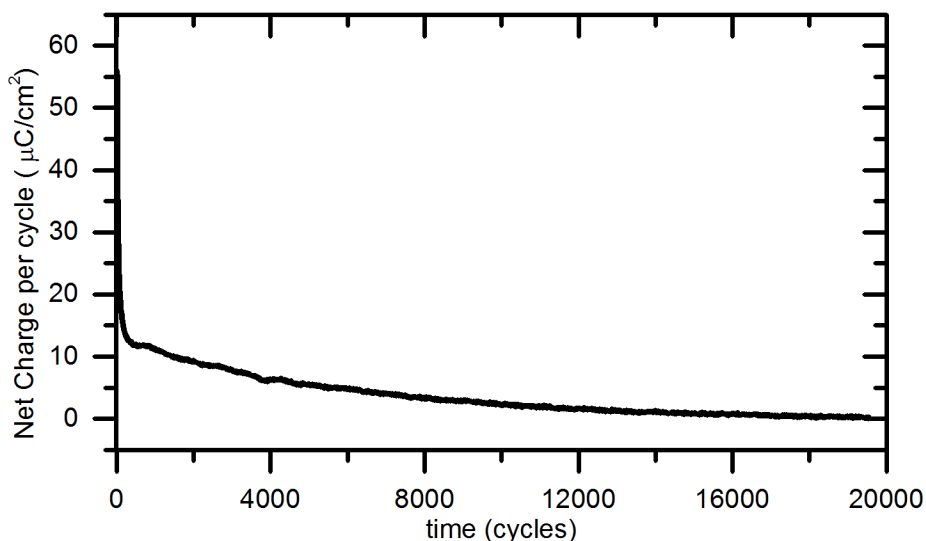
Figure 8.7: Net Charge per cycle for the optimal treatment.

It is also interesting to note is that the net charge transferred during the treatment is more than one monolayer of even a multi-electron process (the charge involved in generating a monolayer by an electrochemical process on Ni will be number of electrons involved multiplied by 257 $\mu C/cm^2$) (Figure 8.7). This opens up two possibilities. The first is that some small degree of dissolution occurs during the optimal treatment. This may seem inconsistent with unmodified morphology seen in chapter 5, but nickel normally dissolves by a step–flow process in sulphate solutions [183], which would leave the surface morphology unaltered. The other possibility is that the $Ni(OH)_x$ structure is more than one mono-layer thick. The visual appearance of treated nickel surface, which ranges from dull grey to a specular green or gold, would tend to support the treated structure containing multiple layers. However, the two possibilities are not mutually exclusive. Further investigations and information gathered from experiments using quartz crystal microbalance or electrochemical scanning tunneling microscopy are required.

8.4 Application to Other Metals

Being able to apply the treatment to other metals would significantly increase its practical importance. The treatment was also attempted on several other metals, and the charge per cycle was used as a guide to try to find optimum parameters on those metals. Ti, Fe, Mo, Co, 316L steel, Sn, Cu, and Al were all tried. Unfortunately, only some limited success was found with

89

Cobalt (see Figure 6.9). This effort did not represent an exhaustive search of the parameter space for these metals, so perhaps a more thorough search would find optimum parameters for other metals. Partly, the charge per cycle strategy was hampered by having to explore voltages that were within the HER or OER region (which was the case for the successful parameters for Co). When this was not an issue, the charge per cycle graphs for these metals fell into either the oxidation biased or reduction biased pattern. Further, only for Fe, of the non-Ni metals investigated, could both types of charge per cycle graph be seen. However, when the parameters were tuned from oxidation biased to reduction biased in Fe, there was always a rapid switching between the two modes. In Ni there are optimal parameters that can be found if the tuning is done carefully as demonstrated in this thesis. This suggests a point of attack in determining what metals the treatment is appropriate for. If the reason for this difference could be found it would indicate the property of Ni that allows the square wave treatment to work on it and allow this quality to be sought in other materials. The answer to this problem remains, at this stage, an open question.

8.5 Conclusions

Several practical concerns related to the treatment were addressed in this chapter. The cost of maintaining a particular electrolyte for the treatment is offset by the fact that it seems that any salts and acid will work, as long as the pH and conductivity is matched (and Cl^- is avoided). The running cost of treating an electrode was determined to be negligible. The cost of The cost of equipment may not be negligible, if large electrodes (>1000 cm^2) are to be treated, but this is a onetime cost. Additionally, it may also be mitigated by rounding the edges of the square wave.

Online monitoring of the current signal was seen to give valuable insights into the status of the process. Whether or not the treatment is proceeding as planned can be gleaned from the charge transferred each cycle. This information can even be used to tune the treatment parameters during a treatment. This allows for faster adaptability to variable conditions (e.g. electrode geometry, changing uncontrolled environmental conditions, etc.), and opens the possibility of automatic control of the process.

The online monitoring during the treatment also contributes to the understanding of the treatment. The dissolution of the surface caused by reduction biased parameters is evident in the charge per cycle graphs as the sustained net charge flow. Oxidation biased parameters, on the

other hand, are seen to form a marginally reactive layer within the first five minutes, and then change very little. The optimal parameters are a mix between these cases, though the net charge flow in this case is the construction of the $Ni(OH)_x$. Additionally, the charge per cycle provides evidence of the progressive nature of the construction. Application of the treatment to other metals will, no doubt, be aided by on-line monitoring.

9   Conclusions and Outlook

9.1   Conclusions

9.1.1   HER Treatment

The evidence from chapter 5 and 6 clearly shows that Ni electrodes subjected to the electrochemical square wave treatment have significantly higher activity than untreated nickel. The electrodes treated with the optimal parameters were found to have an exchange current of 0.18 A/m^2, compared to untreated nickel with 0.01 A/m^2, which is one order of magnitude of gain. Recall that platinum has an exchange current density of 4 A/m^2. So, it is not quite at platinum levels of activity, but it is only one order of magnitude off (whereas untreated Nickel is two orders of magnitude off). The Tafel slope was also reduced, from 121 mV/decade in untreated nickel to 106 mV/decade in treated nickel. This signifies that the treated electrode performs even better at higher potentials. The activity is also seen to be from a bifunctional cause. This is seen from the dependence of their activity on the pH of the solution.

Electrodes treated with the electrochemical square wave treatment were seen to be very stable. In the three electrode stability experiment (Figure 5.2d) showed that over the course of 20 hours the electrode appears to be very stable, hardly losing any activity at all. The lengthier two electrode experiment (Figure 6.8), at a higher current density, showed that a treated electrode will eventually return to the activity of an untreated electrode, but it will take several weeks. Considering that at any point a previously used electrode may be re-treated to regain the lost activity this loss appears to be a minor problem.

9.1.2   Urea Electrooxidation

In addition to being active for the HER, the electrochemical square wave treatment (with slightly different parameters) is capable of increasing the activity for the urea electrooxidation. A treated electrode can achieve 7 times the current at 0.96 V vs MSE, which increases to 35 times the current after 12 hours (as the treated electrode has far greater stability).

9.1.3   Strategy

The strategy for the modification of Nickel surface for increased catalytic activity toward the HER was seen to work as expected. The activity increase can be seen to be intrinsic. Indeed,

AFM measurements show no difference in roughness, while the increase in activity is linked with a new peak seen on the CV of treated Ni, indicating the activity is related to a new phase on the surface. Further, the fact that the activity is bifunctional denotes it is intrinsic. Finally, the need to adjust the parameters of the treatment to obtain the active UOR catalysts clearly indicates that the activity comes from modified surface chemistry, and not from an increased surface roughness, i.e. the activity is intrinsic.

Further, the treated surface is the proposed $Ni(OH)_x$ state. The XPS and EDX data show that the surface must also be like $Ni(OH)_2$, and it must be bifunctional. However, not identical, as seen in the CVs. The phase that is associated with the increased activity, identified by CV and double potential step experiment, is easier to oxidize than oxidizing Ni to $Ni(OH)_2$. Combined, the surface must be similar to $Ni(OH)_2$ toward XPS, be bifunctional, and have a phase which is easier to oxidized than a Ni surface: all a description of the $Ni(OH)_x$ structure.

Finally, the treatment works through the promotion of the non-electrochemical place exchange reaction, as explained in first two papers. First, that the proposed $Ni(OH)_x$ structure has been created is very suggestive that the treatment works in the specified way. Further, the shape of the parameter-activity space can be explained by appeal to this mechanism for the treatment, for both the HER and the UOR electrodes. Combining these two points with the charge per cycle, indicating the treatment proceeds vi**a** a step-by-step process arriving in situation of a kind of imposed dynamic equilibrium, leads to the conclusion that the treatment process works as hypothesized.

9.2 Future Work and Outlook

Since the treatment is a novel way to modify a nickel surface this work opens up several possible avenues of research. Some of them are listed here:

- **Basic Research into the structure and formation of $Ni(OH)_x$:** Further Experiment investigation into the exact mechanism of the treatment is important. The theory expressed explains the evidence well, but some details remain unexplored. The exact structure of $Ni(OH)_x$, and the reactions involved its further oxidation (basically, explaining in detail the anodic side of the CV) would be of interest for the future development of the treatment. The following is suggested in decreasing priority:

- o Further scanning probe microscopy (SPM) investigation. The reason these techniques will be important is that they can give information on an atomic resolution. Since the special properties of $Ni(OH)_x$ are thought to come from its special arrangement on the surface this technique is very applicable. The effects of the treatment on different planes of single crystal Ni electrodes could be investigated ex-situ. More ambitiously, SPM may be used to investigate the effects of the treatment in-situ. The challenge for this would revolve around magnitude of t_h and t_l, since these are much smaller than time it takes to image a surface with SPM. Perhaps some sort of average image over several cycles would be possible.

- o Electrochemical quartz microbalance (EQCM) studies. This tool would be used in two ways. The first is as an ex-situ investigation. There are several current waves in the CV of a treated electrode that are not fully explained. Knowing the change in mass during these current waves would greatly aid in their understanding. The second way is as an in-situ technique, during the treatment. The time scale involved in EQCM is longer than the either t_h or t_l, so it would not be able to show the anodic and cathodic mass change per cycle, but like SPM, the average over several cycles would still be useful.

- o In-situ spectroscopy: EIS or optical (FTIR, Raman, Ellipsometry). These techniques require detailed models of the surface to be effective, but when that is known they can provide detailed information, if further investigation is required at this point in development.

- **Other reactions**: The treated nickel surface should be extended more fully to other reactions. Herein we have already seen a detailed study of treated electrodes for the UOR, and preliminary data has been shown for Nitrate reduction, and ethanol and methanol oxidation. The three reactions for which preliminary data has been presented can be studied in more detail, and further reactions should be tested. Practically speaking, the best starting point would be to look for similar reactions to those already studies. This would further expand the range of use of the treatment. However, scientifically speaking, searching for other reactions that are not catalysed is of more interest. This is because these will offer more insight into the exact working of the treated surfaces.

- **Other metals**: The application of the treatment to other metals would be useful. It could provide catalysts for other reactions, or alternatives for the reactions studied here. More ambitiously, since the treatment oxidizes the surface in a novel way, applying it to other metals could yield surfaces useful in a wide range of applications that need specially engineered surfaces. To find metals that the treatment can be used with, a brute force survey could be made over different metals and treatment parameters. Alternately, as suggested in Chapter 6, the cause of the difference between Fe and Ni during the treatment could be investigated in detail.

- **Automatic control**: Implementation of an automatic control systems based on the heuristic presented in chapter four could be implemented. This could be important for producing consistent results from the treatment in variable conditions.

- **Reduction of peak current**: To reduce equipment requirements of the treatment the peak current seen during the treatment should be reduced. This can be accomplished by rounding off the edges of the square wave. A thorough study must be done to determine parameters for the lowest possible peak current, while still obtaining optimal results from the treatment.

- **Rapid switching of voltage**: The way that quickly changing the electrochemical potential was used in this work to promote a certain intermediary may be of interest elsewhere. Some other process that uses a switching voltage to generate a unique effect, other than this work, already exist. For example, preventing the buildup of H_2 during metal electrodeposition [184], creating thick hydroxide layers [185], and prevent the build up a disperse titanium dioxide when growing it on a CNT [186]. Our treatment acts slightly differently than the methods of those studies. It promotes the production of an intermediate which leads to a unique final result. Finding another reaction appropriate for this kind of technique would be the first challenge. There should be a non-electrochemical reaction in the overall mechanism which produces an intermediate that in larger concentrations than normally seen would combine to make an interesting product. To this end, a survey of electrochemical reactions whose mechanisms are well understood in the literature could be made to further this investigation.

10 References

[1] E. Bakker, "Electrochemical Sensors," *Anal. Chem.,* vol. 76, pp. 3285-3298, 06/01, 2004.

[2] Z. Chen, D. Higgins, A. Yu, L. Zhang and J. Zhang, "A review on non-precious metal electrocatalysts for PEM fuel cells," *Energy Environ. Sci.,* vol. 4, pp. 3167-3192, 2011.

[3] Y. Shao, S. Park, J. Xiao, J. Zhang, Y. Wang and J. Liu, "Electrocatalysts for Nonaqueous Lithium–Air Batteries: Status, Challenges, and Perspective," *ACS Catal.,* vol. 2, pp. 844-857, 05/04, 2012.

[4] G. Chen, "Electrochemical technologies in wastewater treatment," *Separation and Purification Technology,* vol. 38, pp. 11-41, 7/15/, 2004.

[5] K. Zeng and D. Zhang, "Recent progress in alkaline water electrolysis for hydrogen production and applications," *Prog. Energ. Combust.,* vol. 36, pp. 307-326, 6, 2010.

[6] S. Chu and A. Majumdar, "Opportunities and challenges for a sustainable energy future," *Nature,* vol. 488, pp. 303, 2012.

[7] L. Jörissen, "Prospects of hydrogen as a future energy carrier," in *Fuel Cells in the Waste-to-Energy Chain* Springer London, 2012, pp. 189-203.

[8] J. Andrews and B. Shabani, "Re-envisioning the role of hydrogen in a sustainable energy economy," *Int J Hydrogen Energy,* vol. 37, pp. 1184-1203, 1, 2012.

[9] D. Stolten, *Hydrogen and Fuel Cells.* Wiley, 2010.

[10] M. B. I. Janjua and R. L. Le Roy, "Electrocatalyst performance in industrial water electrolysers," *Int J Hydrogen Energy,* vol. 10, pp. 11-19, 1985.

[11] A. Ursua, L. M. Gandia and P. Sanchis, "Hydrogen Production From Water Electrolysis: Current Status and Future Trends," *Proceedings of the IEEE,* vol. 100, pp. 410-426, 2012.

[12] E. Endoh, H. Otouma and T. Morimoto, "Advanced low hydrogen overvoltage cathode for chlor-alkali electrolysis cells," *Int J Hydrogen Energy,* vol. 13, pp. 207-213, 1988.

[13] A. Bard and L. R. Faulkner, *Electrochemical Methods: Principles and Applications.* John Wiley and Sons, 2001.

[14] C. H. Hamann, A. Hamnett and W. Vielstich, *Electrochemistry.* Weinheim,De: Wiley-VCH, 2007.

[15] S. Machado and L. Avaca, "The hydrogen evolution reaction on nickel surfaces stabilized by H-absorption," *Electrochim. Acta,* vol. 39, pp. 1385-1391, 1994.

[16] R. Woods, A. Henglein and A. Bard, *Electroanalytical Chemistry.* Marcel Dekker New York, 1976.

[17] Trasatti S. and Petrii O. A., "Real surface area measurements in electrochemistry," vol. 63, pp. 711, 2015-08-05T03:44:01.852+02:00 ER -, 1991.

[18] C. G. Zoski, *Handbook of Electrochemistry.* Elsevier, 2006.

[19] D. S. Hall, D. J. Lockwood, C. Bock and B. R. MacDougall, "Nickel hydroxides and related materials: a review of their structures, synthesis and properties," *Proceedings of the Royal Society of London A: Mathematical, Physical and Engineering Sciences,* vol. 471, 12/24, 2014.

[20] M. Rajamathi, P. Vishnu Kamath and R. Seshadri, "Polymorphism in nickel hydroxide: role of interstratification," *J. Mater. Chem.,* vol. 10, pp. 503-506, 2000.

[21] M. Rajamathi, G. N. Subbanna and K. P. Vishnu, "On the existence of a nickel hydroxide phase which is neither α nor β," *Journal of Materials Chemistry,* vol. 7, pp. 2293-2296, 1997.

[22] D. S. Hall, D. J. Lockwood, S. Poirier, C. Bock and B. R. MacDougall, "Raman and Infrared Spectroscopy of α and β Phases of Thin Nickel Hydroxide Films Electrochemically Formed on Nickel," *J Phys Chem A,* vol. 116, pp. 6771-6784, 06/28, 2012.

[23] W. Visscher and E. Barendrecht, "Absorption of hydrogen in reduced nickel oxide," *J. Appl. Electrochem.,* vol. 10, pp. 269-274, 1980.

[24] L. M. M. de Souza, F. P. Kong, F. R. McLarnon and R. H. Muller, "Spectroscopic ellipsometry study of nickel oxidation in alkaline solution," *Electrochim. Acta,* vol. 42, pp. 1253-1267, 1997.

[25] A. Seyeux, V. Maurice, L. H. Klein and P. Marcus, "In situ scanning tunnelling microscopic study of the initial stages of growth and of the structure of the passive film on Ni(111) in 1 mM NaOH(aq)," *J. Solid State Electrochem.,* vol. 9, pp. 337-346, 2005.

[26] M. Jain, A. L. Elmore, M. A. Matthews and J. W. Weidner, "Thermodynamic considerations of the reversible potential for the nickel electrode," *Electrochim. Acta,* vol. 43, pp. 2649-2660, 6/16/, 1998.

[27] P. Oliva, J. Leonardi, J. F. Laurent, C. Delmas, J. J. Braconnier, M. Figlarz, F. Fievet and A. d. Guibert, "Review of the structure and the electrochemistry of nickel hydroxides and oxy-hydroxides," *J. Power Sources,* vol. 8, pp. 229-255, 1982.

[28] W. Visscher and E. Barendrecht, "Investigation of thin-film α- and β-Ni(OH)2 electrodes in alkaline solutions," *Journal of Electroanalytical Chemistry and Interfacial Electrochemistry,* vol. 154, pp. 69-80, 9/23/, 1983.

[29] D. S. Hall, C. Bock and B. R. MacDougall, "The Electrochemistry of Metallic Nickel: Oxides, Hydroxides, Hydrides and Alkaline Hydrogen Evolution," *J. Electrochem. Soc.,* vol. 160, pp. F235-F243, 01/01, 2013.

[30] A. Visintin, W. E. Triaca and A. J. Arvia, "A phenomenological approach to hydrous nickel oxide electrodes prepared by applying periodic potential routines," *J. Appl. Electrochem.,* vol. 26, pp. 493-502, 1996.

[31] B. Beverskog and I. Puigdomenech, "Revised Pourbaix diagrams for nickel at 25–300 °C," *Corros. Sci.,* vol. 39, pp. 969-980, 5, 1997.

[32] J. Gregori, J. J. García-Jareño, D. Giménez-Romero and F. Vicente, "Growth of passive layers on nickel during their voltammetric anodic dissolution in a weakly acid medium," *Electrochim. Acta,* vol. 52, pp. 658-664, 10/25/, 2006.

[33] F. Vicente, J. Gregori, J. García-Jareño and D. Giménez-Romero, "Cyclic voltammetric generation and electrochemical quartz crystal microbalance characterization of passive layer of nickel in a weakly acid medium," *J. Solid State Electrochem.,* vol. 9, pp. 684-690, 2005.

[34] J. Gregori, J. J. García-Jareño, D. Giménez-Romero, A. Roig and F. Vicente, "Anodic Dissolution of Nickel across Two Consecutive Electron Transfers: Calculation of the Ni(I) Intermediate Concentration," *J. Electrochem. Soc.,* vol. 154, pp. 371-377, 2007.

[35] M. R. Barbosa, S. G. Real, J. R. Vilche and A. J. Arvia, "Comparative Potentiodynamic Study of Nickel in Still and Stirred Sulfuric Acid-Potassium Sulfate Solutions in the 0.4–5.7 pH Range," *J. Electrochem. Soc.,* vol. 135, pp. 1077-1085, May 01, 1988.

[36] A. J. Bard, R. Parsons and J. Jordan, *Standard Potentials in Aqueous Solution.* CRC press, 1985.

[37] S. G. Real, M. R. Barbosa, J. R. Vilche and A. J. Arvia, "Influence of Chloride Concentration on the Active Dissolution and Passivation of Nickel Electrodes in Acid Sulfate Solutions," *J. Electrochem. Soc.,* vol. 137, pp. 1696-1702, 1990.

[38] M. Nakamura, N. Ikemiya, A. Iwasaki, Y. Suzuki and M. Ito, "Surface structures at the initial stages in passive film formation on Ni(1 1 1) electrodes in acidic electrolytes," *J. Electroanal. Chem.,* vol. 566, pp. 385-391, 5/15, 2004.

[39] J. Scherer, B. M. Ocko and O. M. Magnussen, "Structure, dissolution, and passivation of Ni(111) electrodes in sulfuric acid solution: an in situ STM, X-ray scattering, and electrochemical study," *Electrochim. Acta,* vol. 48, pp. 1169-1191, 4/20/, 2003.

[40] R. Subbaraman, D. Tripkovic, D. Strmcnik, K. Chang, M. Uchimura, A. P. Paulikas, V. Stamenkovic and N. M. Markovic, "Enhancing Hydrogen Evolution Activity in Water Splitting by Tailoring Li+-Ni(OH)2-Pt Interfaces," *Science,* vol. 334, pp. 1256-1260, December 02, 2011.

[41] N. Danilovic, R. Subbaraman, D. Strmcnik, K. Chang, A. P. Paulikas, V. R. Stamenkovic and N. M. Markovic, "Enhancing the Alkaline Hydrogen Evolution Reaction Activity through the Bifunctionality of Ni(OH)2/Metal Catalysts," *Angew. Chem. Int. Ed. Engl.,* vol. 51, pp. 12495-12498, 2012.

[42] W. Schmickler and E. Santos, *Interfacial Electrochemistry.* Springer Berlin Heidelberg, 2010.

[43] H. Wang, H. S. Casalongue, Y. Liang and H. Dai, "Ni(OH)2 Nanoplates Grown on Graphene as Advanced Electrochemical Pseudocapacitor Materials," *J. Am. Chem. Soc.,* vol. 132, pp. 7472-7477, 06/02, 2010.

[44] Y. Luo, G. Duan and G. Li, "Synthesis and characterization of flower-like β-Ni(OH)2 nanoarchitectures," *J. Solid State Chem.,* vol. 180, pp. 2149-2153, 7, 2007.

[45] Y. Ren and L. Gao, "From Three-Dimensional Flower-Like α-Ni(OH)2 Nanostructures to Hierarchical Porous NiO Nanoflowers: Microwave-Assisted Fabrication and Supercapacitor Properties," *J Am Ceram Soc,* vol. 93, pp. 3560-3564, 11/01, 2010.

[46] S. L. Medway, C. A. Lucas, A. Kowal, R. J. Nichols and D. Johnson. "In situ studies of the oxidation of nickel electrodes in alkaline solution," *J. Electroanal. Chem. 587(1),* pp. 172-181. 2006. . DOI: 10.1016/j.jelechem.2005.11.013.

[47] N. Kitakatsu, V. Maurice, C. Hinnen and P. Marcus, "Surface hydroxylation and local structure of NiO thin films formed on Ni(111)," *Surf Sci,* vol. 407, pp. 36-58, 6/10, 1998.

[48] L. R. Furenlid, M. W. Renner, K. M. Smith and J. Fajer, "Structural consequences of nickel versus macrocycle reductions in F430 models: EXAFS studies of a Ni(I) anion and Ni(II) .pi. anion radicals," *J. Am. Chem. Soc.,* vol. 112, pp. 1634-1635, 02/01, 1990.

[49] C. Gosden, J. B. Kerr, D. Pletcher and R. Rosas, "The electrochemistry of square planar macrocyclic nickel complexes and the reaction of Ni(I) with alkyl bromides: Tetradentate Schiff base complexes," *Journal of Electroanalytical Chemistry and Interfacial Electrochemistry,* vol. 117, pp. 101-107, 1/10/, 1981.

[50] M. F. Kibria, M. S. Mridha and A. H. Khan, "Electrochemical studies of a nickel electrode for the hydrogen evolution reaction," *Int J Hydrogen Energy,* vol. 20, pp. 435-440, 6, 1995.

[51] L. B. Albertini, A. C. D. Angelo and E. R. Gonzalez, "A nickel molybdenite cathode for the hydrogen evolution reaction in alkaline media," *J Appl Electrochem,* vol. 22, pp. 888-892, 1992.

[52] N. Krstaji, M. Popovi, B. Grgur and M. Vojnovi, "On the kinetics of the hydrogen evolution reaction on nickel in alkaline solution:: Part I. The mechanism," *J. Electroanal. Chem.,* vol. 512, pp. 16-26, 2001.

[53] P. Sabatier, *Catalysis in Organic Chemistry.* 8 Warren St, New York: D. Van Norstrand Company, 1922.

[54] S. Trasatti, "Work function, electronegativity, and electrochemical behaviour of metals: III. Electrolytic hydrogen evolution in acid solutions," *Journal of Electroanalytical Chemistry and Interfacial Electrochemistry,* vol. 39, pp. 163-184, 9, 1972.

[55] B. Conway and G. Jerkiewicz, "Relation of energies and coverages of underpotential and overpotential deposited H at Pt and other metals to the 'volcano curve'for cathodic H2 evolution kinetics," *Electrochim. Acta,* vol. 45, pp. 4075-4083, 2000.

[56] E. Santos, P. Quaino and W. Schmickler, "Theory of electrocatalysis: hydrogen evolution and more," *Phys. Chem. Chem. Phys.,* vol. 14, pp. 11224-11233, 2012.

[57] P. Quaino, F. Juarez, E. Santos and W. Schmickler, "Volcano plots in hydrogen electrocatalysis – uses and abuses," *Beilstein Journal of Nanotechnology,* vol. 5, pp. 846-854, 2014.

[58] B. Hammer and J. K. Nørskov, "Theoretical surface science and catalysis—calculations and concepts," in *Advances in Catalysis; Impact of Surface Science on Catalysis* Academic Press, 2000, pp. 71-129.

[59] M. Raney, "Method of producing Finely Divided Nickel," 16281910, May 10, 1927, 1927.

[60] J. Freel, W. J. M. Pieters and R. B. Anderson, "The structure of Raney nickel: I. Pore structure," *Journal of Catalysis,* vol. 14, pp. 247-256, 7, 1969.

[61] H. Wendt, H. Hofmann and V. Plzak, "Materials research and development of electrocatalysts for alkaline water electrolysis," *Mater. Chem. Phys.,* vol. 22, pp. 27-49, 6, 1989.

[62] J. Fournier, D. Miousse and J. Legoux, "Wire-arc sprayed nickel based coating for hydrogen evolution reaction in alkaline solutions," *Int J Hydrogen Energy,* vol. 24, pp. 519-528, 6, 1999.

[63] G. Schiller, R. Henne and V. Borck, "Vacuum plasma spraying of high-performance electrodes for alkaline water electrolysis," *J. Therm. Spray Technol.,* vol. 4, pp. 185-194, 1995.

[64] S. Tanaka, N. Hirose and T. Tanaki, "Evaluation of Raney–nickel cathodes prepared with aluminum powder and tin powder," *Int J Hydrogen Energy,* vol. 25, pp. 481-485, 5/1/, 2000.

[65] L. Birry and A. Lasia, "Studies of the Hydrogen Evolution Reaction on Raney Nickel—Molybdenum Electrodes," *J. Appl. Electrochem.,* vol. 34, pp. 735-749, 2004.

[66] K. R. Koboski, E. F. Nelsen and J. R. Hampton, "Hydrogen evolution reaction measurements of dealloyed porous NiCu," vol. 8, pp. 1-7, 2013.

[67] R. Solmaz and G. Kardas, "Hydrogen evolution and corrosion performance of NiZn coatings," *Energy Conversion and Management,* vol. 48, pp. 583-591, 2007.

[68] G. Sheela, M. Pushpavanam and S. Pushpavanam, "Zinc-nickel alloy electrodeposits for water electrolysis," *Int J Hydrogen Energy,* vol. 27, pp. 627-633, 2002.

[69] J. Balej, J. Divisek, H. Schmitz and J. Mergel, "Preparation and properties of raney nickel electrodes on Ni-Zn base for H2 and O2 evolution from alkaline solutions Part I: electrodeposition of Ni-Zn alloys from chloride solutions," *J. Appl. Electrochem.,* vol. 22, pp. 705-710, 1992.

[70] T. Boruciński, S. Rausch and H. Wendt, "Raney nickel activated H2-cathodes Part II: Correlation of morphology and effective catalytic activity of Raney-nickel coated cathodes," *J. Appl. Electrochem.,* vol. 22, pp. 1031-1038, 1992.

[71] L. Chen and A. Lasia, "Hydrogen Evolution Reaction on Nickel-Molybdenum Powder Electrodes," *J. Electrochem. Soc.,* vol. 139, pp. 3458-3464, 1992.

[72] L. Chen and A. Lasia, "Study of the Kinetics of Hydrogen Evolution Reaction on Nickel-Zinc Alloy Electrodes," *J. Electrochem. Soc.,* vol. 138, pp. 3321-3328, 11/01, 1991.

[73] S. Rausch and H. Wendt, "Morphology and Utilization of Smooth Hydrogen-Evolving Raney Nickel Cathode Coatings and Porous Sintered-Nickel Cathodes," *J. Electrochem. Soc.,* vol. 143, pp. 2852-2862, 09/01, 1996.

[74] M. Ledendecker, G. Clavel, M. Antonietti and M. Shalom, "Highly Porous Materials as Tunable Electrocatalysts for the Hydrogen and Oxygen Evolution Reaction," *Adv. Funct. Mater.,* vol. 25, pp. 393-399, 2015.

[75] M. Shalom, V. Molinari, D. Esposito, G. Clavel, D. Ressnig, C. Giordano and M. Antonietti, "Sponge-like Nickel and Nickel Nitride Structures for Catalytic Applications," *Adv Mater,* vol. 26, pp. 1272-1276, 2014.

[76] I. Brown and S. Sotiropoulos, "Preparation and characterization of microporous Ni coatings as hydrogen evolving cathodes," *J. Appl. Electrochem.,* vol. 30, pp. 107-111, 2000.

[77] I. J. Brown and S. Sotiropoulos, "Electrodeposition of Ni from a high internal phase emulsion (HIPE) template," *Electrochim. Acta,* vol. 46, pp. 2711-2720, 5/15, 2001.

[78] V. Ganesh and V. Lakshminarayanan, "Preparation of high surface area nickel electrodeposit using a liquid crystal template technique," *Electrochim. Acta,* vol. 49, pp. 3561-3572, 2004.

[79] J. K. Lee, Y. Yi, H. J. Lee, S. Uhm and J. Lee, "Electrocatalytic activity of Ni nanowires prepared by galvanic electrodeposition for hydrogen evolution reaction," *Catalysis Today,* vol. 146, pp. 188-191, 2009.

[80] P. C. Chen, Y. M. Chang, P. W. Wu and Y. F. Chiu, "Fabrication of Ni nanowires for hydrogen evolution reaction in a neutral electrolyte," *Int J Hydrogen Energy,* vol. 34, pp. 6596-6602, 2009.

[81] C. S. Hsu, H. B. Lee, C. S. Lin and C. Y. Lee, "Study on the Electrodeposition of Ni-P Nanowires and Their Electrocatalytic Properties," *Metallurgical and Materials Transactions A,* vol. 41, pp. 768-774, 2010.

[82] L. M. Abrantes and J. P. Correia, "Polypyrrole incorporating electroless nickel," *Electrochim. Acta,* vol. 45, pp. 4179-4185, 8/31/, 2000.

[83] E. Navarro-Flores and S. Omanovic, "Hydrogen evolution on nickel incorporated in three-dimensional conducting polymer layers," *Journal of Molecular Catalysis A: Chemical,* vol. 242, pp. 182-194, 2005.

[84] D. A. Dalla Corte, C. Torres, P. d. S. Correa, E. S. Rieder and C. d. F. Malfatti, "The hydrogen evolution reaction on nickel-polyaniline composite electrodes," *Int J Hydrogen Energy,* vol. 37, pp. 3025-3032, 2012.

[85] H. Hu, Y. Fan and H. Liu, "Hydrogen production in single-chamber tubular microbial electrolysis cells using non-precious-metal catalysts," *Int J Hydrogen Energy,* vol. 34, pp. 8535-8542, 2009.

[86] H. Hu, Y. Fan and H. Liu, "Optimization of NiMo catalyst for hydrogen production in microbial electrolysis cells," *Int J Hydrogen Energy,* 2010.

[87] M. A. McArthur, L. Jorge, S. Coulombe and S. Omanovic, "Synthesis and characterization of 3D Ni nanoparticle/carbon nanotube cathodes for hydrogen evolution in alkaline electrolyte," *J. Power Sources,* vol. 266, pp. 365-373, 11/15/, 2014.

[88] L. Kang, R. Wang, L. Kong, H. Li, J. Zhang and Y. Luo, "Fabrication of Ni nanoparticles on ordered mesoporous carbon using an immersion-electrodeposition method," *Mater Lett,* vol. 64, pp. 2064-2067, 10/15/, 2010.

[89] M. H. Miles, "Evaluation of electrocatalysts for water electrolysis in alkaline solutions*," *J. Electroanal. Chem.,* vol. 60, pp. 89-96, 1975.

[90] M. M. Jaksic, "Hypo-hyper-d-electronic interactive nature of interionic synergism in catalysis and electrocatalysis for hydrogen reactions," *Int J Hydrogen Energy,* vol. 26, pp. 559-578, 2001.

[91] J. G. Highfield, E. Claude and K. Oguro, "Electrocatalytic synergism in Ni/Mo cathodes for hydrogen evolution in acid medium: a new model," *Electrochim. Acta,* vol. 44, pp. 2805-2814, 4/1/, 1999.

[92] J. M. Jakšić, M. V. Vojnović and N. V. Krstajić, "Kinetic analysis of hydrogen evolution at Ni-Mo alloy electrodes," *Electrochim. Acta,* vol. 45, pp. 4151-4158, 2000.

[93] S. D. De la Torre, D. Oleszak, A. Kakitsuji, K. Miyamoto, H. Miyamoto, R. Martínez-S, F. Almeraya-C, A. Martínez-V and D. Rios-J, "Nickel-molybdenum catalysts fabricated by mechanical alloying and spark plasma sintering," *Materials Science and Engineering A,* vol. 276, pp. 226-235, 2000.

[94] L. M. Rodriguez-Valdez, I. Estrada-Guel, F. Almeraya-Calderón, M. A. Neri-Flores, A. Martínez-Villafaņe and R. Martínez-Sánchez, "Electrochemical performance of hydrogen evolution reaction of Ni–Mo electrodes obtained by mechanical alloying," *Int J Hydrogen Energy,* vol. 29, pp. 1141-1145, 2004.

[95] E. Navarro-Flores, Z. Chong and S. Omanovic, "Characterization of Ni, NiMo, NiW and NiFe electroactive coatings as electrocatalysts for hydrogen evolution in an acidic medium," *Journal of Molecular Catalysis A: Chemical,* vol. 226, pp. 179-197, 2005.

[96] J. Divisek, H. Schmitz and J. Balej, "Ni and Mo coatings as hydrogen cathodes," *J. Appl. Electrochem.,* vol. 19, pp. 519-530, 1989.

[97] N. Krstajic, V. Jovic, L. Gajic-Krstajic, B. Jovic, A. Antozzi and G. Martelli, "Electrodeposition of Ni-Mo alloy coatings and their characterization as cathodes for hydrogen evolution in sodium hydroxide solution," *Int J Hydrogen Energy,* vol. 33, pp. 3676-3687, 2008.

[98] J. Y. Huot, M. L. Trudeau and R. Schulz, "Low Hydrogen Overpotential Nanocrystalline Ni-Mo Cathodes for Alkaline Water Electrolysis," *J. Electrochem. Soc.,* vol. 138, pp. 1316-1321, 05/01, 1991.

[99] M. Metikos-Hukovic, Z. Grubac, N. Radic and A. Tonejc, "Sputter deposited nanocrystalline Ni and Ni-W films as catalysts for hydrogen evolution," *Journal of Molecular Catalysis A: Chemical,* vol. 249, pp. 172-180, 2006.

[100] M. Wang, Z. Wang, Z. Guo and Z. Li, "The enhanced electrocatalytic activity and stability of NiW films electrodeposited under super gravity field for hydrogen evolution reaction," *Int J Hydrogen Energy,* vol. 36, pp. 3305-3312, 2011.

[101] D. E. Brown, M. N. Mahmood, M. C. M. Man and A. K. Turner, "Preparation and characterization of low overvoltage transition metal alloy electrocatalysts for hydrogen evolution in alkaline solutions," *Electrochim. Acta,* vol. 29, pp. 1551-1556, 1984.

[102] M. Jafarian, O. Azizi, F. Gobal and M. G. Mahjani, "Kinetics and electrocatalytic behavior of nanocrystalline CoNiFe alloy in hydrogen evolution reaction," *Int J Hydrogen Energy,* vol. 32, pp. 1686-1693, 2007.

[103] R. Solmaz and G. Kardas, "Electrochemical deposition and characterization of NiFe coatings as electrocatalytic materials for alkaline water electrolysis," *Electrochim. Acta,* vol. 54, pp. 3726-3734, 2009.

[104] M. H. Tang, C. Hahn, A. J. Klobuchar, J. W. D. Ng, J. Wellendorff, T. Bligaard and T. F. Jaramillo, "Nickel-silver alloy electrocatalysts for hydrogen evolution and oxidation in an alkaline electrolyte," *Phys. Chem. Chem. Phys.,* vol. 16, pp. 19250-19257, 2014.

[105] S. H. Ahn, H. Park, I. Choi, S. J. Yoo, S. J. Hwang, H. Kim, E. Cho, C. W. Yoon, H. Park, H. Son, J. M. Hernandez, S. W. Nam, T. Lim, S. Kim and J. H. Jang, "Electrochemically fabricated NiCu alloy catalysts for hydrogen production in alkaline water electrolysis," *Int J Hydrogen Energy,* vol. 38, pp. 13493-13501, 10/17/, 2013.

[106] R. Solmaz, A. Döner, I. Sahin, A. O. Yüce, G. Kardas, B. YazIcI and M. Erbil, "The stability of NiCoZn electrocatalyst for hydrogen evolution activity in alkaline solution during long-term electrolysis," *Int J Hydrogen Energy,* vol. 34, pp. 7910-7918, 2009.

[107] C. Fan, D. L. Piron and P. Paradis, "Hydrogen evolution on electrodeposited nickel-cobalt-molybdenum in alkaline water electrolysis," *Electrochim. Acta,* vol. 39, pp. 2715-2722, 1994.

[108] C. Lupi, A. Dell'Era and M. Pasquali, "Nickel–cobalt electrodeposited alloys for hydrogen evolution in alkaline media," *Int J Hydrogen Energy,* vol. 34, pp. 2101-2106, 2009.

[109] C. González-Buch, I. Herraiz-Cardona, E. Ortega, J. García-Antón and V. Pérez-Herranz, "Synthesis and characterization of macroporous Ni, Co and Ni–Co electrocatalytic deposits for hydrogen evolution reaction in alkaline media," *Int J Hydrogen Energy,* vol. 38, pp. 10157-10169, 8/21/, 2013.

[110] D. S. P. Cardoso, L. Amaral, D. M. F. Santos, B. Šljukić, C. A. C. Sequeira, D. Macciò and A. Saccone, "Enhancement of hydrogen evolution in alkaline water electrolysis by using nickel-rare earth alloys," *Int J Hydrogen Energy,* vol. 40, pp. 4295-4302, 4/6/, 2015.

[111] J. K. Nørskov, T. Bligaard, A. Logadottir, J. R. Kitchin, J. G. Chen, S. Pandelov and U. Stimming, "Trends in the Exchange Current for Hydrogen Evolution," *J. Electrochem. Soc.,* vol. 152, pp. J23-J26, 03/01, 2005.

[112] J. Greeley, T. F. Jaramillo, J. Bonde, I. Chorkendorff and J. K. Nørskov, "Computational high-throughput screening of electrocatalytic materials for hydrogen evolution," *Nat. Mater.,* vol. 5, pp. 909-913, 2006.

[113] J. Greeley and J. K. Nørskov, "Large-scale, density functional theory-based screening of alloys for hydrogen evolution," *Surf Sci,* vol. 601, pp. 1590-1598, 3/15/, 2007.

[114] M. E. Bjorketun, A. S. Bondarenko, B. L. Abrams, I. Chorkendorff and J. Rossmeisl, "Screening of electrocatalytic materials for hydrogen evolution," *Phys. Chem. Chem. Phys.,* vol. 12, pp. 10536-10541, 2010.

[115] X. Zhao, Y. Ding, L. Ma, X. Shen and S. Xu, "Structure, morphology and electrocatalytic characteristics of nickel powders treated by mechanical milling," *Int J Hydrogen Energy,* vol. 33, pp. 6351-6356, 2008.

[116] Y. Sürme, A. A. Gürten and K. Kayakırılmaz, "Electrodeposition, characterization and long term stability of NiW and NiWZn coatings on copper substrate in alkaline solution," vol. 19, pp. 803-812, 2013.

[117] M. Wang, Z. Wang and Z. Guo, "Electrodeposited free-crack NiW films under super gravity filed: Structure and excellent corrosion property," *Mater. Chem. Phys.,* vol. 148, pp. 245-252, 11/14/, 2014.

[118] S. E. F. Kleijn, S. C. S. Lai, M. T. M. Koper and P. R. Unwin, "Electrochemistry of Nanoparticles," *Angew. Chem. Int. Ed.,* vol. 53, pp. 3558-3586, 04/01, 2014.

[119] N. Tian, Z. Y. Zhou, S. G. Sun, Y. Ding and Z. L. Wang, "Synthesis of tetrahexahedral platinum nanocrystals with high-index facets and high electro-oxidation activity," *Science,* vol. 316, pp. 732, 2007.

[120] C. Hu, C. Lin and T. Wen, "Textural and electrochemical properties of Watts nickel-deposited titanium electrodes," *Mater. Chem. Phys.,* vol. 44, pp. 233-238, 6, 1996.

[121] A. Pătru, P. Antitomaso, R. Sellin, N. Jerez, P. L. Taberna and F. Favier, "Size and strain dependent activity of Ni nano and micro particles for hydrogen evolution reaction," *Int J Hydrogen Energy,* vol. 38, pp. 11695-11708, 9/10/, 2013.

[122] M. A. Domínguez-Crespo, E. Ramírez-Meneses, A. M. Torres-Huerta, V. Garibay-Febles and K. Philippot, "Kinetics of hydrogen evolution reaction on stabilized Ni, Pt and Ni–Pt nanoparticles obtained by an organometallic approach," *Int J Hydrogen Energy,* vol. 37, pp. 4798-4811, 3, 2012.

[123] M. A. Domínguez-Crespo, E. Ramírez-Meneses, V. Montiel-Palma, A. M. Torres Huerta and H. Dorantes Rosales, "Synthesis and electrochemical characterization of stabilized nickel nanoparticles," *Int J Hydrogen Energy,* vol. 34, pp. 1664-1676, 2009.

[124] P. Quaino, E. Santos, G. Soldano and W. Schmickler, "Recent Progress in Hydrogen Electrocatalysis," *Advances in Physical Chemistry,* vol. 2011, pp. 14, 2011.

[125] M. Even, "Determination of the Electrochemical Active Surface Area of Nickel Electrodes," 2011.

[126] I. Herraiz-Cardona, E. Ortega, J. G. Antón and V. Pérez-Herranz, "Assessment of the roughness factor effect and the intrinsic catalytic activity for hydrogen evolution reaction on Ni-based electrodeposits," *Int J Hydrogen Energy,* vol. 36, pp. 9428-9438, 8, 2011.

[127] A. Lasia, "Modeling of experimental data," in *Electrochemical Impedance Spectroscopy and its Applications* Springer New York, 2014, pp. 301-321.

[128] I. Herraiz-Cardona, E. Ortega and V. Pérez-Herranz, "Impedance study of hydrogen evolution on Ni/Zn and Ni–Co/Zn stainless steel based electrodeposits," *Electrochim. Acta,* vol. 56, pp. 1308-1315, 1/1, 2011.

[129] R. Subbaraman, D. Tripkovic, K. Chang, D. Strmcnik, A. P. Paulikas, P. Hirunsit, M. Chan, J. Greeley, V. Stamenkovic and N. M. Markovic, "Trends in activity for the water electrolyser reactions on 3d M(Ni,Co,Fe,Mn) hydr(oxy)oxide catalysts," *Nat. Mater.,* vol. 11, pp. 550-557, 2012.

[130] L. Wang, C. Lin, D. Huang, J. Chen, L. Jiang, M. Wang, L. Chi, L. Shi and J. Jin, "Optimizing the Volmer Step by Single-Layer Nickel Hydroxide Nanosheets in Hydrogen Evolution Reaction of Platinum," *ACS Catal.,* vol. 5, pp. 3801-3806, 05/13, 2015.

[131] M. Gong, W. Zhou, M. Tsai, J. Zhou, M. Guan, M. Lin, B. Zhang, Y. Hu, D. Wang, J. Yang, S. J. Pennycook, B. Hwang and H. Dai, "Nanoscale nickel oxide/nickel heterostructures for active hydrogen evolution electrocatalysis," *Nat Commun,* vol. 5, 08/22/, 2014.

[132] R. Gordon, M. Bertram and T. Graedel, "Metal stocks and sustainability," *Proc. Natl. Acad. Sci. U. S. A.,* vol. 103, pp. 1209, 2006.

[133] B. R. Blair, "The role of near-earth asteroids in long-term platinum supply," 2000, pp. 5.

[134] B. E. Conway, B. Barnett, H. Angerstein-Kozlowska and B. V. Tilak. A surface-electrochemical basis for the direct logarithmic growth law for initial stages of extension of anodic oxide films formed at noble metals. *J. Chem. Phys. 93(11),* pp. 8361-8373. 1990. . DOI: http://dx.doi.org/10.1063/1.459319.

[135] A. R. T. Morrison, S. S. Hosseiny and R. Wüthrich, "Platinum-like Oxidation of Nickel Surface by Rapidly Switching Voltage to Generate Highly Active Bifunctional Catalysts," *Electrochemistry Communications, vol. 67, pp 22-25,* 2016.

[136] B. E. Conway, "Electrochemical oxide film formation at noble metals as a surface-chemical process," *Prog. Surf. Sci.,* vol. 49, pp. 331-452, 8, 1995.

[137] M. Grdeń, M. Alsabet and G. Jerkiewicz, "Surface Science and Electrochemical Analysis of Nickel Foams," *ACS Appl. Mater. Interfaces,* vol. 4, pp. 3012-3021, 05/10; 2012.

[138] M. C. Biesinger, B. P. Payne, L. W. M. Lau, A. Gerson and R. S. C. Smart, "X-ray photoelectron spectroscopic chemical state quantification of mixed nickel metal, oxide and hydroxide systems," *Surf. Interface Anal.,* vol. 41, pp. 324-332, 2009.

[139] M. Dmochowska and A. Czerwiński. Behavior of a nickel electrode in the presence of carbon monoxide. *J. Solid State Electrochem. 2(1),* pp. 16-23. 1998.

[140] Y. Gorlin and T. F. Jaramillo, "A Bifunctional Nonprecious Metal Catalyst for Oxygen Reduction and Water Oxidation," *J. Am. Chem. Soc.,* vol. 132, pp. 13612-13614, 2010.

[141] H. R. Zare, S. H. Hashemi and A. Benvidi, "Electrodeposited nano-scale islands of ruthenium oxide as a bifunctional electrocatalyst for simultaneous catalytic oxidation of hydrazine and hydroxylamine," *Anal. Chim. Acta,* vol. 668, pp. 182-187, 2010.

[142] M. Grdeń and J. Jagiełło, "Oxidation of electrodeposited cobalt electrodes in an alkaline electrolyte," *J. Solid State Electrochem.,* vol. 17, pp. 145-156, 2013.

[143] P. Klapetek, D. Nečas and C. Anderson, *Gwyddion User Guide.* 2004.

[144] M. Donten, H. Cesiulis and Z. Stojek, "Electrodeposition of amorphous/nanocrystalline and polycrystalline Ni-Mo alloys from pyrophosphate baths," *Electrochim. Acta,* vol. 50, pp. 1405-1412, 2005.

[145] E. Chassaing, N. Portail, A. Levy and G. Wang, "Characterisation of electrodeposited nanocrystalline Ni–Mo alloys," *J. Appl. Electrochem.,* vol. 34, pp. 1085-1091, 2004.

[146] M. Shalom, D. Ressnig, X. Yang, G. Clavel, T. P. Fellinger and M. Antonietti, "Nickel nitride as an efficient electrocatalyst for water splitting," *J. Mater. Chem. A,* vol. 3, pp. 8171-8177, 2015.

[147] T. C. Tan and D. T. Chin, "A.c. corrosion of nickel in sulphate solutions," vol. 18, pp. 831-838, 1988.

[148] A. N. Rollinson, G. L. Rickett, A. Lea-Langton, V. Dupont and M. V. Twigg, "Hydrogen from urea–water and ammonia–water solutions," *Appl. Catal. , B,* vol. 106, pp. 304-315, 8/11, 2011.

[149] A. N. Rollinson, J. Jones, V. Dupont and M. V. Twigg, "Urea as a hydrogen carrier: a perspective on its potential for safe, sustainable and long-term energy supply," *Energy Environ.Sci.,* vol. 4, pp. 1216-1224, 2011.

[150] A. N. Alexandrova and W. L. Jorgensen, "Why Urea Eliminates Ammonia Rather than Hydrolyzes in Aqueous Solution," *The Journal of Physical Chemistry B,* vol. 111, pp. 720-730, 2007.

[151] B. P. Callahan, Y. Yuan and R. Wolfenden, "The Burden Borne by Urease," *J. Am. Chem. Soc.,* vol. 127, pp. 10828-10829, 2005.

[152] M. Constable, M. Charlton, F. Jensen, K. McDonald, G. Craig and K. W. Taylor, "An Ecological Risk Assessment of Ammonia in the Aquatic Environment," *Hum. Ecol. Risk Assess.,* vol. 9, pp. 527-548, 03/01; 2003.

[153] W. Simka, J. Piotrowski and G. Nawrat, "Influence of anode material on electrochemical decomposition of urea," *Electrochim. Acta,* vol. 52, pp. 5696-5703, 5/10, 2007.

[154] C. Carlesi Jara, S. Giulio, D. Fino and P. Spinelli, "Combined direct and indirect electroxidation of urea containing water," *J. Appl. Electrochem.,* vol. 38, pp. 915-922, 2008.

[155] S. Di Giulio, C. Carlesi Jara, D. Fino, G. Saracco, V. Specchia and P. Spinelli, "Fate of Organic Nitrogen during Electrooxidation over Conductive Metal Oxide Anodes," *Ind. Eng. Chem. Res.,* vol. 46, pp. 6783-6787, 2007.

[156] R. L. King and G. G. Botte, "Investigation of multi-metal catalysts for stable hydrogen production via urea electrolysis," *J. Power Sources,* vol. 196, pp. 9579-9584, 11/15, 2011.

[157] D. Wang, W. Yan and G. G. Botte, "Exfoliated nickel hydroxide nanosheets for urea electrolysis," *Electrochemistry Communications,* vol. 13, pp. 1135-1138, 10, 2011.

[158] V. Vedharathinam and G. G. Botte, "Understanding the electro-catalytic oxidation mechanism of urea on nickel electrodes in alkaline medium," *Electrochim. Acta,* vol. 81, pp. 292-300, 10/30/, 2012.

[159] V. Vedharathinam and G. G. Botte, "Direct evidence of the mechanism for the electro-oxidation of urea on Ni(OH)2 catalyst in alkaline medium," *Electrochim. Acta,* vol. 108, pp. 660-665, 10/1/, 2013.

[160] W. Yan, D. Wang and G. G. Botte, "Electrochemical decomposition of urea with Ni-based catalysts," *Applied Catalysis B: Environmental,* vol. 127, pp. 221-226, 10/30, 2012.

[161] B. K. Boggs, R. L. King and G. G. Botte, "Urea electrolysis: direct hydrogen production from urine," *Chemical Communications,* pp. 4859-4861, 2009.

[162] R. Ahmad, N. Tripathy and Y. Hahn, "Highly stable urea sensor based on ZnO nanorods directly grown on Ag/glass electrodes," *Sensors Actuators B: Chem.,* vol. 194, pp. 290-295, 2014.

[163] M. Wester, F. Simonis, N. Lachkar, W. K. Wodzig, F. J. Meuwissen, J. P. Kooman, W. H. Boer, J. A. Joles and K. G. Gerritsen, "Removal of Urea in a Wearable Dialysis Device: A Reappraisal of Electro-Oxidation," *Artif. Organs,* vol. 38, pp. 998-1006, 2014.

[164] R. Lan, S. Tao and J. T. S. Irvine, "A direct urea fuel cell - power from fertiliser and waste," *Energy Environ.Sci.,* vol. 3, pp. 438-441, 2010.

[165] W. Yan, D. Wang and G. G. Botte, "Nickel and cobalt bimetallic hydroxide catalysts for urea electro-oxidation," *Electrochim. Acta,* vol. 61, pp. 25-30, 2/1, 2012.

[166] D. Wang, W. Yan, S. H. Vijapur and G. G. Botte, "Enhanced electrocatalytic oxidation of urea based on nickel hydroxide nanoribbons," *J. Power Sources,* vol. 217, pp. 498-502, 11/1, 2012.

[167] M. Wu, R. Ji and Y. Zheng, "Nickel hydroxide electrode with a monolayer of nanocup arrays as an effective electrocatalyst for enhanced electrolysis of urea," *Electrochim. Acta,* vol. 144, pp. 194-199, 10/20/, 2014.

[168] D. Wang, W. Yan, S. H. Vijapur and G. G. Botte, "Electrochemically reduced graphene oxide–nickel nanocomposites for urea electrolysis," *Electrochim. Acta,* vol. 89, pp. 732-736, 2/1, 2013.

[169] L. Wang, M. Li, Z. Huang, Y. Li, S. Qi, C. Yi and B. Yang, "Ni-WC/C nanocluster catalysts for urea electrooxidation," *J. Power Sources,* vol. 264, pp. 282-289, 10/15, 2014.

[170] D. A. Daramola, D. Singh and G. G. Botte, "Dissociation Rates of Urea in the Presence of NiOOH Catalyst: A DFT Analysis," *J Phys Chem A,* vol. 114, pp. 11513-11521, 11/04, 2010.

[171] V. Vedharathinam and G. G. Botte, "Experimental Investigation of Potential Oscillations during the Electrocatalytic Oxidation of Urea on Ni Catalyst in Alkaline Medium," *J. Phys. Chem. C,* vol. 118, pp. 21806-21812, 09/25, 2014.

[172] A. R. T. Morrison, L. Juillac, S. Guyomart and R. Wüthrich, "Optimization of the Square Wave Treatment of Nickel to Produce Highly Active Bifunctional Catalyst for the Hydrogen Evolution," *Submitted,* 2016.

[173] K. Ye, D. Zhang, F. Guo, K. Cheng, G. Wang and D. Cao, "Highly porous nickel@carbon sponge as a novel type of three-dimensional anode with low cost for high catalytic performance of urea electro-oxidation in alkaline medium," *J. Power Sources,* vol. 283, pp. 408-415, 6/1, 2015.

[174] Y. Miao, L. Ouyang, S. Zhou, L. Xu, Z. Yang, M. Xiao and R. Ouyang, "Electrocatalysis and electroanalysis of nickel, its oxides, hydroxides and oxyhydroxides toward small molecules," *Biosensors and Bioelectronics,* vol. 53, pp. 428-439, 3/15, 2014.

[175] I. Danaee, M. Jafarian, F. Forouzandeh, F. Gobal and M. G. Mahjani, "Electrocatalytic oxidation of methanol on Ni and NiCu alloy modified glassy carbon electrode," *Int J Hydrogen Energy,* vol. 33, pp. 4367-4376, 2008.

[176] (). *Alfa Aesar Web Page*. Available: https://www.alfa.com/en/.

[177] "Environmental Protection Act, Revised Regulations of Ontario 1990, Regulation 347: GENERAL - WASTE MANAGEMENT," pp. 1-1, 2016.

[178] C. S. Turchi, H. F. Mehos and M. F. Link, "Design and Cost of Solar Photocatalytic Systems for Groundwater Remidiation," *Remediation: The Journal of Environmental Cleanup Costs, Technologies and Techniques,* 1992.

[179] (). *Hy-Stat-A Hydrogen Plants on-site and on-demand* [Hydrogenics Corperation]. Available: http://pdf.directindustry.com/pdf/hydrogenics/hystat-a-hydrogen-generator-plant/33492-75126.html.

[180] (). *MT Series 100 kW to 2000 kW+* [Magna-Power]. Available: http://www.magna-power.com/products/programmable-dc-power-supplies/mt-series#specifications.

[181] V. Srinivasan and J. W. Weidner, "Studies on the Capacitance of Nickel Oxide Films: Effect of Heating Temperature and Electrolyte Concentration," *J. Electrochem. Soc.,* vol. 147, pp. 880-885, 03/01, 2000.

[182] B. E. Conway and L. Bai, "Determination of the adsorption behaviour of 'overpotential-deposited' hydrogen-atom species in the cathodic hydrogen-evolution reaction by analysis of potential-relaxation transients," *J. Chem. Soc. , Faraday Trans. 1,* vol. 81, pp. 1841-1862, 1985.

[183] V. Maurice, L. H. Klein and P. Marcus, "Atomic-scale investigation of the localized corrosion of passivated nickel surfaces," *Surf. Interface Anal.,* vol. 34, pp. 139-143, 08/01, 2002.

[184] K. Nielsch, F. Müller, A. P. Li and U. Gösele, "Uniform nickel deposition into ordered alumina pores by pulsed electrodeposition," *Adv Mater,* vol. 12, pp. 582-586, 2000.

[185] A. Visintin, A. C. Chialvo, W. E. Triaca and A. J. Arvia, "The electroformation of thick hydrous nickel hydroxide films through the application of periodic potential signals," *Journal of Electroanalytical Chemistry and Interfacial Electrochemistry,* vol. 225, pp. 227-239, 1987.

[186] S. Albu, D. Kim and P. Schmuki, "Growth of Aligned TiO2 Bamboo-Type Nanotubes and Highly Ordered Nanolace," *Angewandte Chemie,* vol. 120, pp. 1942-1945, 02/22, 2008.